Assessment of the Repeatability and Sensitivity of the Thermoelectric Perfusion Probe

Brent Earl Ellis, B.S.

Thesis submitted to the faculty of the

Virginia Polytechnic Institute and State University

in partial fulfillment of the requirements for the degree of

Master of Science

in

Mechanical Engineering

APPROVED:

Elaine P. Scott, Ph.D., Co-Chair

Thomas E. Diller, Sc.D., Co-Chair

Otto Lanz, DVM, Diplomate ACVS

December 6, 2006

Blacksburg, Virginia

Keywords: blood perfusion, tissue phantom, finite difference, thermal diffusion probe

Assessment of the Repeatability and Sensitivity of the Thermoelectric Perfusion Probe

Brent Earl Ellis

ABSTRACT

The Thermoelectric Perfusion Probe is a completely electronic system that cyclically heats and cools tissue to measure blood perfusion. The probe produces the thermal event with a thermoelectric cooler and then measures the resulting heat flux and temperatures: the arterial temperature and the sensor temperature (the temperature between the heat flux gage and the skin). The Thermoelectric Perfusion Probe was validated and calibrated on a phantom tissue test stand, a system that simulates perfusion with known, controlled flow. With the new pressed sensor technology, a thermocouple sealed to a heat flux gage, the sensor temperature and the heat flux are simultaneously recorded. The pressed sensor tests validated the program used to predict perfusion for the Thermoelectric Perfusion Probe. This perfusion estimation program can determine the tissues perfusion regardless of how the thermal event is created (i.e. convective cooling, convective heating, conductive heating).

Based on experimentation, the Thermoelectric Perfusion Probe displays good repeatability and sensitivity for continuously measuring perfusion. The sensitivity and repeatability of the Thermoelectric Perfusion Probe was proven when the perfusion estimates were compared to the perfusion estimates predicted by the Convective Perfusion Probe, a previously validated perfusion probe, and the CFD Flow Model, a computational model of the phantom tissue test stand.

Acknowledgments

I would like to thank my family and friends for supporting me through this process. My parents, Charles and Sherrin always encouraged me and provided me with monetary support throughout my education, gas and girls are expensive. I would like to thank my sister, Amanda and her husband Chuck for providing me with guidance through the college years. Brittney, thank for being there, because lets face it I am different and SPECIAL.

I would like to thank my advisors Dr. Tom Diller & Elaine Scott and the rest of the Heat Transfer Lab. Dr. Diller had a knack for fixing lab equipment in 10 minutes when it would take me 10 hours. Dr. Scott always was willing to point out the NUMEROUS grammatical mistakes in my papers. Tricia provided me with comical relief, Ashvin provided me with theoretical expertise, and, Leah was God sent because she kept me organized.

Contents

List of Figures

List of Tables

List of Equations

Chapter 1 Introduction

Blood perfusion, the blood flowing at the capillary level, is an extremely important component of human physiology. Blood perfusion is responsible for providing the oxygen and nutrients required by cells and removing waste products. Blood perfusion is extremely complex and therefore appears non-directional at the macroscopic level. The non-directional flow is due to the intricacy of the structure found in the capillary bed. The blood flow at the venous and arterial level is related to blood perfusion; however, there can be perfusion abnormalities in the presence of normal blood flow in the arteries and veins. Blood flow is the velocity of blood through the blood vessels, whereas perfusion is the total amount of blood flowing through the tissue. Blood flow is directional where perfusion is convoluted and considered nondirectional on the macroscopic level. In addition, blood perfusion is a chief component in the thermoregulatory system of the human body.

Due to the vital role that blood plays in maintaining normal and physiologic conditions, the ability to determine blood perfusion has many important clinical applications. Differences in local blood perfusion can be an indicator that the body is responding to an abnormal physiologic or pathologic state. These blood perfusion differences can be used to assess the progression of skin graft healing. Low blood perfusion can also be an indicator of microcirculatory problems in diabetes patients.

Several methods have been developed to determine blood perfusion. These methods include scanning techniques, laser Doppler techniques, and thermal techniques. Laser Doppler techniques do not measure absolute blood perfusion, they estimate perfusion based on velocities. Currently, the scanning techniques are very large and expensive and can't be used in a surgical situation or for long term monitoring. Also, scanning techniques can't determine perfusion in shallow tissue such as skin. An invasive thermal diffusion probe has been developed for measuring absolute perfusion; however, it is limited due to its invasive nature and inability to measure skin perfusion.

Another concept uses the thermal response of tissue to predict perfusion but in a non-invasive manner. The Convective Perfusion Probe at Virginia Tech cools a small

area of tissue and then measures the thermal response of the tissue. The absolute perfusion value for the tissue is predicted from the thermal response. The Convective Perfusion Probe has been shown to be a viable probe to measure perfusion for short periods of time. However, the Convective Perfusion Probe is clumsy and limited because of the pressurized air requirement. It also is not a continuous measurement technique.

The main goal of the research by the blood perfusion group at Virginia Tech is to develop an inexpensive noninvasive blood perfusion probe that can continuously measure blood perfusion. This probe will also be usable in a surgical situation and could be mobile for use in home health care. Currently, the goal is to create a newer version of the blood perfusion probe that will be completely electronic and allow for continuous measurements.

1.1 Goals & Objectives

The overall goal of this research was to develop a next generation blood perfusion probe (Thermoelectric Perfusion Probe) that can continuously monitor perfusion. Therefore this thesis assesses the feasibility of using a thermoelectric cooler (TEC) to create the thermal event for the Thermoelectric Perfusion Probe as compared to Convective Perfusion Probe which uses cooled air for the thermal event. There were several objectives that must be completed to design this system. First, a new phantom tissue test stand had to be developed to allow for testing of the Thermoelectric Perfusion Probe. This phantom tissue test stand allowed for testing on the probe without pathological uncertainties.

The second objective was to alter the Convective Perfusion Probe's perfusion estimation program to adjust for the fact the thermal event would be established by conductive cooling/heating compared to the previous convective cooling. The third objective was to test the sensitivity and repeatability of the Thermoelectric Perfusion Probe. To do this, the phantom tissue test stand was used for testing. The final objective was to compare and contrast the experimental results from the Thermoelectric Perfusion Probe, the Convective Perfusion Probe, and the Fluent® model. For this comparison, the phantom tissue test stand was used.

Several tasks were performed in order to achieve the objectives presented above. These tasks are outlined below.

1. A newer phantom tissue test stand was designed and built that was more robust and repeatable. This tissue phantom was designed using the 3d modeling program Unigraphics®.
2. The perfusion estimation program was altered to model the Thermoelectric Perfusion Probe instead of the Convective Perfusion Probe.
3. The Thermoelectric Perfusion Probe's perfusion estimation program was altered to use the finite difference information from previous cycles for current cycles (temperature recycling).
4. A routine was developed for running and testing the Thermoelectric Perfusion Probe.
5. A pressed sensor was developed to validate the new Thermoelectric Perfusion Probe's perfusion estimation program with the Convective Perfusion Probe's perfusion estimation program.

1.2 Thesis Organization

This thesis presents the research performed to develop the Thermoelectric Perfusion Probe. First, a literature review of blood perfusion monitoring systems is presented. Also, the significance of this work is explained. Then in Chapter 3, the physical design of the Thermoelectric Perfusion Probe is presented. In Chapter 4, the Thermoelectric Perfusion Probe's perfusion estimation program is explained in detail. Then, the phantom tissue design is presented in Chapter 5. Also presented in Chapter 5 is the Fluent® computational model of the phantom tissue test stand. Chapter 6 presents the results of the experiments performed on the phantom tissue test stand with the Convective Perfusion Probe. Chapter 7 presents the results of testing with the Thermoelectric Perfusion Probe including a comparison of the predicted perfusion values based on the Thermoelectric Perfusion Probe and the predicted perfusion values based on the Fluent® computational model. Chapter 8 presents the conclusions based on the

experimental results. Finally, Chapter 9 presents the recommendations for future research.

Chapter 2 Literature Review

Because of the importance of blood perfusion, several methods, both invasive and noninvasive exist for measuring perfusion. In this chapter, these perfusion measuring methods are reviewed. First, noninvasive imaging techniques to measure perfusion are reviewed. Then, laser Doppler systems that measure perfusion are explained. Finally, thermal measuring systems that measure perfusion are explained. Currently, there is no perfusion measuring system that can continuously measure absolute perfusion.

2.1 Imaging Techniques

Noninvasive imaging techniques, including: Photon Emission Tomography (PET) (*e.g*. Schelbert, 2000), Magnetic Resonance Imaging (MRI) (Montet *et al.*, 2003) and Micro-Computer Tomography (MicroCT) (Prinzen and Bassingthwaighte, 2000) are used to estimate blood perfusion. These systems have produced reliable perfusion estimates in deep tissues; however, they cannot be used in a surgical situation or for long term monitoring. Imaging machines tend to be very large, costly, and require substantial processing time and therefore cannot be used for continuous monitoring.

Magnetic Resonance Imaging (MRI) in conjunction with the arterial spin labeling technique is considered the standard scanning technique for measuring perfusion (Montet *et al*., 2003; Vallee *et al*., 2000; Richardson *et al*., 2001). The technique of arterial spin labeling does not require a contrast agent. In this technique, RF pulses saturate the water in the blood before it enters the area of interest. The spin of the water in the blood is "labeled" and different than the spin of unaffected water. Then, this blood flow exchanges water and nutrients with the tissue of interest and alters this tissue's magnetism. Then, from this change in magnetism the perfusion in the tissue can be calculated for the tissue (Richardson et. al., 2001). This method is usually used to determine perfusion in the brain.

Positron Emission Tomography (PET) can be used to monitor the body's metabolic activity and perfusion. A radioactive tracer, usually N-ammonia or O labeled

water, is placed on a glucose molecule and injected into the blood stream (Schelbert, 2000). The blood distributes the sugar throughout the body, then perfusion is determined by a two step process. First, time activity curves of the location of the tracier are extracted from a dynamic scan (Nuutilia and Kalliokoski, 2000). Then, perfusion is determined based on an arterial input function (Boellaard *et al*., 2005). One problem with PET is that it requires the tracer injection.

PET has the highest resolution of the scanning techniques for determining perfusion. However, it requires expensive equipment and therefore each scan is costly. SPECT is another scanning technique that is similar to PET but utilizes relatively less expensive equipment. SPECT has higher resolution than MRI but not as high as the PET (Kinuya *et al.* 2004*,* Gregory and Thirion, 2005*)*. In SPECT a tracer is used, which has a longer decay time than tracers that are used for PET. These tracers also only emit one gamma ray (PET releases two). This scanning technique has been shown to be problematic when patient movement occurs (Slomka *et al,* 2004).

Micro-Computer Tomography (MicroCT) is a scanning technique that works based on microspheres and CT scanning. In this technique, introduced by Heymann *et al. (*1977*)* microspheres coated in silver are injected into the body. Then, time is given to allow the microspheres to circulate throughout the body. Next, a CT scan (X-ray) takes several 2-D images from different locations (Prinzen and Bassingthwaighte 2000). Then a computer is used to construct a 3-D image based on these 2-D scans. Perfusion can then be determined from the location of the microspheres (Marxen *et al.* 2006)

Overall, these systems tend to be very large, costly, and require some processing time. Therefore, they cannot be used for continuous monitoring. These scanning techniques are very good at measuring noninvasive perfusion in deep tissue. However these systems are limited to use on deep tissue, that is deeper than 1.27 cm (0.5 in). This is because these scanning techniques do not have the spatial resolution needed to obtain perfusion at the skin level. The skin is thinner than the minimum resolution of the scanning techniques. (Dias *et al.*, 2003).

2.2 Laser Doppler Systems

Laser Doppler Flowmetry (LDF) is considered to be the standard technique for instantaneously monitoring the perfusion (Vajkoczky *et al.*, 2000) of the skin. This method works because light is capable of measuring the relatively low speeds at which red blood cells travels through capillaries. LDF has recently been used for monitoring dialysis (Niwayama and Sanaka, 2005), to assess the extent of burn wounds (Mileski, 2003), and to determine whether transplant rejection will occur (Oltean *et al.*, 2005).

Laser Doppler systems are based on the Doppler Effect and the reflecting of light by the red blood cells. A monochromatic light beam is focused on the skin. Then, light is reflected by the red blood cells back to a receiver. The velocity of the red blood cell is determined by the frequency shift (Doppler Effect) caused during the reflection. Also, the number of red blood cells can be determined by the amount of light reflected. Perfusion is then deduced based on these two factors.

A similar method, Laser Doppler Imaging (LDI) is a scanning technique based on Laser Doppler Flowmetry. LDI follows the same basic principles of LDF, except that it eliminates the need of a probe to be affixed to the skin (Svedman *et al*., 1998). The image of the tissue is achieved by sequentially moving the laser beam step by step over the tissue. LDI can image a maximum area of 144 cm^2 in five minutes (Svedman *et al*., 1998). LDI can be advantageous over LDF because the LDI averages the perfusion over a region and gives more reasonable blood perfusion values (Murray *et al.*, 2005). Also, LDI allows for a two dimensional array of perfusion measurements which are represented in a color coded map (Khan and Newton, 2003).

Another system that is similar to laser Doppler imaging is Laser Speckle Contrast Analysis (LASCA). This system originally was developed by Brier and Fercher in 1982. This system is currently being used and developed by Stewart *et al*. (2005), Cheng *et al*. (2004), and Forrestor *et al*. (2004). The main advantage of LASCA is that it can scan at a much faster rate than Laser Doppler Imaging. A CCD camera is used to sense a speckle pattern of the red blood cells over time. Blood perfusion is determined from the resulting images (Cheng *et al.*, 2004).

There are three main problems associated with the laser Doppler perfusion measuring techniques. First, these systems do not allow for absolute perfusion estimates. The perfusion estimates are a function of the number of red blood cells and the velocity of the red blood cells. Red blood cells make a small percentage of the blood, and that percentage varies from person to person. The percentage also varies in a person at different times. Because the percentage varies from person to person the exact amount of blood flowing through the tissue cannot be determined based on the velocity of the red blood cells and the number of red blood cells. Also, there is no Standard Unit for these devices. Therefore, the results can be confusing and have to be interpreted by the physician. There is no way to compare perfusion estimates for different people because everyone will have a different number of red blood cells. Secondly, these systems are sensitive to both placement and movement. If the laser Doppler systems are not properly aligned with the skin, then the systems do not give reasonable perfusion estimates. Any movement of the patient can drastically affect the perfusion measurements. Third, these systems tend to be dependent on a number of factors other than perfusion including: the optical properties of the tissue, the blood, and the optical fibers (Leahy, 1999).

Although there is currently no standard calibration system, laser Doppler systems tend to be calibrated using latex microspheres in Brownian motion in water (Liebert, 1995). Other calibration techniques use polythene tubes with a microsphere suspension (Leahy, 1999). There are three problems with these calibration schemes. First, these systems do not model the non-directional effects of perfusion. Secondly, the microspheres used are much smaller than red blood cells. Finally, the red blood cells do not have a spherical shape as with the microspheres, but are a flexible disk. It is possible the differences between the shape of the microsphere and the red blood cell affect the scattering of the light (Liebert, 1995).

It is not practical to use a laser Doppler system to continuously monitor perfusion for two main reasons. First, this probe is very sensitive to movement. Therefore, it is impractical to put this on a recovering patient who will move during recovery. The second problem with using a laser Doppler system for continuously monitoring is that the system is based on very sensitive fiber optics. Therefore, the measuring device is very fragile and is potentially not durable enough to withstand continuous use on a patient.

2.3 Thermal Systems

A few techniques exist that use the thermal properties of tissue and blood to estimate perfusion. These systems work based on the clearance of thermal energy in the tissue. The most common technique for invasively measuring blood perfusion uses a Thermal Diffusion Probe (TDP). The Convective Perfusion Probe is another method that uses thermal properties of tissue and blood to determine perfusion. These systems allow for absolute measurements of perfusion. All these systems work based on the relationship developed by Pennes.

The Pennes bioheat equation (1948), shown below, can be used to determine perfusion.

$$(\rho C_p)_t \frac{\partial T_t}{\partial t} = k_t \nabla^2 T_t + (\rho C_p \omega)_b (T_a - T_v) + Q_m \qquad 1$$

In Equation 1, T is temperature, t is time, ρ is density, C_p is specific heat, k is thermal conductivity, and ω is blood perfusion. The subscripts t, b, v and a, correspond to tissue, blood, venous, and arterial respectively. Q_m is the heat generation due to metabolic activity. The relationship between temperature and heat transfer in the Pennes equation offers potential for using temperature measurements to estimate perfusion. However, there are a few key assumptions that must be made to determine the perfusion. The tissue is assumed to be homogenous and supplied with arterial blood at the body's core temperature. The blood flow is assumed to be uniform, and the thermal properties of the tissue and the blood are also assumed to be constant.

The Thermal Diffusion Probe (TDP) (Valvano *et al*., 1984; Arkin *et al*., 1986a, b; Bowman, 1985; Vajkoczy *et al*., 2000, Khot *et al*., 2005; *Maitz et al.*, 2005) is the standard thermal perfusion measurement system. In this technique, a thermistor bead is situated at the end of a hypodermic needle which is inserted into the tissue. The thermistor is used to both deposit thermal energy into the tissue and measure the temperature response of the tissue. The power deposition is controlled as a specified function. Several different approaches for specifying this function have been introduced. These include temperature pulse-decay (Arkin *et al*., 1986a; Kress and Roemer, 1987; Yang & Liu, 2004), temperature step function (Kress and Roemer, 1987), constant-power heat-up (Kress and

Roemer, 1987), two-phase, cyclical heating (Arnaud *et al*., 1994), and sinusoidal heating (Liu e*t al*., 1999). Khot *et al.* (2005) and Maitz *et al.*, (2005) used two thermistors: one on the peripheral tissue and one in the tissue region of interest, to determine perfusion. The first thermistor provides information about the baseline temperature and the second thermistor monitors the deep tissue temperature.

The amount of energy dissipated is monitored and controlled to give a constant temperature gradient between the bead and the tissue. The power that is required to maintain this temperature is dependent on the thermal properties of the surrounding tissue, and thus, is a function of perfusion. Perfusion is then determined based on this power dissipation. There is one main limitation with the TDP. The TDP is invasive which limits its abilities as a medical tool. However, the TDP does provide absolute perfusion measurements which make it more reasonable than laser Doppler methods.

Several attempts have been made to develop a noninvasive perfusion probe that works on the same principle as the TDP. These noninvasive techniques usually involve placing a heater on the skin and then measuring the temperature response of the skin, (Patel *et al*., 1987, Li *et al.* 2002, Anderson and Burnside, 1990). These types of probes are limited due to two main problems. First these probes generally have large heat losses to the surroundings. Secondly, these probes tend to measure temperature changes as opposed to heat flux. The temperature changes of the skin are relatively small and therefore difficult to monitor. A promising noninvasive technique that has been developed at Virginia Tech is the Convective Perfusion Probe.

The Convective Perfusion Probe works by inducing a thermal event on tissue and then measuring the heat flux response of the tissue. The thermal response of the tissue depends on the perfusion through the tissue. Therefore, the heat flux response of the tissue to a thermal event is a function of the local blood perfusion, (Cardinali *et. al*, 2002). The Convective Perfusion Probe cools the tissue via convection. The measured heat flux is generated by the temperature gradient between the convectively cooled sensor and the bottom surface of the sensor which is warmed by the underlying tissue. Thus, an absolute perfusion value can be estimated from the heat flux response of the tissue.

The Convective Perfusion Probe is a second generation design with a smaller housing and heat flux sensor then the first generation design, (Cardinal *et. al*, 2002). The Convective Perfusion Probe is shown in Figure 2.1 and has an overall size of 1.27 cm x 1.27 cm x 1.02 cm (0.5 in x 0.5 in x 0.4 in). The Convective Perfusion Probe is comprised of four components: the heat flux sensor, the spacer block, the air inlet piece, and the cap piece. A Vatell® heat flux sensor is attached to the housing with glue. The spacer block has been designed to be a U shape to allow the convective air to cool the heat flux sensor and then to exhaust to the atmosphere. The air inlet piece has a small inlet for cool air to enter, and then has an array of nine small holes. The cap piece is used to make sure everything is air tight and to direct the air flow. The housing for the Convective Perfusion Probe has been designed out of plastic to eliminate heat losses to the surroundings. The heat flux sensor is attached directly to the tissue using double-sided tape. The thermal event is created by convectively cooling the top surface of the sensor. Cooled air is forced through using an array of nine impinging jets. The air cools the heat flux sensor which produces a measurable heat flux response from the tissue. The shape of the resulting heat flux curve is dependent upon the effects of the blood perfusion in the tissue.

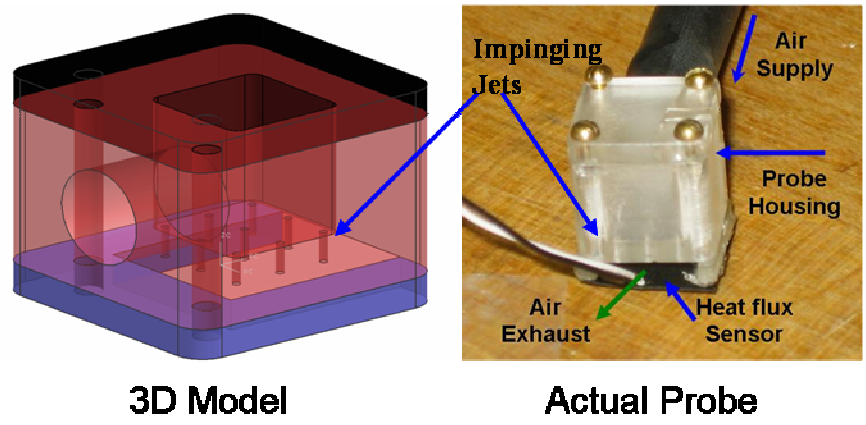

Figure 2.1. The Thermal Convective Probe: a 3D model of the housing (Left), and the actual probe (Right)

The Convective Perfusion Probe has two main advantages for measuring perfusion over other noninvasive thermal methods. First, the Convective Perfusion Probe is designed out of plastic to minimize heat losses to the surroundings. Secondly, the

Convective Perfusion Probe uses heat flux as the driving parameter as apposed to temperature. There is more sensitivity with heat flux changes than with temperature changes. However, one key disadvantage that still exists is that the Convective Perfusion Probe cannot be used for continuous measurements. This is because perfusion is altered when the overall temperature of the tissue is changed, (Janssen *et. al*, 2005). Therefore, if the Convective Perfusion Probe was used for a long period it would cool the tissue. Then, the perfusion would be altered because of this effect and the perfusion estimation would not be representative of the normal tissue perfusion.

2.4 Validation of blood perfusion measuring systems

One of the biggest challenges for all blood perfusion measuring systems is how to validate and calibrate them. Microspheres are used as the standard to validate blood perfusion measuring systems. Most scanning and laser systems have been validated using microspheres. Generally, with the microspheres' technique, colored or radioactive microspheres are injected into the blood of the test subject. Then, the perfusion experiment is completed and the animal is euthanized. The tissue of interest is weighed and then, the number of microspheres it contains is determined. The number of microspheres in the tissue corresponds to the perfusion.

Microspheres can also be used to determine perfusion in humans without harm to the patients. Microspheres are injected into the blood stream and become embedded in the tissue microcirculation. Then a small amount of tissue of interest is harvested and the distribution of the blood flow is determined based on the amount of emitted radiation. Then, the absolute perfusion is determined based on the amount of emitted radiation and the amount of blood withdrawn from an artery down stream, (Heymann *et. al*, 1977).

Experiments proved there is a strong correlation between renal microspheres perfusion estimates and PET estimated perfusion, (Juillard *et. al,* 2000). Also, in 2006 Monnet showed a correlation between the LDF measurements and a microsphere technique on dog stomach walls. Finally, Martin & Bowman (2000) were able to validate the TDP based on the microspheres technique. The microspheres technique is especially good at validating perfusion measuring devices.

A common problem with most blood perfusion measurement systems is developing a reliable way to calibrate them without the presence of physiological variations. These systems can be validated, but calibration is a much more difficult task. Laser Doppler systems have been calibrated, but not in a condition that models perfusion.

Robinson *et. al* (2006) was able to develop a phantom tissue system to test the Convective Perfusion Probe, however this system could not be used for calibration. Therefore, a new system was developed at Virginia Tech that has been used for the calibration and validation of the Convective Perfusion Probe and the Thermoelectric Perfusion Probe. The phantom tissue test stand was created to mimic perfusion and the thermal effects of perfusion while eliminating physiological variations. The system was initially designed using computational fluid dynamics (Fluent®), and then a final design was created that used a porous media in conjunction with a pump and flowmeter to model perfusion in tissue. This system was modeled in Fluent® to validate the experimental results.

2.5 Significance of Work

The literature above demonstrates the need for a device that noninvasively continuously monitors absolute perfusion. Scanning techniques cannot be used for continuous use and can only be used for deep tissue perfusion estimates. Laser Doppler systems do not have the ability to measure absolute perfusion. The Convective Perfusion Probe has been developed into a viable device to measure absolute perfusion. However, this probe cannot be used continuously and lacks mobility. The main objective of the current research was to develop a continuous perfusion monitoring thermal system that would cyclically heat and cool the tissue over a specified time interval. This will allow the overall tissue temperature to be kept constant. This technology will eventually be used to monitor tissue perfusion and could be used for care in several medical situations. The Thermoelectric Perfusion Probe will allow for the early diagnosis of problems, before the tissue has died.

Chapter 3 Thermoelectric Perfusion Probe Design

The Thermoelectric Perfusion Probe is designed to be simple, lightweight and functional. In this chapter the actual design of the Thermoelectric Perfusion Probe is introduced. Then, the data acquisition involved with the probe is introduced. Next, the voltage controller is introduced. Finally, the heat flux sensor with an affixed thermocouple is introduced.

3.1 Physical Design

To allow for continuous measurements, the Thermoelectric Perfusion Probe was developed to utilize a different method of inducing the thermal event. This probe uses a Thermoelectric Cooler (TEC) to create the thermal event. A TEC acts as a miniature heat pump with no moving parts. A Thermoelectric Cooler works based on the Peltier Effect in which a temperature difference is created when current is supplied across two dissimilar materials (Godfrey, 1996). Therefore, by sending the current in one direction; the top side of the TEC will get warmer than room temperature while the bottom will get cooler than room temperature. When the direction of the current is switched, the top side of the TEC becomes cooler than room temperature and the bottom side of the TEC will get warmer than room temperature as seen in Figure 3.1.

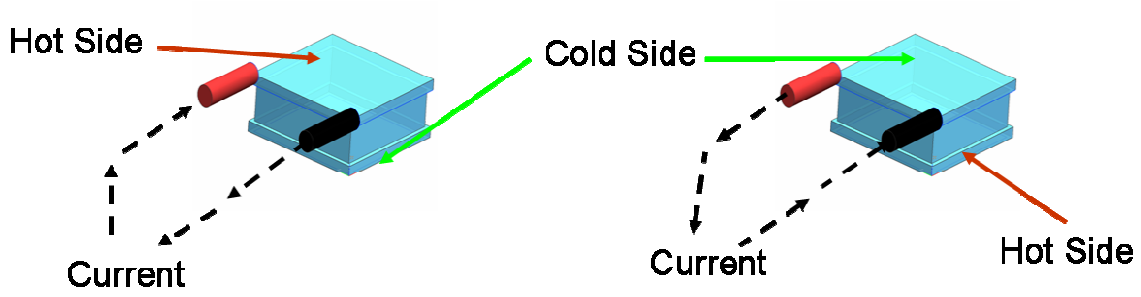

Figure 3.1. A diagram showing how a TEC can be used for sinusoidal heating

The TEC solves both problems associated with the Convective Perfusion Probe. The TEC converts electricity into a thermal event and therefore eliminates the need for an

air supply. Also, the TEC will allow for the thermal event to alternate between heating and cooling. Therefore, the overall tissue temperature will be unaltered over time. When the overall tissue temperature is affected, the perfusion is altered.

The Thermoelectric Perfusion Probe was developed to use a Thermoelectric Cooler to create the thermal event. As can be seen in Figure 3.2, the Thermoelectric Perfusion Probe is constructed from a holding plate, a small TEC, a heat flux sensor, a thermocouple, and a heat sink. Dimensioned drawings for all three parts can be seen in Appendix A. The holding plate is used to hold the probe together and to fix the TEC to the heat sink. Because the TEC in conjunction with room temperature convection is not efficient enough to remove all the required heat, a heat sink is required to disperse excess heat. This will assure that the Thermoelectric Perfusion Probe will not overheat and burn a patient. The heat flux sensor that was fixed to the Thermoelectric Perfusion Probe is the same as the heat flux sensor used on the Convective Perfusion Probe. A thermocouple is used to determine the sensor temperature.

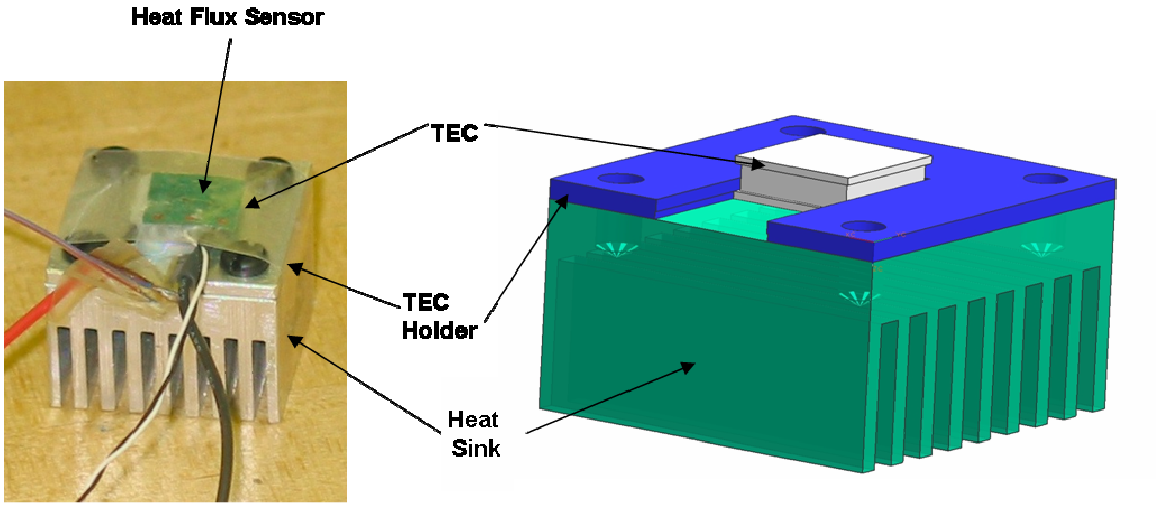

Figure 3.2. The assembled Thermoelectric Perfusion Probe (Left) and the 3D model of the Thermoelectric Perfusion Probe (Right)

3.1.1 The TEC

The TEC used for the Thermoelectric Perfusion Probe was a Melcor CP 1.4-7-10L with overall dimensions of 0.94 cm x 0.94 cm x 0.36 cm (0.37 in x 0.37 in x 0.14 in). This particular TEC is made out of the ceramic material alumina and the solder construction material bismuth tin. This TEC can handle a maximum voltage of 2.06Vand

a maximum current of 2.1Amps. When under maximum voltage, the TEC can produce a temperature difference of 67˚C. While working with the TEC in a circuit, it is the same as working with a high current resistor (Godfrey, 1996).

3.1.2 The Holding Plate

The holding plate has been designed to securely hold the TEC to the heat sink. It is also used to dissipate the heat throughout the heat sink. The holding plate is made out of aluminum. As can be seen from Figure 3.3, the holding plate has a track where the TEC can slide. The bottom of the track has a shelf notch that goes all the way around the sliding track. This shelf notch allows the TEC to be supported from the side and from the top while also insuring good contact between the TEC and heat sink. There are four 10-32 clearance holes that will allow for the hard attachment to the heat sink.

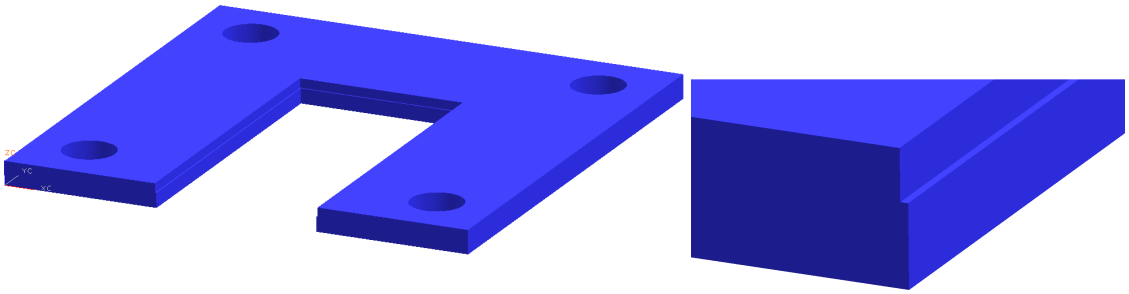

Figure 3.3. A 3d model of the holding plate (Left) and a zoomed in view of the shelf notch (Right).

3.1.3 The Heat Sink

The TEC on the Thermoelectric Perfusion Probe like all other heat pumps will produce heat that must be exhausted to the atmosphere during the heating and cooling cycles. Therefore, the heat sink was designed to remove all excess heat, Figure 3.4 . The heat sink is 2.54 cm x 2.54 cm x 1.02 cm (1 in x 1 in x 0.4 in) in total dimensions and is made of Aluminum. The heat sink has nine fins and has a total surface area of 63.87 cm^2 (9.9 in^2). The heat sink holes were drilled and tapped for 10-32 screws to attach it to the holding plate.

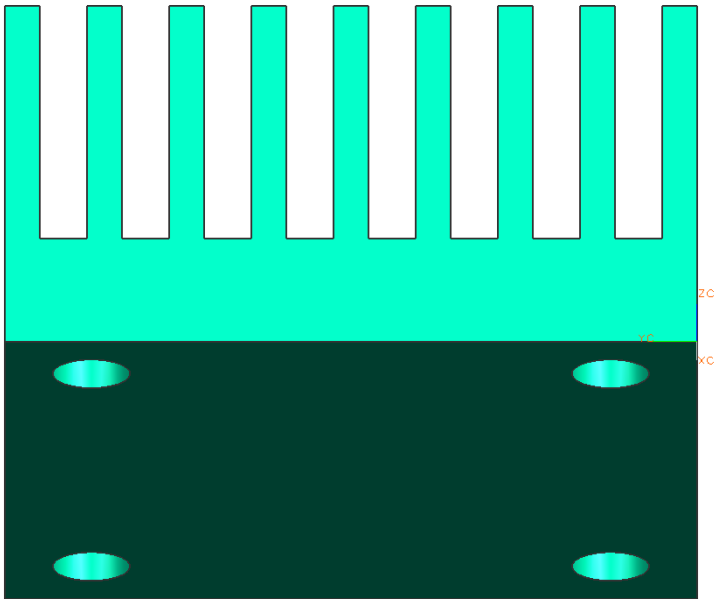

Figure 3.4. The heat sink

3.3 The Voltage Controller

To power the TEC, a special DC voltage controller was developed, Figure 3.5. The voltage controller had four main design criteria. First, the voltage controller had to be able to output a very high current, up to one amp. The TEC can take more current than this; however, this will produce temperatures much higher than is desired. Secondly, the voltage controller had to be able to sustain this high current output for a very long period of time, up to one and a half hours. Third, the voltage controller had to be able to output a variable voltage. The TEC can take voltages up to 2.06V and a controllable voltage is needed so the TEC will be able to heat to the proper temperature. Finally, the voltage controller has to be able to reverse the polarity of the voltage. This is because the requirement for the TEC is to have alternating heating and cooling. The direction of the current must be reversed to obtain the heating effect. A voltage controller had to be built because no other power supply could be found that fit all the criteria.

This voltage controller was built from two AA batteries, two potentiometers, a toggle switch, and a circuit box. The toggle switch allows the user to access either of the batteries. One battery is configured to output a positive voltage; the other battery is configured to output a negative voltage. The voltage controller has the ability to output a

variable voltage from 1.25V to -1.25V, because that is about the voltage that an AA battery can output. The potentiometers adjust the voltage and allows the voltage to be set at any voltage between 0.5V and 1.25V and between -0.5V and -1.25V, to give a total voltage range of 0.5<V<1.25 and -0.5>V>0.5.

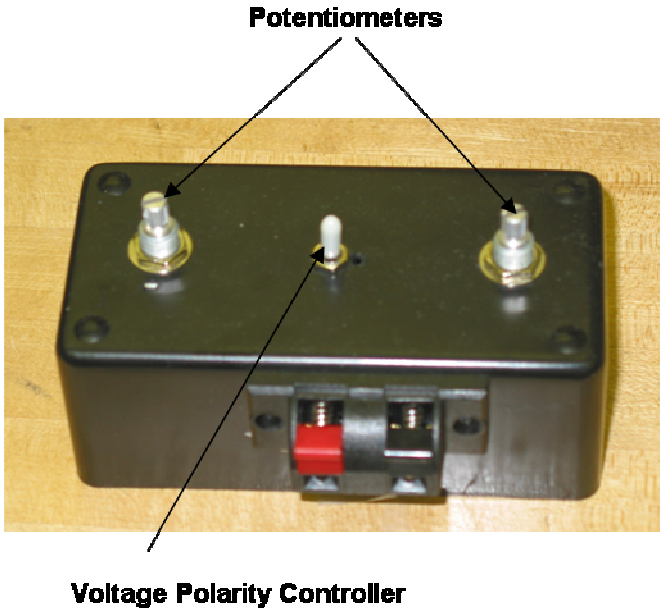

Figure 3.5. The voltage controller.

3.4 A Heat Flux Sensor with an Affixed Thermocouple

As mentioned above there are two temperatures that must be measured in the Thermoelectric Perfusion Probe. The sensor thermocouple will be used to measure the temperature between the heat flux sensor and the skin. Originally, a thin film thermocouple 0.00127 cm (0.0005 in) was sealed in plastic and taped to the bottom of the heat flux sensor as this was used for the majority of the Thermoelectric Perfusion Probe tests. However, this method proved to be problematic because it was hard to insure good contact at all the layers, especially between the heat flux sensor and the thermocouple.

Therefore, a heat flux sensor has been made with a thin film thermocouple laminated to one side of it, Figure 3.6. This laminated sensor is made by placing a layer of heat activated epoxy on the heat flux sensor, followed by a layer of thin plastic, then another layer of epoxy. The thin film thermocouple is placed on top, followed by more epoxy and another layer of plastic. This structure is then hot pressed for an hour at 150˚C

resulting in a sealed sensor with a thin film thermocouple on top of it. The thin film thermocouples for this design were purchased from RDF Corporation. This laminated sensor is advantageous for another reason as well; it will make the heat flux sensor water tight and the sensor can easily be destroyed if it comes into contact with water.

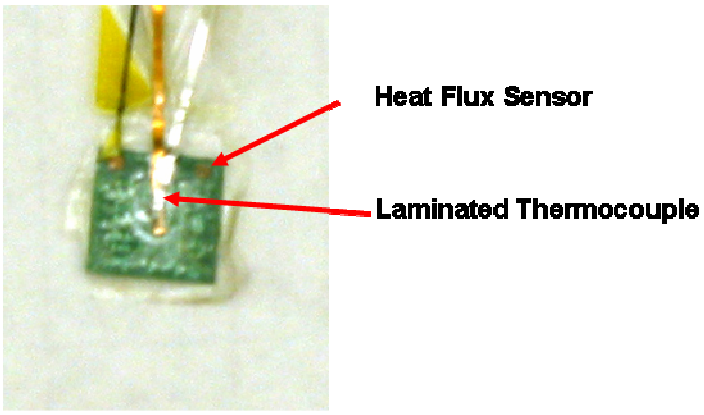

Figure 3.6. A heat flux sensor with a laminated thermocouple. This allows for the sensor temperature to be measured.

Chapter 4 The Thermoelectric Perfusion Probe's Perfusion Estimation Program

In this chapter the perfusion estimation program developed specifically for the Thermoelectric Perfusion Probe is presented. First, the basic principles behind the perfusion estimation program are explained. Then, the programs that were developed to process the recorded experimental data are presented. Finally, the changes that were made to the Convective Perfusion Probe's perfusion estimation program to fit the Thermoelectric Perfusion Probe are presented. All program files are included in Appendix B.

4.1 Basic Principles behind the Perfusion Estimation Program

The Convective Perfusion Probe's perfusion estimation program has been developed to determine the perfusion in the tissue and the contact resistance between the skin and the sensor. A schematic of the process to obtain the perfusion values is shown in Figure 4.1. Basically, the probe records the temperature and heat flux data when the thermal event is imposed. Then, an ADI finite difference model uses a guess for the perfusion estimate and the contact resistance to make a mathematical model of the system. Then, an estimation procedure is used to determine the best guesses for contact resistance and perfusion (Cardinali *et. al*, 2002).

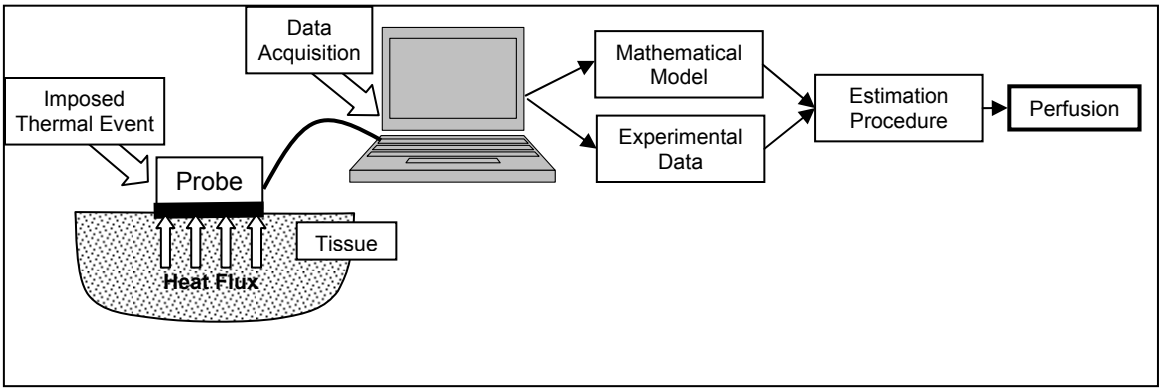

Figure 4.1. A schematic of how perfusion estimates are obtained for the Convective Perfusion Probe

The finite difference model incorporates both the tissue, and the heat flux sensor. The mathematical model is the predicted heat flux curve based on the temperature data

and the current perfusion and contact resistances guesses. Then, a Gaussian elimination scheme is utilized to obtain the best perfusion and contact resistances estimates. Basically, the experimental heat flux and the predicted heat fluxes are compared and new perfusion and contact resistance estimates are made. Then, the finite difference program is rerun to produce a new predicted heat flux curve. This cycle is repeated until the convergence criteria are met or a maximum number of iterations are completed. For a more detailed explanation of the perfusion estimation program please refer to Ashvin Mudaliar's dissertation (2006).

4.2 Data Processing

The data collected for this experiment could not directly be used to determine perfusion. The data were originally recorded in two files: one containing heat flux data and one containing temperature data. The data files had to be altered in two ways to allow reasonable perfusion values to be obtained. First the data had to be combined into one text file that used the same time scale for the heat flux and the temperature measurements. Secondly, the recorded cycle had to be broken up into two different text files. One text file contained the temperature and heat flux data from the cooling portion of the cycle. The other text file contained the temperature and heat flux data from the heating portion of the cycle. Perfusion estimates were then independently obtained for the heating portion of the cycle and the cooling portion of the cycle.

4.2.1 File Combination

When the bulk of the experiments for the TEC were completed, the system was limited because there was only one working amplifier. Therefore, the heat flux data were amplified and recorded by one DAQ while the temperatures were directly measured using another DAQ. This created two problems. First, the heat flux data were collected at 12Hz while the temperature data were recorded at 1Hz. The large discrepancy in sampling frequency was because the DAQ reading the thermocouples was directly reading the temperatures instead of the voltage produced by the thermocouples. The second problem was that the data were recorded in two completely different files and would create problems for data processing.

Therefore, a computer program was developed that would combine the two data files into one file. The program was created so both the heat flux and temperatures are on the same time scale. Also, this program was developed to do this automatically for as many files as were recorded. The program works simply by loading the heat flux and temperature data. Then, the spline function was used interpolate temperature data on the same time scale as the heat flux data. Finally, these data are written to a new text file and the computer code moves on to the next set of files.

4.2.2 Processing Individual Cycles

One problem that remained was how to obtain perfusion estimates from both the heating and cooling portions of the cycle. Originally it was attempted to input the experimental data for the entire cycle and gain a perfusion estimate. However, this proved to provide very poor curve matching, as can be seen from Figure 4.2. As can be seen from the curve, the slope of the predicted heat flux curve for both the cooling and heating portion of the cycle were poorly matched. The parameter estimation produced very low perfusions and a high sum of squares. Therefore, a method had to be developed to deal with the heat flux curve differently.

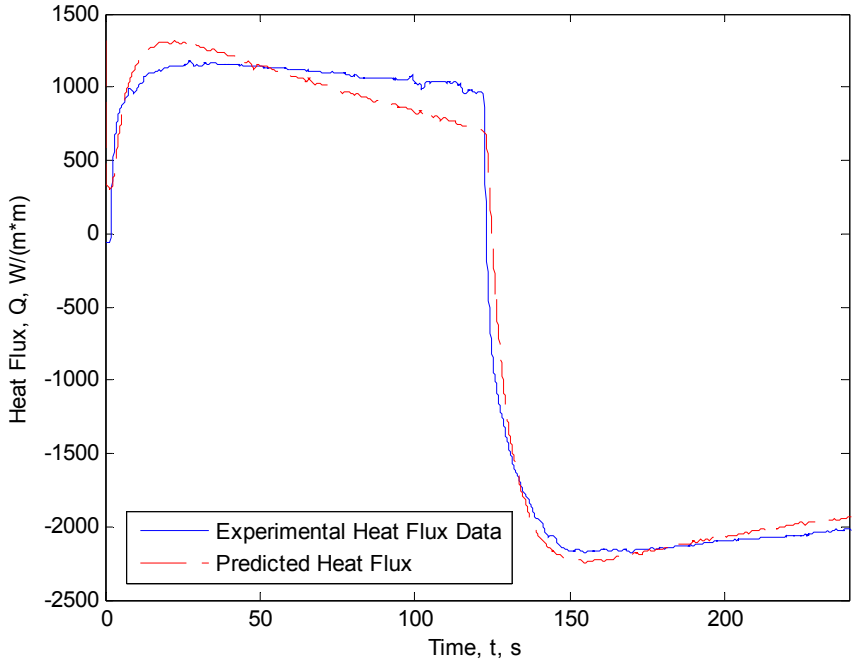

Figure 4.2. The results of parameter estimation when the entire heat flux curve is used

A new method was developed to utilize the data during both the heating and cooling portion of the cycle. It was determined that the best method would be to divide the experimental results and data into two sections: the cooling section and the heating section, Figure 4.3. Then, each section of data was individually placed into the perfusion estimation program. For most experiments, the cooling took place for two minutes and the heating occurred for two minutes.

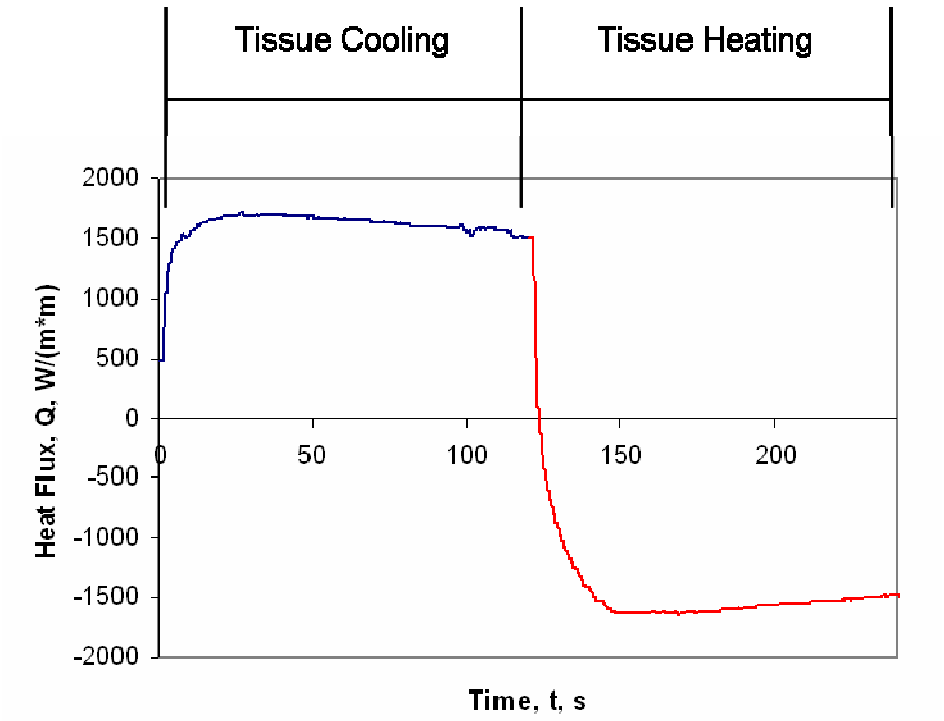

Figure 4.3. A plot of the experimental heat flux curve and how the data is to be broken for the perfusion estimation program.

This change made a significant difference when the experimental heating and cooling data were processed with the finite difference code, Figure 4.4 and Figure 4.5 . As can be seen from the Figures, the curve matching was excellent when the two curves were isolated. For both the cooling portion of the cycle and the heating portion of the cycle the initial conditions and corresponding initial finite difference model were based on the arterial temperature and the top temperatures measured with the Doric thermocouple reader at the beginning of the experiment (discussed later).

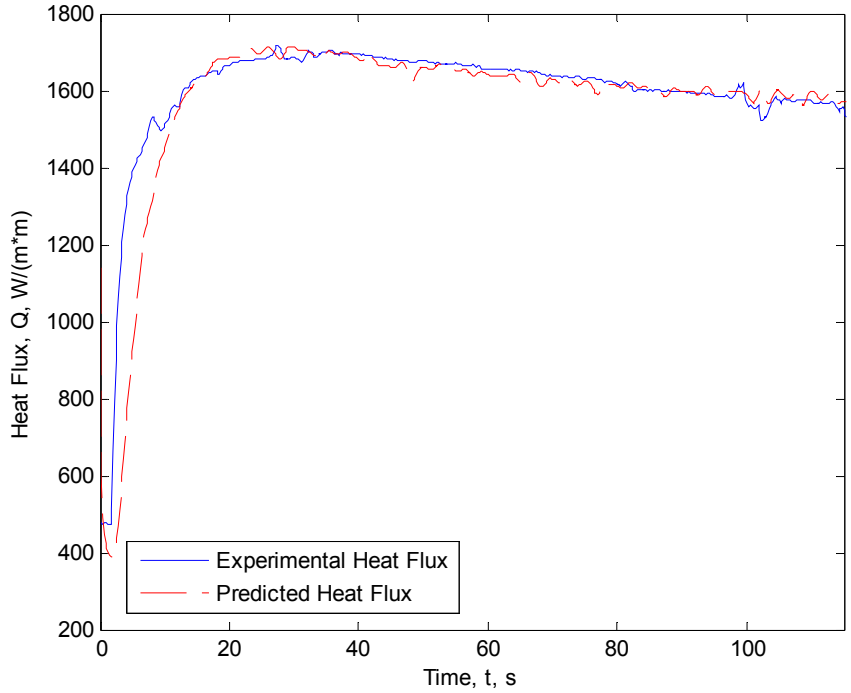

Figure 4.4. The results of parameter estimation when only the cooling portion of the cycle is used.

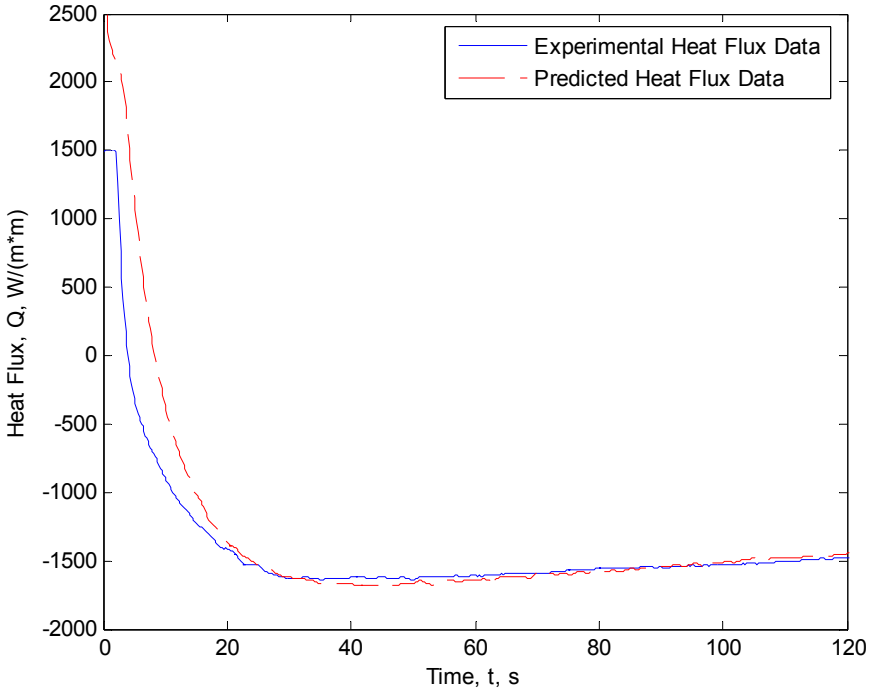

Figure 4.5. The results of parameter estimation when only the heating portion of the cycle is used.

By breaking the cycle into two parts, the perfusion estimation program produced better perfusion estimates, Table 1. The first thing to notice is how the perfusion values were all negative when a full cycle was used for perfusion estimation. This is unrealistic and does not display a trend (a linear trend is expected). Also, using the full cycle resulted in a very high sum of squares. This is indicative of poor curve matching. It is clear from this result that it is much better to break the cycles in half before running the perfusion estimation.

Table 1. The results of perfusion estimation when the cycle is broken up compared to a full cycle.

Flow Rate (cc/min)	Perfusion (mL/mL/s)			Sum of Squares $\left(\left(\frac{W}{m^2}\right)^2\right)$		
	Full Cycle	Cooling	Heating	Full Cycle	Heating	Cooling
0	-0.009	0.011	-0.002	23.081	5.868	4.009
0	-0.008	0.008	-0.003	21.378	5.358	4.146
0	-0.008	0.011	-0.002	28.346	1.955	7.269
5	-0.007	0.017	0.003	34.428	16.172	4.853
5	-0.006	0.024	0.009	41.499	6.012	2.451
5	-0.005	0.021	0.006	36.824	2.708	2.544
10	-0.007	0.020	0.007	38.505	3.356	5.108
10	-0.006	0.029	0.018	52.065	6.934	2.054
10	-0.007	0.028	0.020	52.244	3.978	1.914
20	-0.009	0.029	0.034	64.846	8.067	2.414
20	-0.007	0.038	0.021	64.664	7.469	6.461
20	-0.009	0.039	0.035	64.928	6.649	2.039
30	-0.008	0.054	0.046	78.252	15.656	0.691

The next step was to develop a computer program that would break all the experimental data into the individual components. In total, there were several experiments that were only one cycle and then a few experiments that were many cycles. Therefore, two different computer codes were developed: one to deal with the files with one cycle, and the second to deal with the files with many cycles.

The first program was a combination program that combined the two data files into one and broke the cycles into the heating portion of the cycle and the cooling portion of the cycle. It was developed where a person inputs a text file that contains the list of files to read. Then, the first file is read and the two text files are outputted. The first file contains the information from the cooling portion of the cycle while the second file contains the information from the heating portion of the cycle and has an extra '1' at the

end of the filename. These files are then written to a specified folder and the next experimental file is read.

The second computer program was developed to process files where the experiment had multiple cycles. Therefore, with this program the user inputs the number of total cycles and the length of the cycles. Then, the computer code automatically makes a new text file for each of the heating and cooling sections of the cycles.

4.3 Alterations made to the Convective Perfusion Probe's Perfusion Estimation Program

Overall, there were two key changes that had to be made to the Convective Perfusion Probe's perfusion estimation code to use it to determine perfusion for the Thermoelectric Perfusion Probe. First, the finite difference model had to be altered to match the Thermoelectric Perfusion Probe, Figure 4.6. As can be seen from the Figure there are two big differences. First the sensor temperature (the temperature between the heat flux sensor and the skin) is known with the Thermoelectric Perfusion Probe where it is not known in the case of the Convective Perfusion Probe. Secondly, the Convective Perfusion Probe has a convective boundary condition with the temperature of the convective air being known, while the Thermoelectric Perfusion Probe has a conductive boundary with the temperature at this boundary being unknown. Therefore, the newly altered finite difference code accounts for these differences. The second change that was made to the perfusion estimation code was to use the temperature profile from a previous half cycle on the current cycle. This is needed because using an initial temperature profile based on temperatures recorded at the beginning of the test does not make for a good model when the perfusion estimation is predicting the perfusion long into the test.

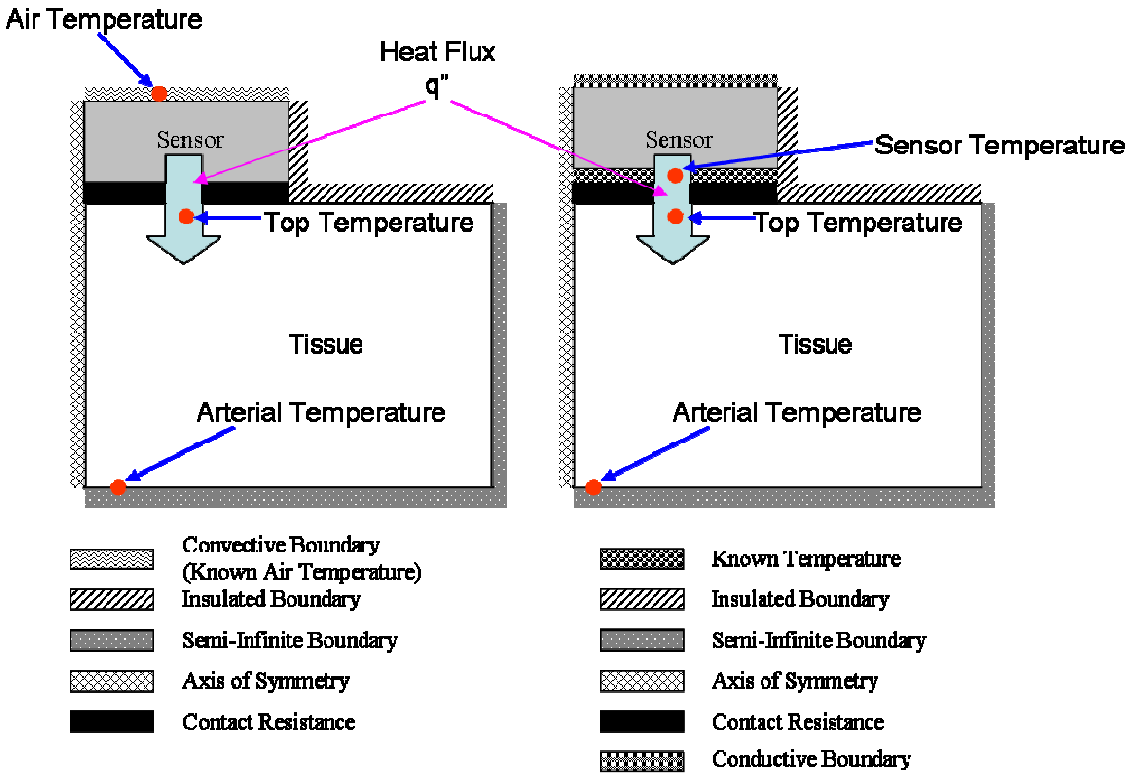

Figure 4.6. A plot of the thermal conditions with the Convective Perfusion Probe (Left) and the Thermoelectric Perfusion Probe (Right).

4.3.1 The Finite Difference Code Changes

As discussed above, the finite difference program had to be altered to match the conditions that exist within the Thermoelectric Perfusion Probe. The initial skin temperature, the temperature measured with a thermocouple in conjunction with the Doric reader placed beside the probe, must be measured along with the convective air temperature for the parameter estimation program of the Convective Perfusion Probe. The skin temperature must be measured in order to set the initial temperature profile. However, until recently it was impossible to continuously and accurately measure the temperature at the skin-heat flux sensor interface (the sensor temperature). With the pressed thermocouple sensor, we can now accurately measure the sensor temperature. Because the temperature between the heat flux sensor and the TEC was not measured, the sensor temperature had to be used in the new perfusion estimation program as the driving temperature for parameter estimation. It would also be preferable to use this measured sensor temperature as the driving temperature for the parameter estimation associated

with the Convective Perfusion Probe. To do this the Convective Perfusion Probe would be fitted with a pressed heat flux sensor. This is because problems in the past have existed when using the air temperature as the driving temperature

The current finite difference model includes the tissue, skin, heat flux sensor, and the convective boundary from the air above it, Figure 4.6. As mentioned above, with the new technology, there is an opportunity to greatly simplify the perfusion estimation code. The current perfusion estimation code has been validated and been tested for stability. Therefore, it is preferable to make minor alterations to the perfusion estimation code and then revalidate.

The Convective Perfusion Probe's perfusion estimation code was altered so that the temperature on the top side of the heat flux sensor is assumed to be the measured sensor temperature, Figure 4.7. This new model is the same thing as setting the boundary condition on the top side of the sensor to a constant temperature, or saying the boundary node experiences infinite convection and is at the same temperature as the convective air. The boundary condition for the current Convective Perfusion Probe code comes into the finite difference code based on Equation 2:

$$C = \left(\frac{1}{h} + \frac{dz}{2 * k_s} \right) \qquad 2$$

where C is a constant that is put into the equations for solving, h is the convective coefficient, dz is the distance between nodes, and k_s is the conductive coefficient in the sensor. Therefore, to adjust the code to the Thermoelectric Perfusion Probe h is infinite and the new equation becomes,

$$C = \left(\frac{dz}{2 * k_s} \right) \qquad 3$$

This equation was then plugged into the finite difference code, making the Thermoelectric Perfusion Probe's perfusion estimation program.

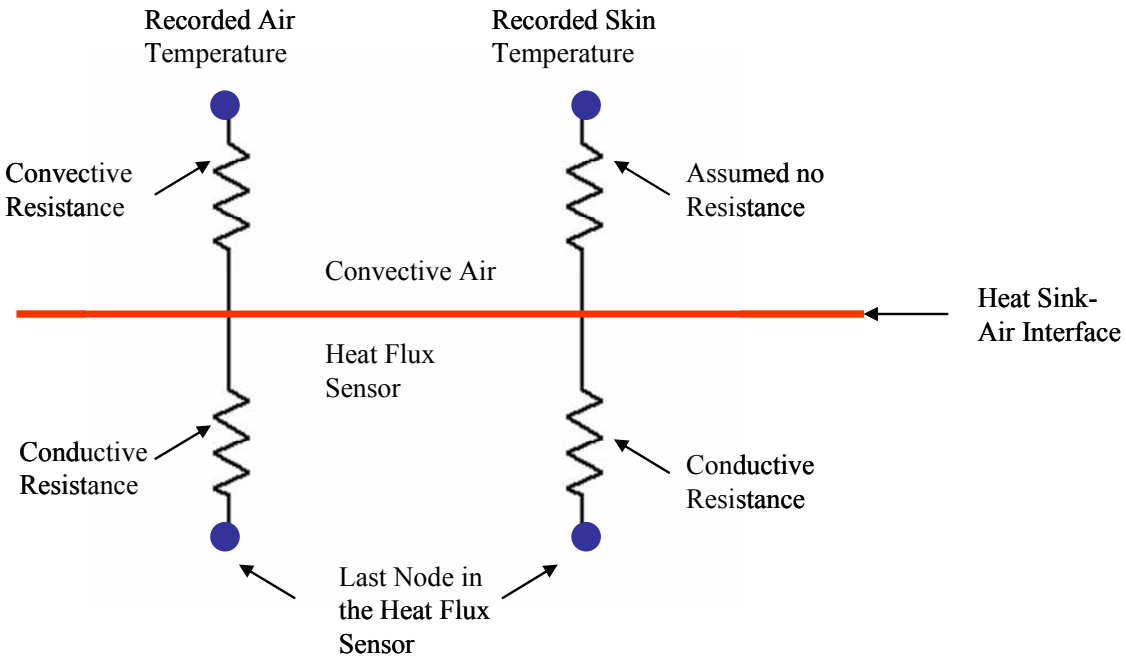

Figure 4.7. The current finite difference model using convection at the top boundary (Left) and the new finite difference model using the sensor temperature (Right).

Overall, a key assumption was made to use the measured sensor temperature as the driving temperature. It is assumed that the contact resistance estimation scheme will be flexible and account for the fact that the location of the recorded temperature differs from the location where the temperature is in the finite difference model. This is a valid assumption because the thermal impedance of the heat flux sensor is very small, and therefore there will be a very small difference in temperature. This assumption will later be tested.

4.3.2 Program Alterations to allow for Temperature Recycling

One problem still existed with running the heating and cooling portions of the cycle through the Thermoelectric Perfusion Probe's perfusion estimation program. The breaking of the cycle does not utilize information from the previous cycle to make a better finite difference model. The initial temperature profile was based on the temperatures measured at the beginning of the experiment. This is a very poor initial temperature profile for cycles that are several minutes from the start of the test. The results are less accurate, require longer computational time, and do not lead to continuous monitoring software, as can be seen in Figure 4.8. The predicted heat flux is almost

infinite at the first time step, and there is a poor match until about 20 seconds. The problem is the uniform initial temperature profile is much different than the actual temperature profile that exists after cooling or heating the tissue. This results in an infinite heat flux and bad curve matching for the first 20 seconds. The next step was to alter the Thermoelectric Perfusion Probe's perfusion estimation program so it can reuse the temperature profile from the previous portion of the cycle on to the next portion of the cycle

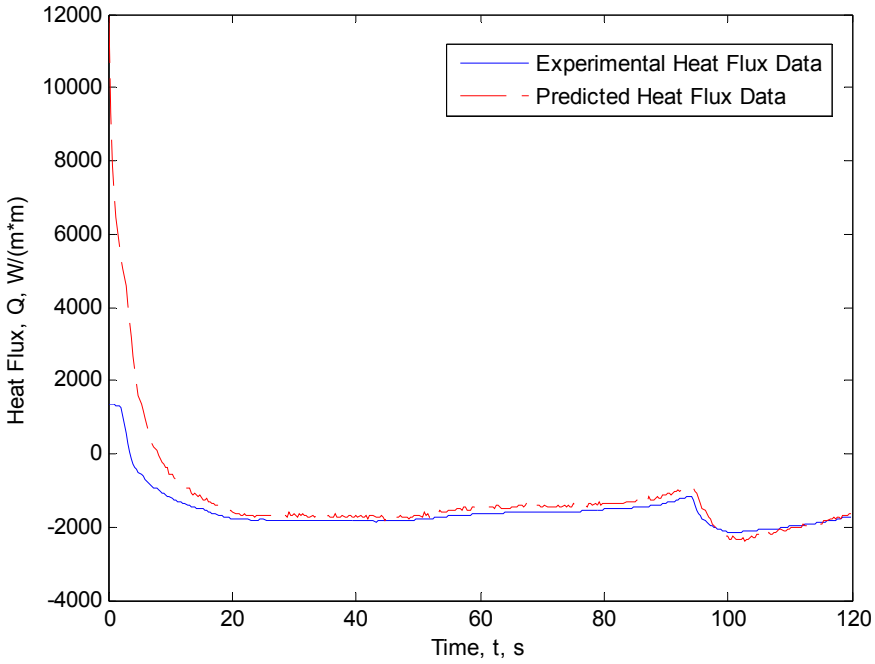

Figure 4.8. The results of parameter estimation when a uniform temperature is used for the heating portion of a cycle

The Thermoelectric Perfusion Probe's perfusion estimation program was altered to have this temperature recycling. The Thermoelectric Perfusion Probe's perfusion estimation program is currently automated to input a file, gain the perfusion estimate and then move to the next file. Therefore, the program will input the data from the cooling section of an experiment, gain the perfusion estimate, and then input the data for the heating section of an experiment. The program marches through the entire time the experiments were run. The finite difference model works by having a 2D array store the finite difference temperature profile and as time moves on this 2D array is updated. The finite difference code, in the perfusion estimation program, was altered to send this 2D

array from the final time step to the parameter estimation program. The parameter estimation program determines the final contact resistance and perfusion. Then, the parameter estimation program was altered to pass the final perfusion, contact resistance, and temperature profile to the driver program. Then, the driver program starts the perfusion estimation on the new temperature file and sends this array of temperatures that was from the last time step of the previous portion of the cycle to the parameter estimation code. Finally, this temperature profile is passed to the finite difference code and the initial temperature profile is set to be the same as the last temperature profile for the previous perfusion estimation. Figure 4.9 gives a schematic of how the array is passed in the program.

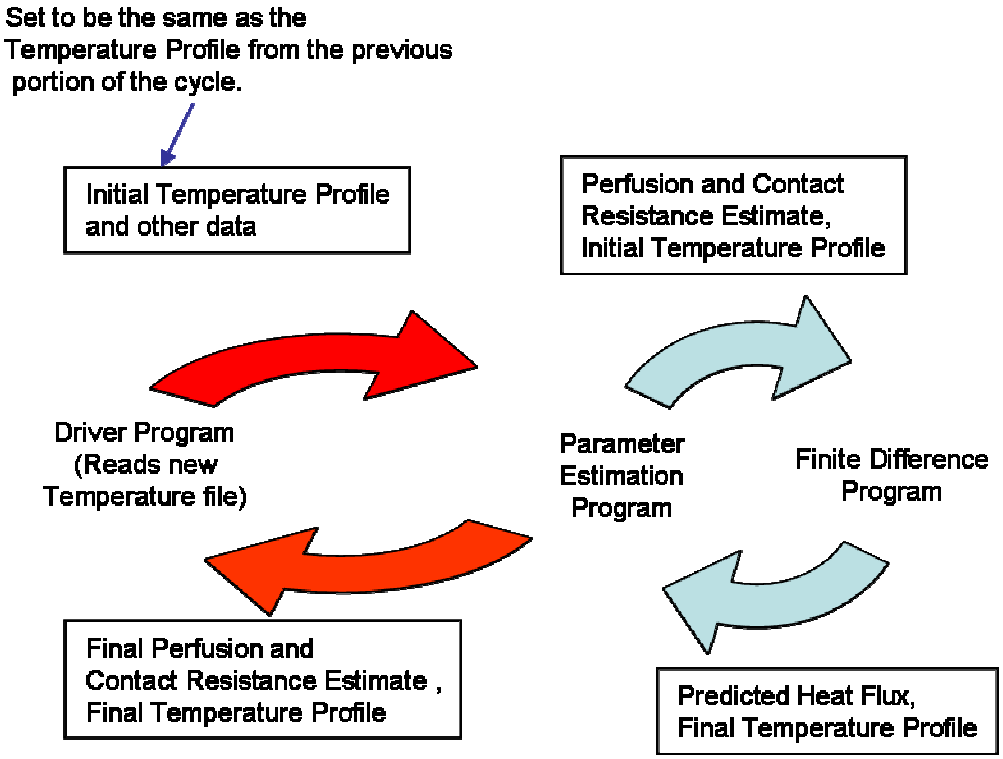

Figure 4.9. A schematic of how the variables are passed through the perfusion estimation program

This addition made an enormous difference when it came to the curve matching, Figure 4.10. As can be seen from the Figure the curve matching is much better at the beginning of the time. The predicted heat flux does not go infinite. Also, the time where good curve matching occurs is at four seconds compared to the previous 20 second curve cycle. As can be seen in Table 2 overall the sum of squares and the perfusion estimates

were better when temperature recycling was used. The sum of squares is indicative of how well the predicted curve matched the experimental data. The smaller the sum of squares the better the match. The average sum of squares, for both cooling and heating, decreased drastically when using temperature recycling.

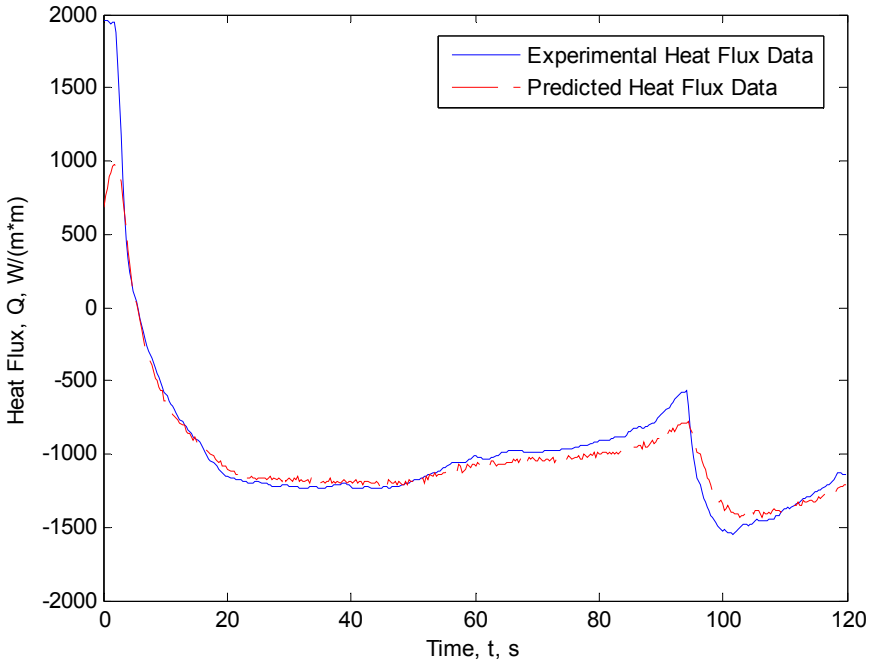

Figure 4.10. The results of parameter estimation when the previous temperature profile is used for the beginning temperature profile of the finite difference model.

Table 2. A summary of results using Temperature Recycling

Flow Rate (cc/min	Perfusion				Sum of Squares			
	Original Processing		Temperature Recycling		Original Processing		Temperature Recycling	
	Cooling	Heating	Cooling	Heating	Cooling	Heating	Cooling	Heating
0	0.0001	0.0046	0.0037	0.0104	2.7917	38.9611	2.7917	8.3926
5	0.0014	N/A	0.0094	N/A	10.8472	N/A	1.1476	N/A
10	0.0071	0.0219	0.0172	0.0252	1.5248	2.7044	1.7151	0.3535
20	0.0164	0.0394	0.0302	0.0533	9.1104	2.0015	2.2549	0.2133
30	0.0308	0.0557	0.0359	0.0782	3.8334	1.9638	5.6150	0.6690
20	0.0214	0.0370	0.0365	0.0498	1.5405	2.1089	0.7078	0.1352
10	0.0066	0.0234	0.0219	0.0223	2.7058	18.0905	0.5754	2.0006
5	-0.0012	0.0099	0.0116	0.0087	5.1208	3.4661	0.2559	0.1325
0	-0.0046	0.0070	0.0052	0.0030	10.9976	3.6755	0.5992	0.1361
5	-0.0057	0.0123	0.0075	0.0033	13.5311	15.9346	0.4628	10.0808
10	0.0010	0.0216	0.0185	0.0269	12.0216	4.2438	1.5130	0.2391
20	0.0109	0.0414	0.0385	0.0422	5.9813	3.7155	0.9597	0.9472
30	0.0333	0.0497	0.0464	0.0585	5.6481	6.7602	1.4419	0.3531
20	0.0213	0.0420	0.0350	0.0504	4.3294	2.0773	1.0632	0.2163
10	0.0083	0.0235	0.0241	0.0282	2.7521	3.0713	0.5865	0.3042
5	0.0000	0.0236	0.0086	-0.0033	10.9162	62.7426	0.7243	48.2734
0	-0.0015	0.0068	0.0033	0.0043	11.8909	8.1816	1.8574	0.2578
Average Sum of Squares					6.7966	11.2312	1.4670	4.5440

Chapter 5 The Phantom Tissue Model

It is very difficult to calibrate the Thermoelectric Perfusion Probe by using animal tests. This is due to the uncertainty in physiological factors. Therefore, a new phantom tissue system has been developed to test the Thermoelectric Perfusion Probe. The new phantom tissue test stand was based on older generations. However, the new phantom tissue test stand was made to be more repeatable, easier to use, and dynamic. In this section, the phantom tissue test stand is introduced. First, the design criteria for the phantom tissue test stand are presented. Then, the initial computational model that was used to develop the phantom tissue model is described. Next, the actual phantom tissue test stand is presented. Then, the final computational model is presented. This computational model was used to validate the phantom tissue test stand. Finally, the experimental procedure is discussed.

5.1 Design criteria

The phantom tissue model was designed to mimic the non-directional flow of blood, to match the blood perfusion in the capillary bed. The phantom tissue model was simulated in the commercial computational fluid dynamics software (Fluent®) to help validate the experimental results.

Due to the large range of blood perfusion values reported for human tissues (i.e. 0.0002 – 0.05 mL/mL/s) and physiological factors, it is impossible to assess the measurement accuracy of any blood perfusion measuring devices *in vivo*. The phantom tissue test stand was developed to closely model perfusion while eliminating physiological factors. There were six main criteria to be fulfilled by the phantom tissue model including: mimicking non-directional flow, having a constant temperature at the inlet, having thermal properties similar to blood, having controlled variability in flow, having a tissue simulator, and being repeatable.

The phantom test stand was designed to properly model perfusion. Perfusion is non-directional at the macroscopic level; therefore the working fluid for the test stand also has

this non-directional flow. Blood perfusion is supplied by arterioles, which contain blood at a constant temperature. The tissue simulator in the test stand is supplied by a working fluid at a constant temperature. Also, because the blood perfusion probe depends on the thermal properties of the tissue and blood, the test stand contains thermal properties similar to that of blood and tissue.

5.2 Initial Computational Study

To determine the best way to design a phantom tissue test stand, a rigorous computational study was completed to test different perfusion simulator ideas. The goal was to determine the best way to develop the test stand before investing the time to construct it. Once this study was completed the test stand was built and the computational model was modified to exactly model the experimental setup.

To meet the objectives of the experimental design, a very basic model was developed for our phantom tissue simulator, Figure 5.1. The basic design of the setup would be to bring the working fluid into an inlet, through a porous matrix, and then out. It was determined that water would be the working fluid, since water has the same thermal properties as blood.

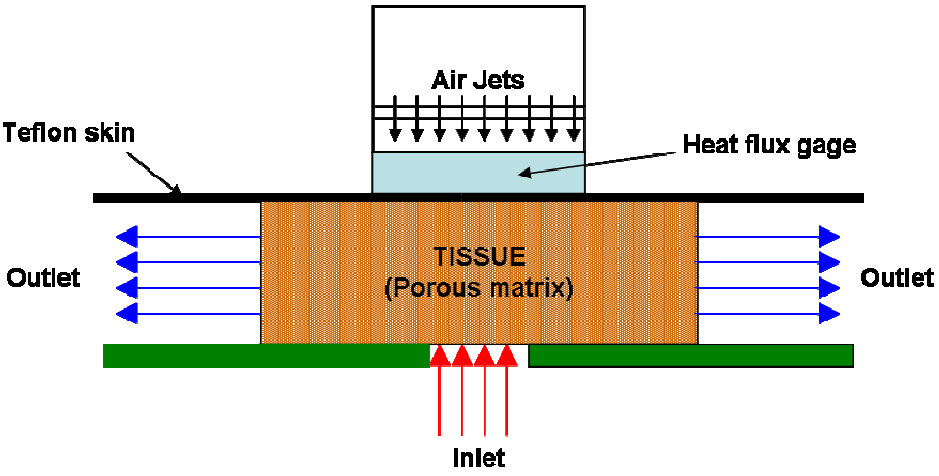

Figure 5.1. A schematic of the initial computational model

Once this basic model was developed, a 2D model was developed in Gambit 2.2.30® and was solved using Fluent®. Several configurations and specifications were tested and the final model was developed, Figure 5.2. This model has the water inlet

entering from the bottom, against gravity, into a flat plate. This configuration was chosen over other entrance configurations because it allowed the water to be evenly distributed through the porous matrix. Also, several porosities and porous media thicknesses were tested to determine which setup would allow the water to both be non-directional and to rise to the skin simulator. It was determined that a porosity of 95% with a thickness of about 1.27 cm (0.5 in) would provide non-directional flow throughout the porous media. The porosity of the sponge was determined based on the wet and dry weight of the sponge. The model proved that the width and length of porous matrix did not have any affect on the heat flux measured during the applied thermal event; however, the thickness did affect the heat flux response. Also the smaller porous matrix size helped to achieve more uniform flow throughout the porous matrix. A schematic of the flow involved in this model is also shown in Figure 5.2.

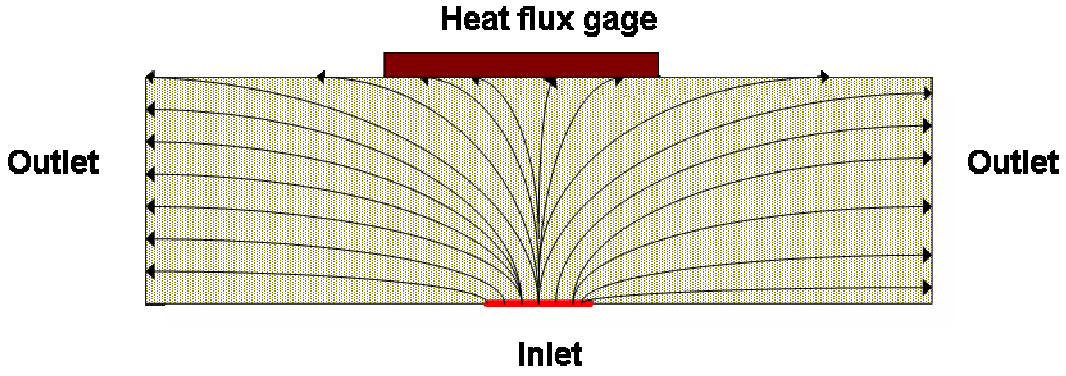

Figure 5.2. A Fluent® model of the phantom tissue with path lines

As can be seen in the Figure, the water flows into the porous matrix and then proceeds to spread out to the outlets. The heat flux sensor placed on the top of the tissue is modeled as solid with properties of the sensor. A convective boundary condition is applied to the top face of the sensor on which the air impinges. A contact resistance was incorporated between the sensor and the tissue interface as thermal resistance.

5.3 The Phantom Tissue Model Setup

Once the basic computational model was developed, the experimental setup was devised. The goal of the experimental setup was to make it simple, adjustable, and to fulfill the objectives presented earlier. The final experimental test stand was first

developed using the 3-D modeling program Unigraphics®. The final design was then physically built and assembled.

The final design of the experimental setup can be seen in Figure 5.3. As can be seen from the Figure, the entire setup is enclosed in a tank that is completely filled with water. This design can be broken up into two main parts: the water regulator system and the actual tissue simulator. The water regulator system includes a pump, a flow controller, and a heater. The tissue simulator system includes a skin simulator, a porous matrix, and a structural support system.

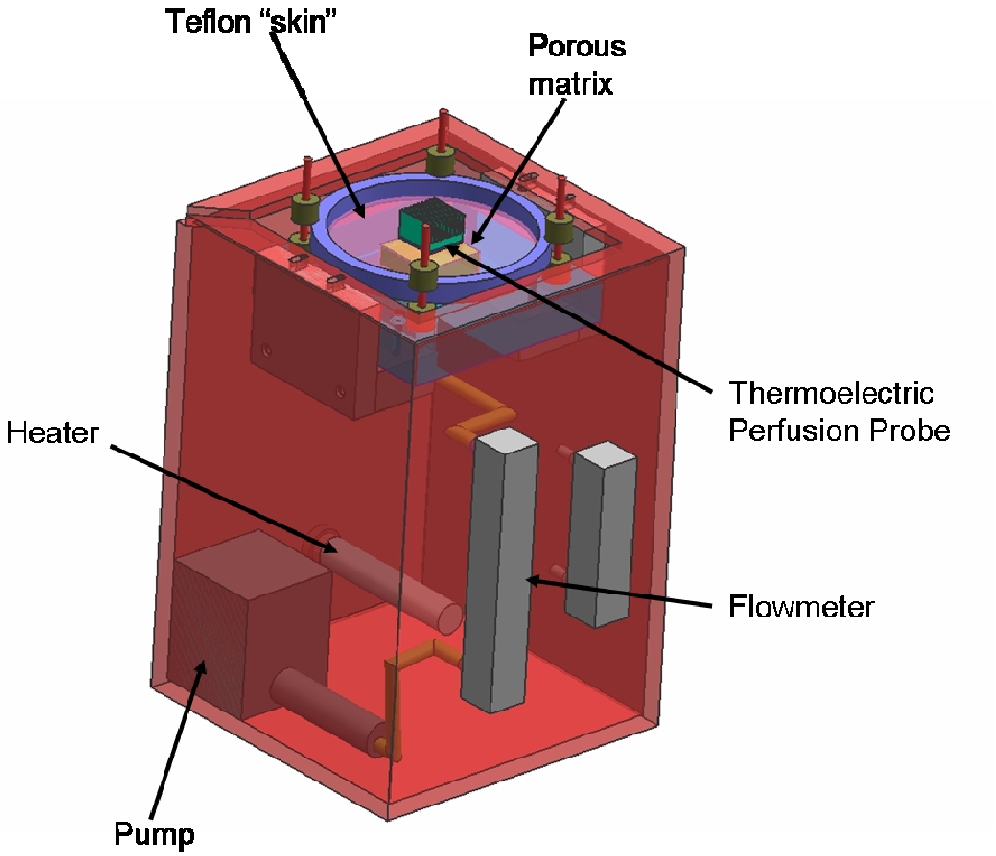

Figure 5.3. Schematic of the phantom tissue test stand.

One of the main objectives of this test stand was to supply blood into the tissue simulator at a constant temperature and flow rate. For this reason, a Plexiglas™ tank was used to enclose the phantom tissue test stand. The bottom area of the tank stored water maintained at a constant temperature. The water was maintained at 37°C, the core temperature of the human body, by a temperature controller in conjunction with a

cartridge heater, Figure 5.4. Also, the water was supplied to the tissue simulator at a controllable flow rate. The water bath served as storage reservoir to ensure that the flow rate into the porous material remained constant. The flow into the tissue was provided by a centrifugal pump that pumped water from the water bath directly through a flowmeter, Dwyer Instruments Inc. Visi-Float®, model VFB-82-BV (2-30 cc/min flow range). The water was then directed from the flowmeter into the tissue simulator. A 0.635 cm (0.25 in) diameter inlet was used for the water flowing into the porous matrix. The test stand also has leveling feet to ensure tank level is adjustable which in turn allows for adjusting all internal components.

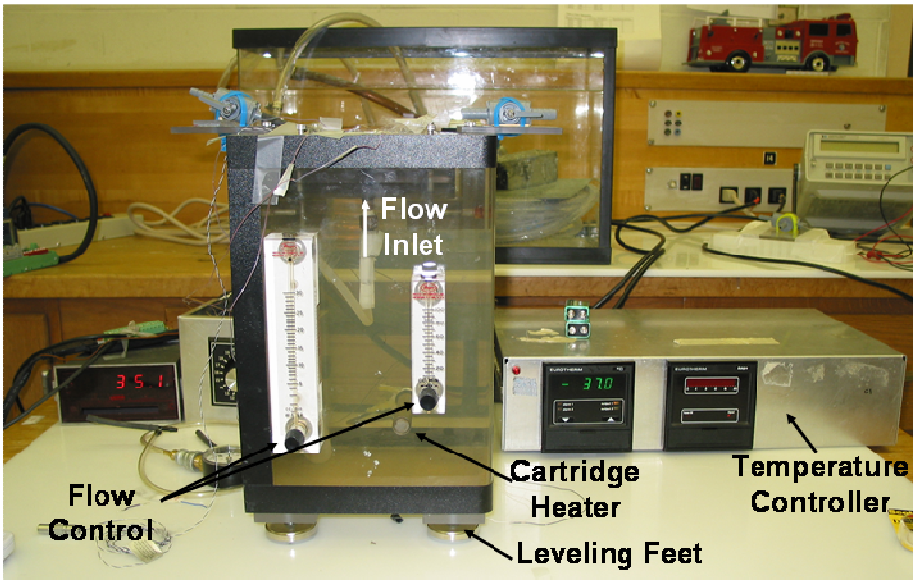

Figure 5.4. The water controller system

The tissue simulator system was devised to be adjustable. Based on the computational study as discussed before, water and a 95% porous matrix are used to simulate blood and tissue, respectively. The tissue simulator is made of seven parts, Figure 5.5. The system is mounted to the Plexiglas™ tank by two Plexiglas™ brackets. The inlet plate, which rests on the brackets, is a 12.7 cm x 12.7 cm x 2.54 cm (5 in x 5 in x 1 in) piece of Plexiglas™ with a NPT tapped hole in the center for the water inlet. Also, this piece supports the entire tissue simulator section. Above the center hole of the inlet plate, a 4 cm x 4 cm x 1.27 cm (1.57 in x 1.57 in x 0.5 in) porous matrix was placed. On top of the porous matrix lies the skin simulator, Teflon™. The Teflon™ sheet is kept taut by a fabric hoop. The supports for the fabric hoop are adjustable to insure that the porous

matrix is not compressed. The Thermoelectric Perfusion Probe is then attached to the Teflon™ using double-sided tape. The water flows through the inlet plate and into the porous matrix where it becomes non-directional. The water then exits through all sides of the porous matrix into the water bath. Drawings for the experimental setup can be seen in Appendix C.

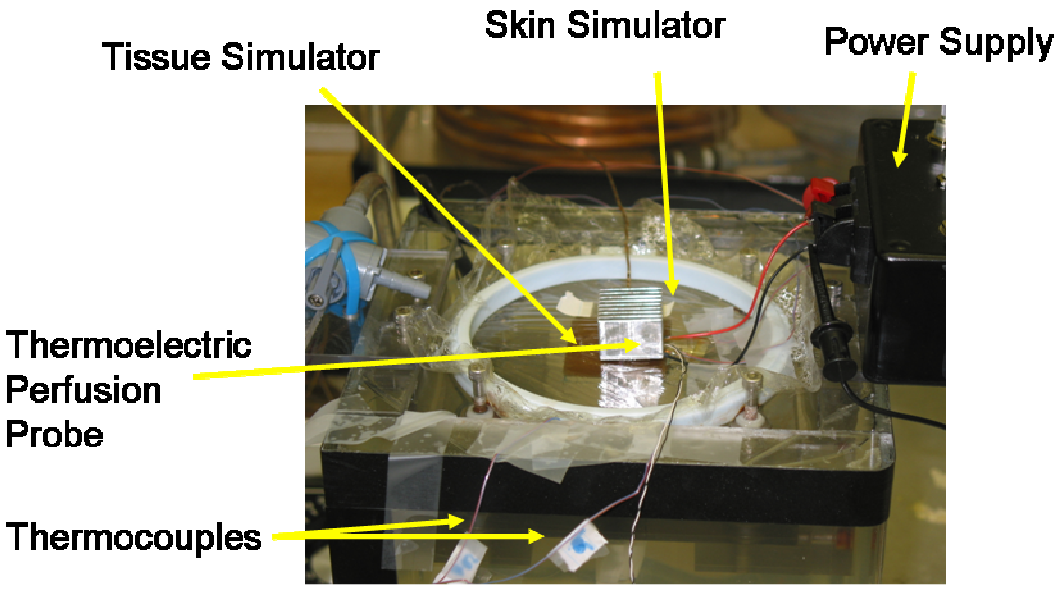

Figure 5.5. Photograph of the Experimental Test Setup.

5.4 Final Computational Model

Once the experimental setup was built and exact dimensions were known, a final Gambit® model could be developed. This model is the same as the initial model, only the dimensions differ. A fully developed velocity profile was used in the Fluent® model at the inlet. The sensor's heat flux from the computational model is calculated based on Fourier's law of conduction and an area weighted temperature difference average between the top and the bottom face of the heat flux sensor. The momentum and energy equations for Fluent® were solved using a second-order upwind scheme and the unsteady formulation was carried out using the first-order implicit scheme. The computational model was set to run for 60 seconds with a time step of 0.1s, to compare with the experimental results.

Two models were created to validate the finite difference model and the experimental setup. A flow model was developed to provide a direct comparison with the experimental conditions, while an energy source model was developed to provide a comparison between the Fluent® and the finite difference models used in the estimation procedure.

The flow model allowed for validation of the heat flux response of the phantom tissue test stand. To validate the heat flux response, the temperatures recorded during the experiments are inserted into the computational model. Then, Fluent® solved the momentum and energy equations to produce the heat flux curve. The final Fluent® model with boundary conditions is presented in Figure 5.6. As can be seen in the Figure, this is a 2D axis symmetric model. This model was built using the Convective Perfusion Probe, instead of the Thermoelectric Perfusion Probe. Also presented in the Figure is an example temperature profile of the sensor and porous matrix. Based on this model it appears the probe has a thermal penetration of 0.10 cm (0.04 in).

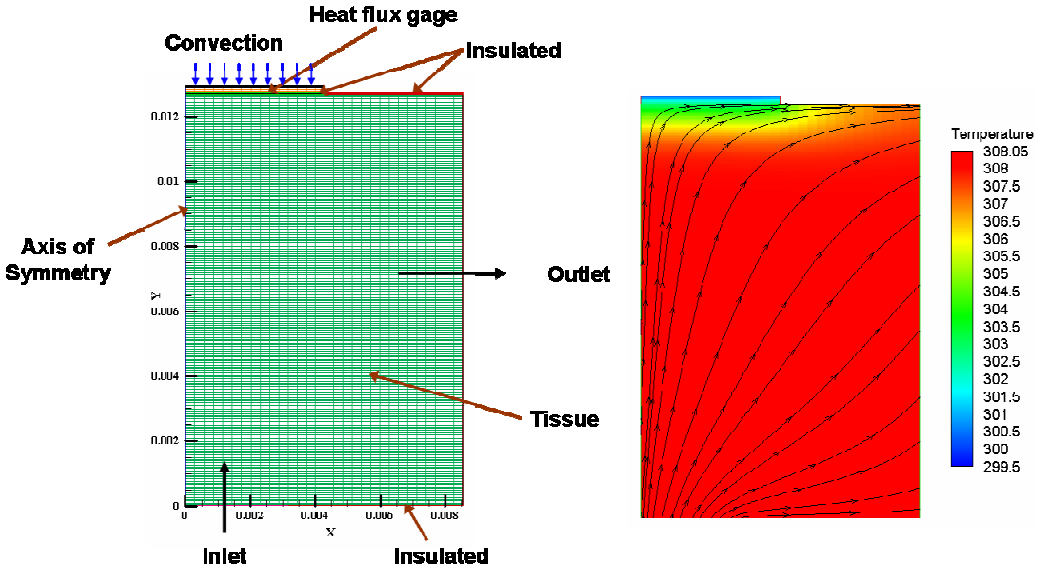

Figure 5.6. The final computational model with a temperature profile for an experimental test.

The computational model was also used to validate the perfusion estimates and contact resistance produced by the parameter estimation code. In Fluent®, perfusion was simulated by adding an energy source term as a function of the local temperature (which

results in the Pennes bioheat equation). The inlet flow under this condition was set to 0 cc/min. The contact resistance and perfusion values were determined from the experimental data using the parameter estimation program. These values were then introduced into the computational model by adjusting the wall thickness (contact resistance) and the energy source term (perfusion). Then, the simulation was completed by Fluent® producing an expected heat flux curve. This produced heat flux curve matched the experimental heat flux curve.

5.5 Experimental Design Plan

Testing on the phantom tissue model was completed with both the Convective Perfusion Probe and the Thermoelectric Perfusion Probe. The overall goal of all the experiments was to prove the Thermoelectric Perfusion Probe can continuously monitor perfusion and to demonstrate the value of the pressed sensor.

Table 3 summarizes the Convective Perfusion Probe's experiments and the purpose of the experiments. More information about these experiments and the results of these experiments will be presented in Chapter 6. Table 4 summarizes the Thermoelectric Perfusion Probe's experiments and the objectives of these experiments. More information about these experiments and the results of these experiments will present in Chapter 7.

Table 3. The Convective Perfusion Probe Experiments

Experiment type	Data Acquisition System	Number of Experiments	Objectives	Result
Sensitivity and Repeatability Tests for the Convective Perfusion Probe fitted with a pressed sensor.	The newer data acquisition system with the high speed 16bit DAQ implemented.	21 total experiments: 3 experiments at each flowrate: 0, 5, 10, 15, 20, 25, and 30 cc/min	To compare the Thermoelectric Perfusion Probe's Program to the Convective Perfusion Probe's Program	The Thermoelectric Perfusion Probe's program was validated
			To test the pressed sensor	The pressed sensor worked

Table 4. The Thermoelectric Perfusion Probe Experiments

Experiment type	Data Acquisition System	Number of Experiments	Objectives	Result
Sensitivity Experiments	The old data acquisition system with 2 24bit DAQs implemented	13 total experiments, one cycle per experiment 3 experiment at each flowrate: 0, 5, 10, and 20 cc/min, 1 experiment at a flowrate of 30 cc/min	To see the sensitivity of the Thermoelectric Perfusion Probe	Both heating and cooling portions of the cycle were sensitive.
Continuous Experiments	The old data acquisition system with 2 24bit DAQs implemented	1 total experiment, 17 total cycles, 2 cycles at 30 cc/min, 3 cycles at 0 cc/min, 4 cycles at each flowrate: 5, 10, and 20 cc/min	To see if the Thermoelectric Perfusion Probe will overheat	The Probe Temperature stayed reasonable
			To see if the Thermoelectric Perfusion Probe was sensitive and repeatable continuously	The Probe worked continuously and was repeatable
			To determine the effects of tissue recycling	Temperature Recycling helped results
			To determine what happens to perfusion estimates when ramping up/down occurs	Randomness occurred except at 30 cc/min flow rates
Combined Results from the Sensitivity and Continuous Experiments	The old data acquisition system with 2 24bit DAQs implemented	14 total experiments: 30 total cycles, 3 cycles at 30 cc/min, 6 cycles at 0 cc/min, 7 cycles at each flowrate: 5, 10, and 20 cc/min	To see the overall comparison of the Thermoelectric Perfusion Probe to the CFD Flow model	The Thermoelectric Perfusion Probe showed the same trend as the CFD Flow model

Chapter 6 Convective Perfusion Probe Experiments

The final version of the Thermoelectric Perfusion Probe's perfusion estimation program with temperature recycling used the continuously recorded sensor temperature as the driving temperature for parameter estimation, as discussed in Chapter 4. For this program to work, it is not important how the thermal event is created. Therefore, perfusion estimates can be obtained from the final version of the Thermoelectric Perfusion Probe's perfusion estimation program when the Convective Perfusion Probe is fitted with a pressed sensor. Also, with this configuration of the Convective Perfusion Probe fitted with a pressed sensor, perfusion estimates can still be obtained from the Convective Perfusion Probe's perfusion estimation program. This is assuming both the air temperature and sensor temperature are continuously recorded. Both temperatures have to be recorded because the air temperature is the driving temperature for the Convective Perfusion Probe's perfusion estimation program and the sensor temperature is the driving program for the Thermoelectric Perfusion Probe perfusion estimation program.

The Convective Perfusion Probe was fitted with the pressed sensor and then experiments were conducted on the phantom tissue test stand. Perfusion estimates from the experimental data was then determined using the final version of the Thermoelectric Perfusion Probe's perfusion estimation program, and using the Convective Perfusion Probe's perfusion estimation program. The final version of the Thermoelectric Perfusion Probe's perfusion estimation program, the one with temperature recycling, was the same program that was used to gain final perfusion values for the Thermoelectric Perfusion Probe (discussed later). Because these experiments weren't continuous temperature recycling didn't impact the results. Temperature recycling is only implemented when experiments are continuous. There were two objectives for these experiments. The first objective was to validate the Thermoelectric Perfusion Probe's perfusion estimation program with the Convective Perfusion Probe's perfusion estimation program. The Convective Perfusion Probe's perfusion estimation program has been previously

validated, see Ashvin Mudaliar's dissertation (2006). The second objective was to prove that reasonable perfusion estimates can be gained from a pressed sensor.

6.1 Experimental Setup

The Convective Perfusion Probe experiments required five measurements to be recorded: four temperature measurements and a heat flux measurement. The Convective Perfusion Probe requires the arterial temperature of the blood, the top temperature, the sensor temperature, and the convective air temperature. Two thermocouples were placed at the top (top temperature) and bottom of the porous media (arterial temperature). Both of these thermocouples were placed in the center of the inlet and the center of the porous media, Figure 6.1. Two more thermocouples were used to measure the air temperature, and the sensor temperature. The thermocouples are labeled as follows in Figure 6.1: 1) air, 2) sensor, 3) top of porous media, and 4) bottom (arterial) of porous media. The porous media had overall dimensions of

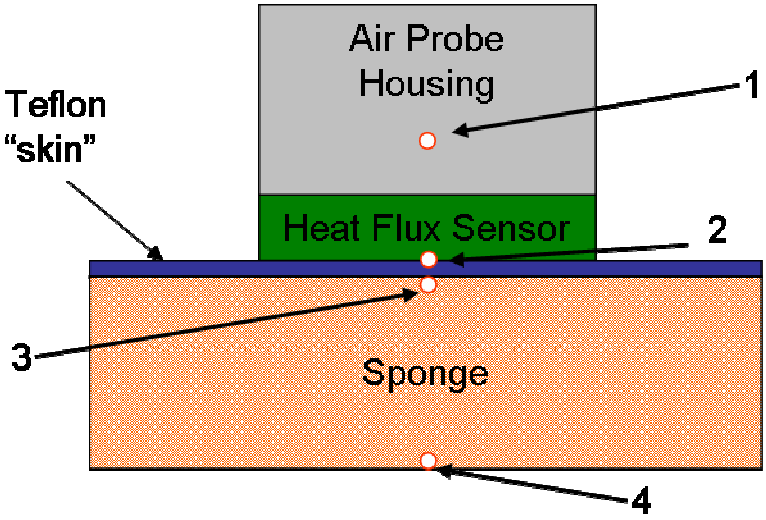

Figure 6.1. A schematic of the arrangement of the thermocouples in the Convective Perfusion Probe experiments

The temperatures were measured using T-type thermocouples made of Copper and Constantan. The arterial temperature and the top temperature are required to set the initial conditions in the finite difference program. The convective air temperature is the driving temperature for the Convective Perfusion Probe's perfusion estimation program.

The sensor temperature is the driving temperature for the Thermoelectric Perfusion Probe's perfusion estimation program.

A Pentium 4 processor laptop was the base of the data acquisition system for the testing with the Convective Perfusion Probe, Figure 6.2. National Instrument's LabView 7.1 in conjunction with a 16 bit, high performance multifunction National Instrument DAQ-Pad 6015 data acquisition system was used to record the voltage signals corresponding to the heat flux sensor and the temperatures. These signals were amplified by 100 gain amplifiers. A Doric thermocouple reader was used to measure the reference temperature.

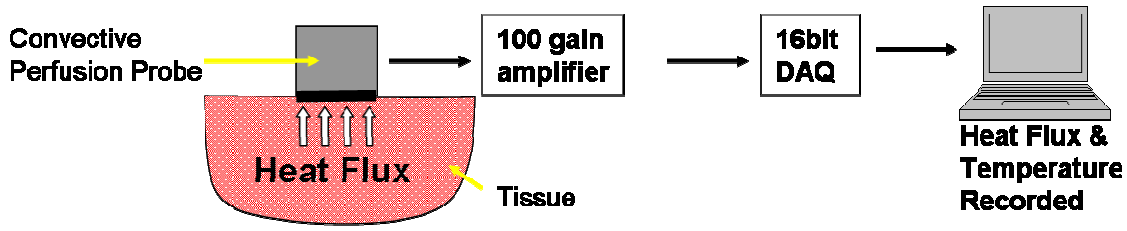

Figure 6.2. A schematic of the Data Acquisition for the Convective Perfusion Probe.

6.2 Experimental Procedure

The Convective Perfusion Probe was fitted with a pressed sensor and experimentation was completed on the phantom tissue model at seven flow rates: 0, 5, 10, 15, 20, 25, and 30 cc/min. At each flow rate, three experiments were conducted. Then, the experimental data were entered into both the Convective Perfusion Probe's perfusion estimation program and the Thermoelectric Perfusion Probe's perfusion estimation program, outlined in Chapter 4. Table 5 displays the procedure for Convective Perfusion Probe tests. The first twenty seconds a maximum flow rate was used to clear the cooled water from a previous experiment. Then, the flowrate was set to the required flowrate. After, one minute the data acquisition starts. After another minute the thermal event is induced. The first minute of data acquisition is used to remove any offsets.

Table 5. Convective Perfusion Probe's Experimental Procedure

Step	Procedure	Time
1	Set the flow meter to maximum flow possible	0 sec
2	Set the flow rate to the desired flow rate for experimental run	20 sec
3	Start the data acquisition (heat flux and temperature)	60 sec
4	Induce the cooling even	120 sec
5	Stop Data Acquisition	180 sec

6.3 Experimental Results

All of the experimental perfusions were compared for the two perfusion estimation programs, as can been seen in Figure 6.3. As shown in the Figure, both perfusion estimation programs displayed similar results and showed reasonable repeatability.

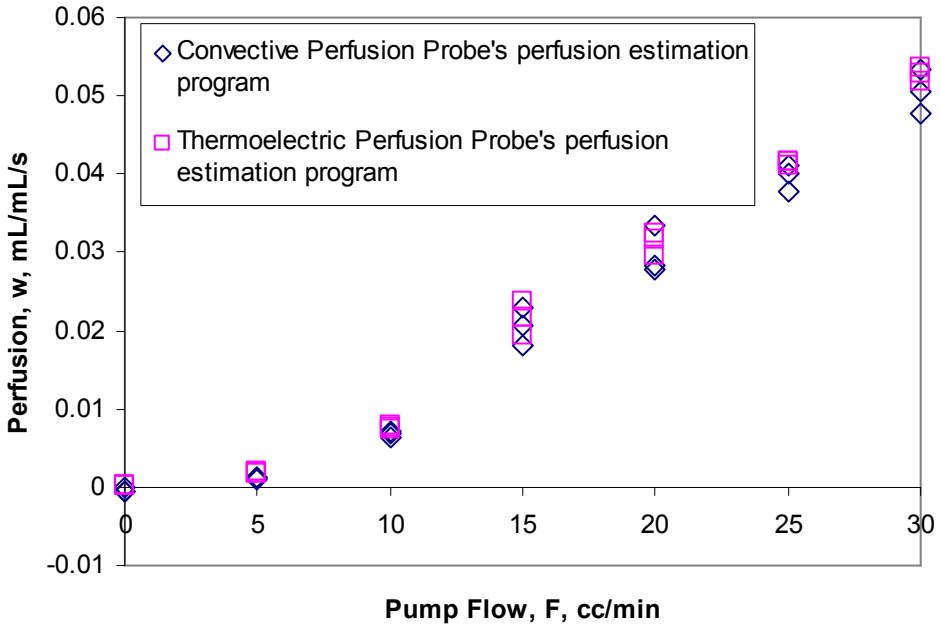

Figure 6.3. Perfusion Estimates for the two different estimation programs. These results are from the same experimental data sets.

The average perfusion values produced from the two different perfusion estimation programs are presented in Figure 6.4 with the 95% confidence intervals. The

offset for the perfusion estimates based on the Thermoelectric Perfusion Probe's estimation program was -0.0004 mL/mL/s, which is negligible. The offset for the perfusion estimates based on the Convective Perfusion Probe's estimation program was 0.0002 mL/mL/s, and was also negligible. These small offsets are very encouraging results. This Figure clearly shows that the two perfusion estimation programs produced very close results.

The averages of the Convective Perfusion Probe's perfusion estimation program results and the Thermoelectric Perfusion Probe's perfusion estimation program results are within a 95% confidence interval of each other. Also, it is very interesting that the Thermoelectric Perfusion Probe's estimation program produced less variability, as defined by a smaller confidence interval, than the Convective Perfusion Probe's estimation program. The small discrepancies between the two programs are probably due to experimental errors associated with using thermocouples.

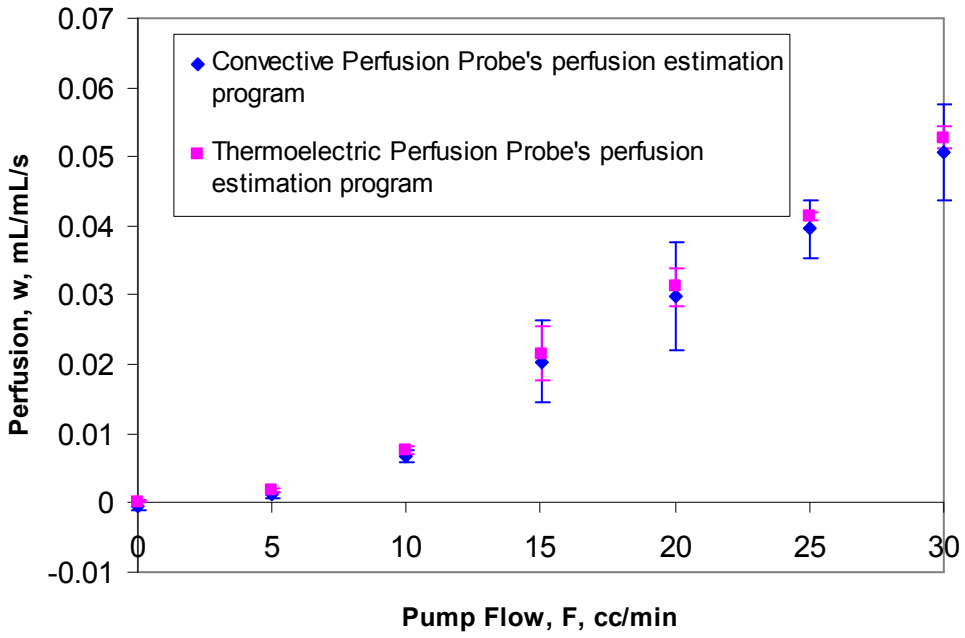

Figure 6.4. Average Perfusion Values for the two different perfusion estimation programs.

Table 6 displays all the perfusion estimates and the sum of squares for the Convective Probe Experiments. Overall, the two perfusion estimation systems had small sum of squares. The Thermoelectric Perfusion Probe's Perfusion Estimation Program had a smaller average sum of squares than the Convective Perfusion Probe's Perfusion

Estimation Program. With these small sums of squares it is clear that both perfusion estimation programs had reasonable curve matches.

Table 6. Comparison of the two perfusion estimation programs

Flowrate	Perfusion		Sum of Squares	
	Convective Perfusion Probe's Perfusion Estimation Program	Thermoelectric Perfusion Probe's Perfusion Estimation Program	Convective Perfusion Probe's Perfusion Estimation Program	Thermoelectric Perfusion Probe's Perfusion Estimation Program
0	-0.0005	0.0002	0.8892	0.4998
0	0.0000	0.0002	0.4616	0.1816
0	-0.0006	0.0003	0.8721	0.3877
5	0.0012	0.0021	0.7346	0.4783
5	0.0009	0.0017	1.2739	0.5792
5	0.0013	0.0019	0.7621	0.4362
10	0.0063	0.0073	0.8898	0.9874
10	0.0068	0.0078	0.7988	0.6526
10	0.0071	0.0077	0.7413	0.5447
15	0.0180	0.0194	0.3181	1.0164
15	0.0205	0.0216	1.1366	1.0288
15	0.0228	0.0237	0.5630	0.4303
20	0.0335	0.0324	0.5131	0.4990
20	0.0283	0.0318	0.5402	0.9385
20	0.0278	0.0296	0.6887	0.9318
25	0.0377	0.0415	0.8037	0.5530
25	0.0410	0.0417	0.6480	0.6909
25	0.0400	0.0411	0.4606	0.5234
30	0.0478	0.0519	0.6772	0.4013
30	0.0534	0.0528	0.5517	0.1782
30	0.0506	0.0536	0.6783	0.7090
Average Sum of Squares			0.7144	0.6023

6.4 Experimental Conclusions

Based on the experimentation with the Convective Perfusion Probe, the Thermoelectric Perfusion Probe's perfusion estimation program was validated with the Convective Perfusion Probe's perfusion estimation program. The Convective Perfusion Probe's perfusion estimation program has been proven to be accurate (Mudaliar *et al*., 2006). These results show promise for simplifying the Convective Perfusion Probe or the Convective Perfusion Probe's perfusion estimation program. It is also possible to make the Convective Perfusion Probe's perfusion estimation program more robust. These

results indicate that the Convective Perfusion Probe could be developed to record one less temperature. Also if all temperatures are recorded, then the Convective Perfusion Probe could have two different methods for determining perfusion. Therefore, the two perfusion estimates can be compared and if large inconsistencies occur then there is a high likelihood of experimental error.

Chapter 7 Thermoelectric Perfusion Probe Experiments

There are three main objectives associated with the experimentation on the Thermoelectric Perfusion Probe. The first objective was to prove that the Thermoelectric Perfusion Probe shows similar sensitivity and repeatability to the Convective Perfusion Probe and the Fluent® Model. The second objective was to prove that the heat sink is sufficient to remove the required heat from the Thermoelectric Perfusion Probe and to maintain the probe at a constant temperature. The third objective was to show that the Thermoelectric Perfusion Probe can be used for continuous perfusion measurements. Testing for the Thermoelectric Perfusion Probe was completed on the phantom tissue test stand.

7.1 Experimental Setup

Overall, the Thermoelectric Perfusion Probe required five measurements to be recorded. This includes four temperature measurements and a heat flux measurement. The Thermoelectric Perfusion Probe requires the arterial temperature of the blood, the temperature of the sensor, the top temperature, and the temperature between the TEC and the heat sink. The temperature between the TEC and the heat sink was only used to verify that the heat sink was sufficient. In the future only the sensor and arterial temperature will need to be measured.

Two thermocouples were placed at the top (top temperature) and bottom of the porous media (arterial temperature). Both of these thermocouples were placed in the center of the inlet and the center of the porous media, Figure 7.1. Two more thermocouples were used to measure the temperature of the heat sink, and the temperature of the sensor. The thermocouples are labeled as follows in Figure 7.1: 1) heat sink, 2) sensor, 3) top of porous media, and 4) bottom (arterial) of porous media. The overall dimensions of the porous media were 4 cm x 4 cm x 1.27 cm (1.57 in x 1.57 in x 0.5 in).

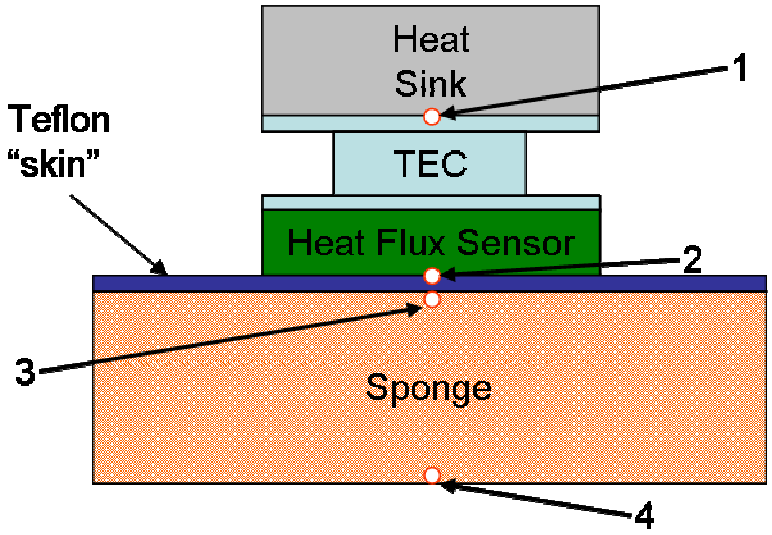

Figure 7.1. A schematic of the arrangement of the thermocouples in the test setup.

T-type thermocouples were used in the experiments. The arterial temperature was required for the finite difference program. The sensor temperature was continuously monitored and has dual purposes. The sensor temperature was used to set the initial conditions in the finite element model, and it was used as the driving temperature for the finite difference model. Also, the Thermoelectric Perfusion Probe required good conduction between the heat flux sensor and the TEC. Therefore, it was not practical to have a thermocouple in between those two components. The temperature between the TEC and the heat sink was required to determine if the heat sink is adequately removing heat.

The data acquisition for the experimentation on the Thermoelectric Perfusion Probe required two 24 bit DAQ's along with a Doric thermocouple reader and one amplifier. A schematic of the data acquisition can be seen below in Figure 7.2. The arterial temperature and the top temperature were measured using the Doric thermocouple reader. The other two thermocouples were connected directly to a 24 bit DAQ. The DAQ directly converted the thermocouple voltage to a temperature. The temperatures were then recorded by a P4 desktop using Labview 7.1. The heat flux signal was amplified and then connected to another 24 bit DAQ. The heat flux signal was then recorded by a P4 Laptop using Labview 7.1.

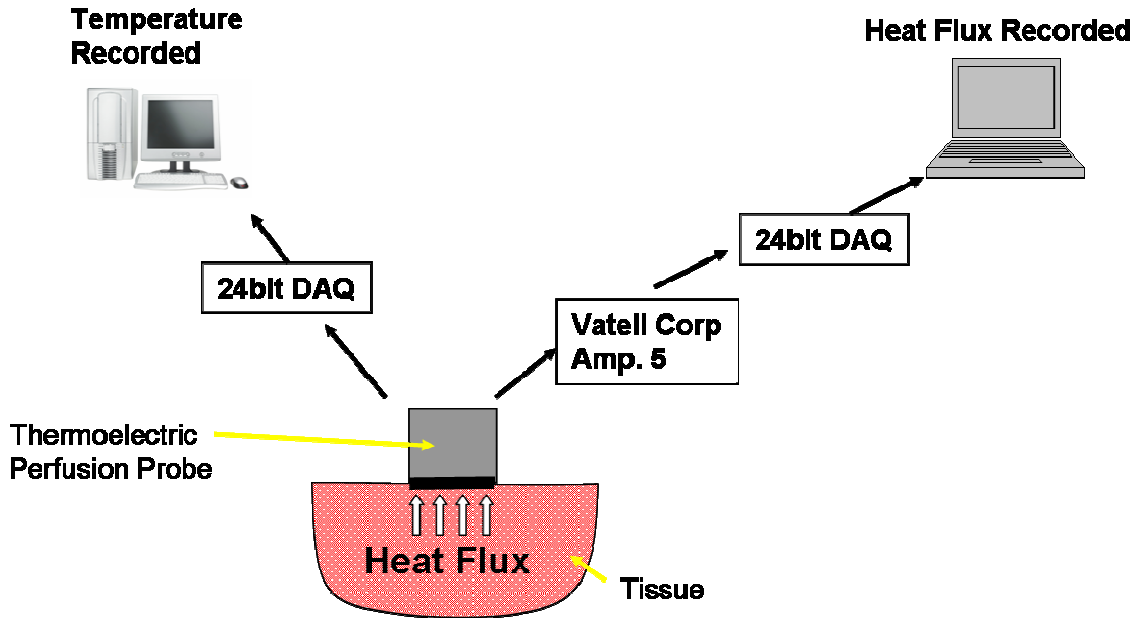

Figure 7.2. A schematic of the Data Acquisition for the Thermoelectric Perfusion Probe.

7.2 Experimental Procedure

To ensure repeatability, an identical data acquisition and experimental procedure was used for all tests. Overall, there were several different experiments that were completed. The first step in the experimental procedure was to equilibrate the temperature within the porous matrix. To do this, the porous matrix was flushed at a maximum flow rate for 20 seconds. Then, the flow was set to the desired flow rate and allowed to equilibrate for 40 seconds. Data acquisition began after one minute. The first minute of data acquisition was used to determine the offset in the heat flux signal. Then, the cooling thermal event was initiated with the Thermoelectric Perfusion Probe.

The thermal event for the Thermoelectric Perfusion Probe was initiated by placing a positive voltage across the TEC, resulting in skin cooling. Then, after two minutes, the voltage was switched and heating was initiated. The tissue was then heated for two minutes. Unless, this was the last cycle, the cooling event was then initiated. This procedure for alternating heating and cooling can occur until the desired number of cycles was reached. Table 7 summarizes the experimental procedure timeline for the testing with the Thermoelectric Perfusion Probe.

Table 7: Summary of the experimental procedure for the phantom test

Step	Procedure	Time
1	Set the flow meter to maximum flow possible	0 sec
2	Set the flow rate to the desired flow rate for experimental run	20 sec
3	Start the data acquisition (heat flux and temperature)	60 sec
4	Alternatively Heating and cooling	120 sec
5	Stop Data Acquisition	Number of Cycles*Cycle Time

Several tests were completed using different cycle times, different numbers of cycles and by varying the voltage to drive the TEC. Overall, it was found that the 4 minute cycle length tests gave the best results, and therefore they were used as the standard. Also, tests were completed at a wide variety of input voltages: ranging from 0.5V to 1.25V. It was found that due to sensitivity issues with the heat flux sensor, it was best to use large voltages which result in high heat fluxes. Also, tests were completed with varying flowrates during the experiment. This procedure was used for both experiments: the sensitivity tests and the continuous tests

7.3 The Thermoelectric Perfusion Probe's Sensitivity Results

The next section discusses the sensitivity experiment results for the Thermoelectric Perfusion Probe. The goal was to prove the Thermoelectric Perfusion Probe had the same sensitivity as the Convective Perfusion Probe. The Convective Perfusion Probe has been proven to be very sensitive and provide reasonable perfusion values during animal tests (Ellis *et al.*, 2006) and during phantom tissue tests (Mudaliar *et al.*, 2006). Currently, the temperature controlling system on the Thermoelectric Perfusion Probe has not been refined enough for animal testing, therefore testing for the sensitivity of Thermoelectric Perfusion Probe had to be completed on the phantom tissue test stand.

Experiments with the Thermoelectric Perfusion Probe were conducted on the phantom tissue test stand where the skin was exposed to two minutes of cooling and then two minutes of heating, for an overall cycle time of four minutes. During this time, the

sensor temperature and the temperature at the heat sink-TEC interface (probe temeperature) were measured continuously, while the top temperature and the arterial temperature were measured at the beginning of the test. As prior stated, many other cycle times were tried; however the four minute cycle period produced the best results. An example of the experimental heat flux data is shown in Figure 7.4. It is important to note that the shape of the heat flux curve produced by the Thermoelectric Perfusion Probe is slightly different than the curves produced by the Convective Perfusion Probe (Appendix D). The Thermoelectric Perfusion Probe slowly ramps up to the desired cooling temperature, whereas the Convective Perfusion Probe immediately has convective air at the desired temperature. The experimental sensor temperature data are presented in Figure 7.4. As can be seen in the Figure the temperature at the sensor decreases until equilibrium is met for the cooling portion of the cycle.

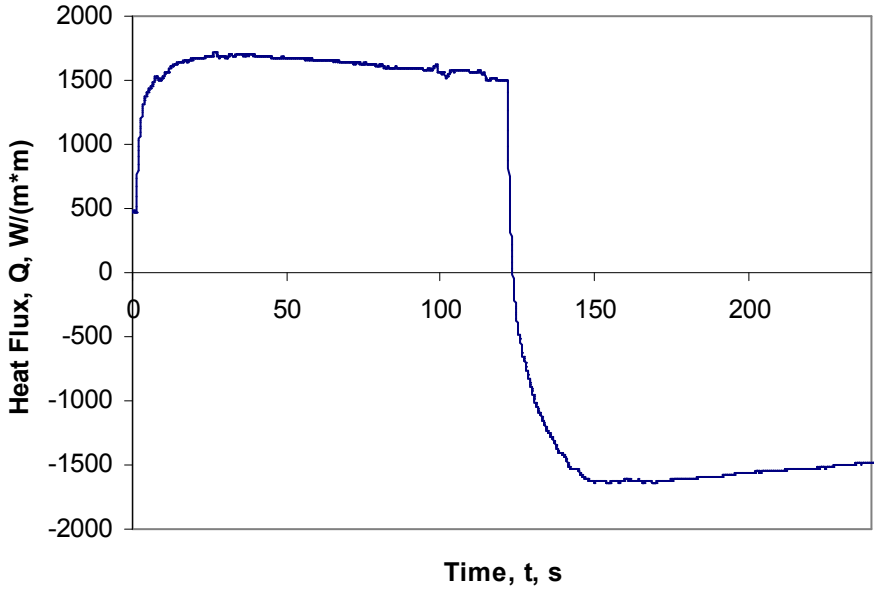

Figure 7.3. Experimental heat flux for a full cycle of testing at a flowrate of 0 cc/min.

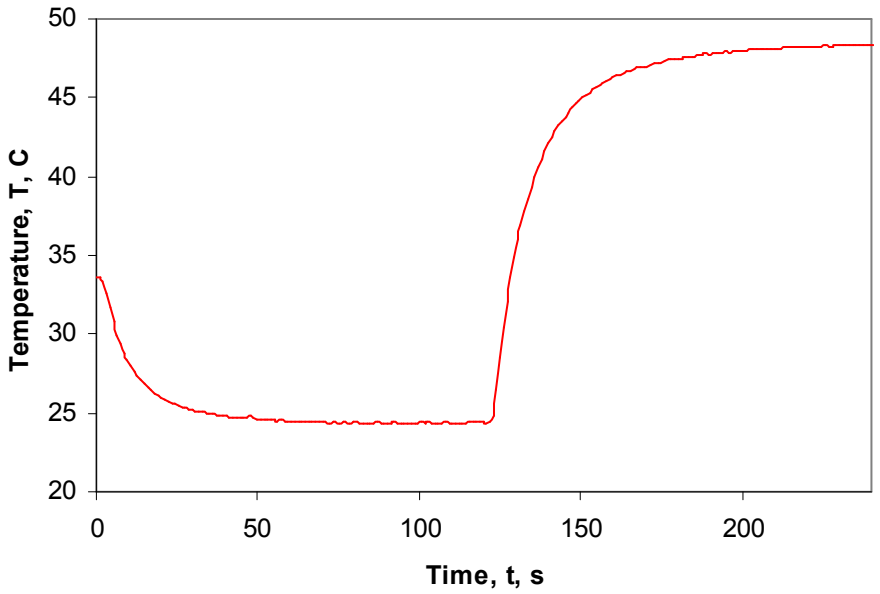

Figure 7.4. Experimental sensor temperature for a full cycle of testing at a flowrate of 0 cc/min.

The next step was to determine if the Thermoelectric Perfusion Probe proved to be repeatable. Therefore, multiple tests were completed at various flow rates. These tests were completed for flow rates of 0, 5, 10, 20, 25 and 30 cc/min. Figure 7.5 displays an example repeatability graph produced by the tests. As can be seen from the graph, all three experiments displayed very similar curves. A repeatability graph for heating appears in Appendix D.

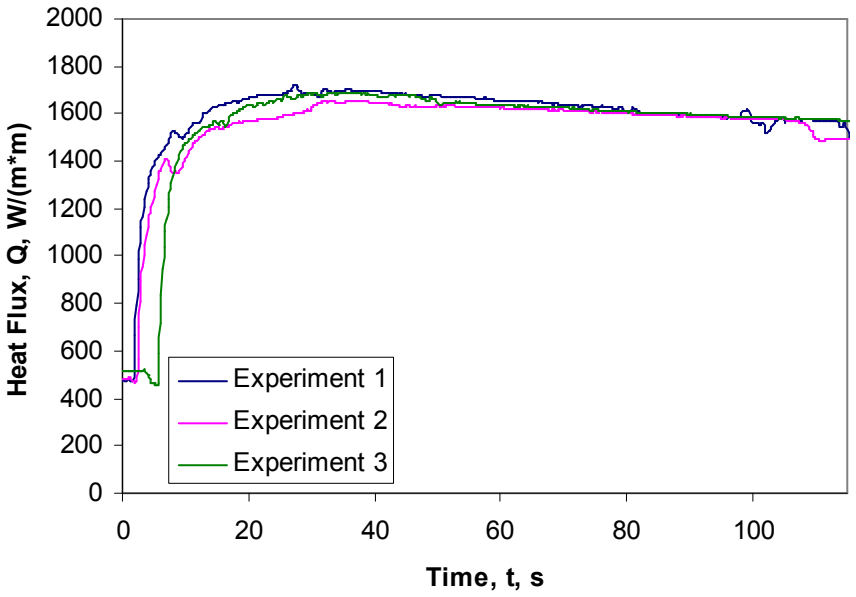

Figure 7.5. Experimental heat flux curves at a 0 cc/min flowrate for the tissue cooling portion of a cycle.

As with the Convective Perfusion Probe, the Thermoelectric Perfusion Probe must have very good sensitivity. A sensitivity study was performed to compare the heat flux curves for the Thermoelectric Perfusion Probe, Figure 7.6. As expected at a flow rate of 30c/min, there is a higher heat transfer than at 0 cc/min. This was the same results that appear using the Convective Perfusion Probe. Also, the heating portion of the cycle produced similar results as can be seen in Appendix D.

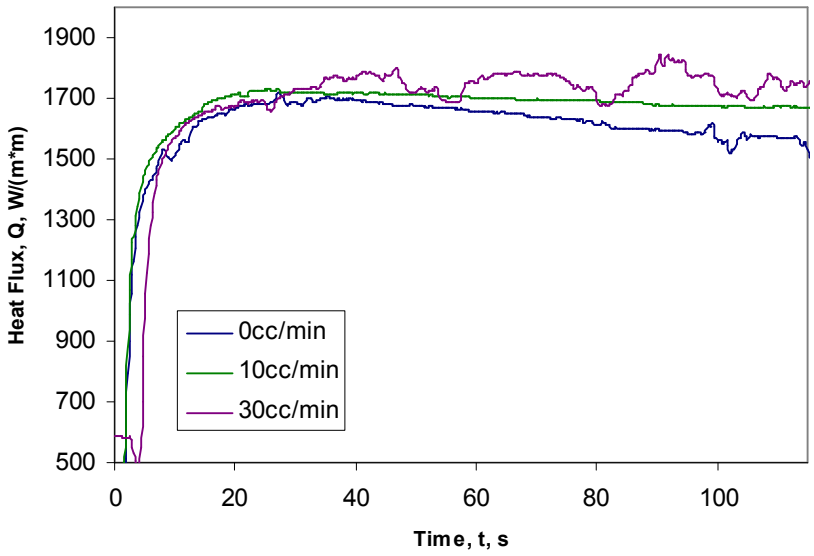

Figure 7.6. Experimental heat flux curves for 0, 10, and 30 cc/min flowrates for the cooling portion of a cycle.

It is important to note that the repeatability and sensitivity of the Thermoelectric Perfusion Probe cannot be tested by simply looking at the heat flux curves. The heat flux is related to the temperature difference between the skin and the heat flux sensor. The temperature difference is determined by the perfusion in the tissue and the amount of power the TEC is consuming. Therefore, because the voltage cannot be kept constant, differences appeared along the heat flux curves. This difference was just due to the variable power consumption by the TEC.

The only way to truly test the sensitivity and repeatability of the Thermoelectric Perfusion Probe was to compare the perfusion values at different flow rates. Therefore, perfusion estimates based on the heat flux and temperature data were produced using the Thermoelectric Perfusion Probe's perfusion estimation program, Figure 7.7. The perfusion estimates were produced with the newest version of the Thermoelectric Perfusion Probe's perfusion estimation program which included temperature recycling (discussed earlier). The perfusion estimates were grouped into two groups: perfusion estimates produced during the tissue cooling and perfusion estimates produced during tissue heating. The perfusions produced from the cooling portion of the cycle appeared to be slightly higher than the perfusion produced from the heating portion of the cycle. Overall, both the perfusion values from cooling portion of the cycle and the perfusion

values from the heating portion of the cycle followed an upward linear trend. This is to be expected because perfusion increases with an increase in flow rate.

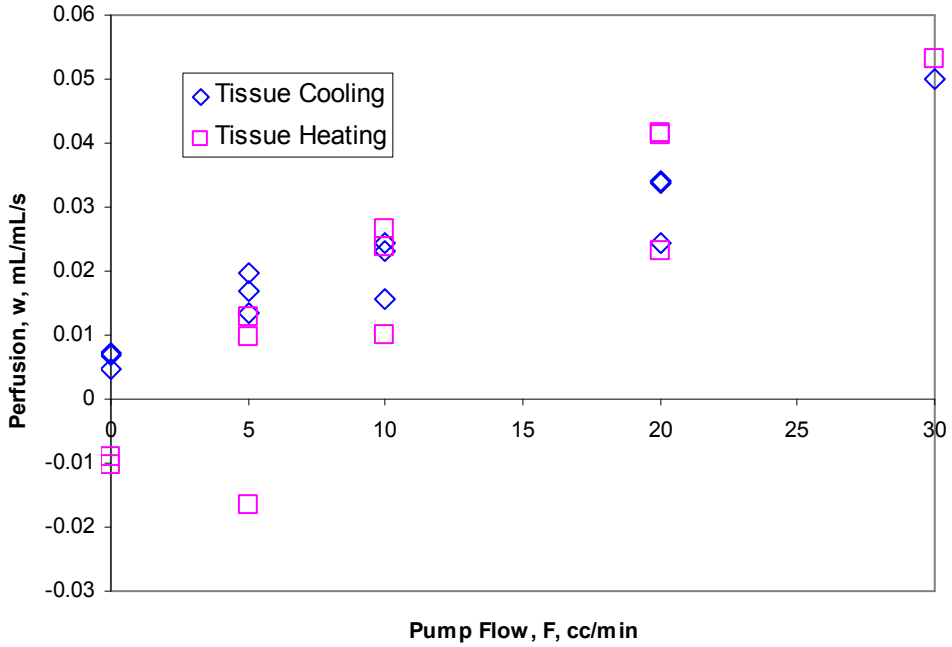

Figure 7.7. Perfusion values from the sensitivity tests.

The next step was to gain a better comparison between the results produced from tissue cooling and tissue heating. The average perfusion values for both tissue cooling and tissue heating are plotted for each flow rate, Figure 7.8. Also the overall average at each flow rate (the average of the cooling perfusion values and the heating perfusion values) is presented with its 95% confidence interval. Tissue cooling produced an offset of 0.0062 mL/mL/s, while tissue heating had an offset of -0.0097 mL/mL/s. The overall offset when tissue heating and tissue cooling were averaged was -0.0017 mL/mL/s. The graph is recreated in Appendix D with the offsets removed. As can be seen in the Figure it appears that at lower flow rates, the cooling portion of the cycle produced higher perfusion values than the heating portion of the cycle. At high flow rates the heating portion of the cycle produced higher perfusion values. The confidence interval was not placed on the 30 cc/min data point because it was large and skewed the scale of the graph.

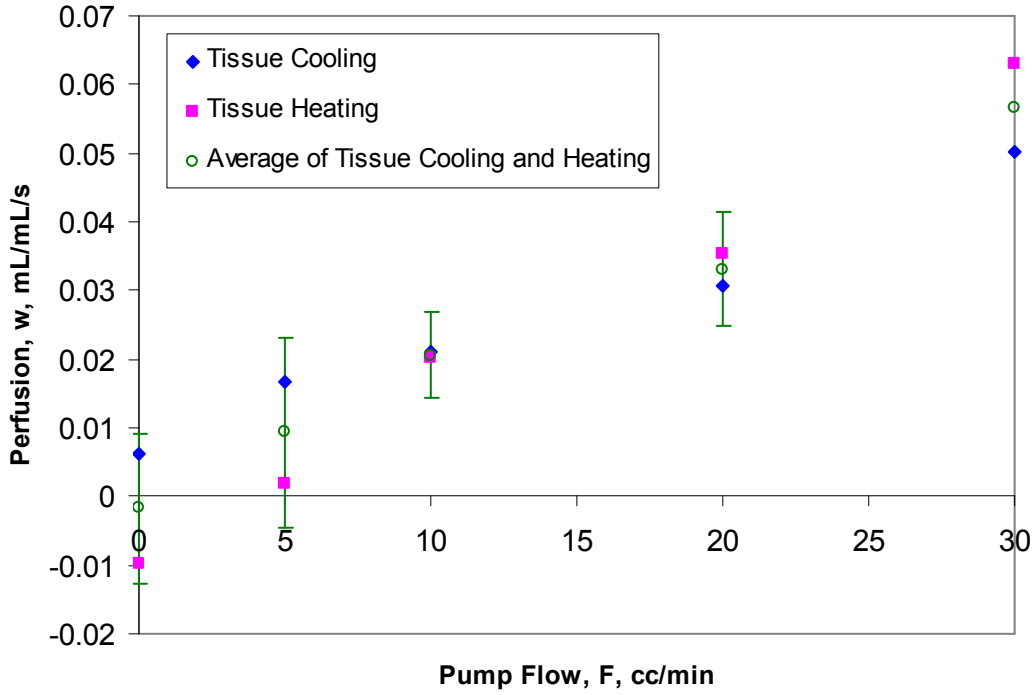

Figure 7.8. Average perfusion values for Tissue Cooling and Tissue Heat ing for a single cycle

7.4 The Thermoelectric Perfusion Probe's Continuous Monitoring Results

For this research to produce a viable medical device, it is desired that this device work continuously. Therefore, this section discusses the results of extended time Thermoelectric Perfusion Probe experiments that were conducted to simulate continuous monitoring. A 69 minute test (17 cycles), was conducted on the phantom tissue test stand. During the test, the sensor temperature and the probe temperature were continuously measured while the top temperature and the arterial temperature were measured at the beginning of each cycle. If this device is truly continuous then accurate perfusion estimates should be obtainable from each of the 34 half cycles. To test if the Thermoelectric Perfusion Probe was producing accurate results, the flow rate was altered during this extended test. Figure 7.9 displays the experimental heat flux along with a diagram of the flow during that period of time. Therefore, after each cycle the flow rate was either increased or decreased. The flow rate was not drastically changed after each cycle so it was assumed that the time it took for the pump to ramp up or down to the new flow rate was negligible and would not affect the perfusion predictions. This curve was

then broken into 34 (17 cooling portions and 17 heating portions) different files, as discussed in the Chapter 4.

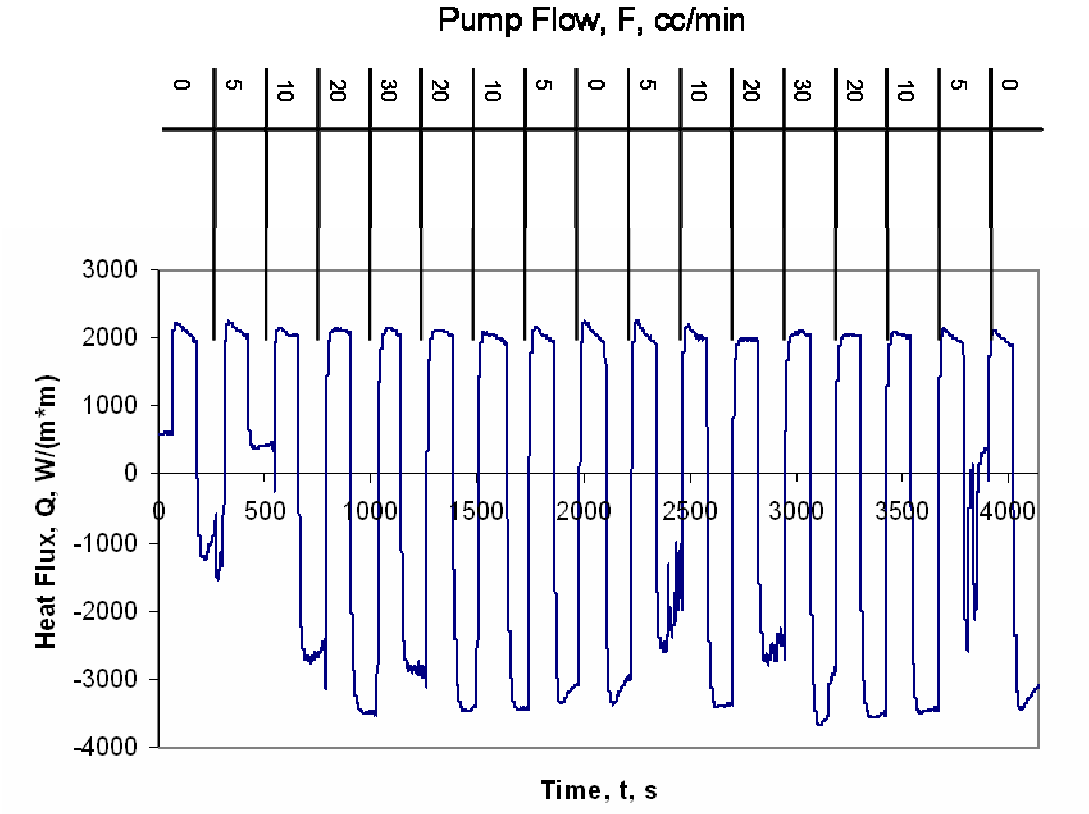

Figure 7.9. A plot of the experimental heat flux data during the 69 minute test. The flow rate was changed every 4 minutes.

7.4.1 Heat Sink Sufficiency Results

For the Thermoelectric Perfusion Probe to be a viable medical device, then it must be assured that the patients' safety be maintained while the probe is being utilized. The TEC will produce heat that must be exhausted to the environment. If the heat is not properly exhausted then the entire probe will warm to a temperature that could burn the patient. Burning, is patient specific, however, it normally occurs at 42-46˚C. Therefore, a heat sink was designed and built to remove all the excess heat while keeping the overall probe temperature reasonable. After the probe was assembled with the TEC, several lengthy tests were conducted to test the effectiveness of the heat sink.

To test the heat sink's capabilities, the maximum and minimum voltage the voltage controller could output was used for testing. The maximum voltage was sent to

the TEC for two minutes, and then the minimum voltage was sent to the TEC for two minutes. Then the temperature at the heat sink-TEC interface (probe temperature) was monitored along with the sensor temperature, Figure 7.10. The room temperature during the experiment was 25.9˚C. The probe temperature rose above the atmospheric temperature until the heat produced by the thermoelectric cooler was equal to the heat loss by the heat sink through convection to the atmosphere. The important thing to notice is how the average probe temperature over a cycle remains constant at 35˚C after the initial ramp up period. This was 9.1˚C above the atmospheric temperature. Therefore, if this probe was used at room temperature 22˚C, the probe temperature would be 31.2˚C which is comparable to skin temperature. This is a safe working temperature. In a medical situation the sensor temperature would be maintained between 25˚C and 42˚C. As can be seen from the results, the sensor temperature for this test was above the range the Thermoelectric Perfusion Probe would operate in a medical situation. The jagged temperatures in some of the heating and cooling portions of the cycle were not experimental errors, but real temperature differences caused by disruption of the voltage controller. When the voltage controller is disrupted the output voltage is changed.

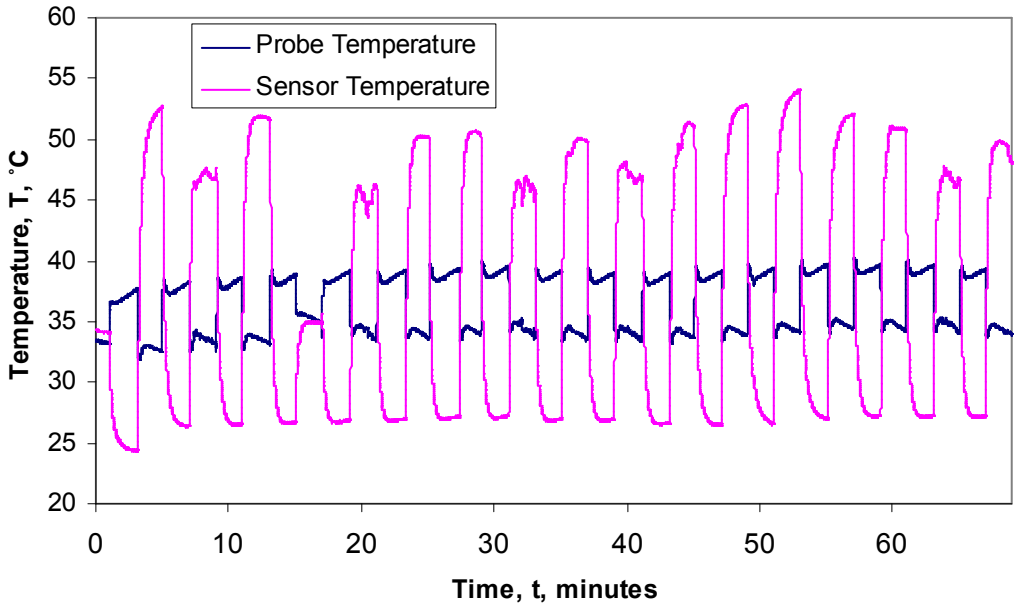

Figure 7.10. The temperature profiles produced by the Thermoelectric Perfusion Probe when the TEC is allowed to consume its maximum recommended voltage.

7.4.2 Continuous Test Results with the First Version (Without Temperature Recycling) of the Thermoelectric Perfusion Probe's Perfusion Estimation Program

After, this extended test was performed; the initial goal was to determine if perfusion estimates could be obtained from these long experiments. The heat flux and temperature from all 34 different files (17 cooling and 17 heating) were processed with the first version of the Thermoelectric Perfusion Probe's perfusion estimation program. The first version of the Thermoelectric Perfusion Probe did not have temperature recycling.

As discussed above the arterial temperature and the top temperature was recorded at the beginning of each cycle during the long test. These temperatures were used to make the initial temperature profile for the cooling portion of a cycle. These temperatures were also used to make the initial temperature profile for the heating portion of the cycle. Perfusion estimates were obtained from all the heating/cooling portions of the cycle and plotted in Figure 7.11.

There was a strong upward trend for both tissue cooling and tissue heating portions of the cycle. There was not a significant amount of scatter for the data for the heating perfusion estimates and the cooling perfusion estimates. Also, because the flow rates were varied throughout the experiment, this graph proves that the Thermoelectric Perfusion Probe could work for long periods of time without losing accuracy. As discussed above there were some areas of sporadic and jagged heat flux. However, these sections of the data still produced good perfusion estimates. This meant the sporadic heat flux actually occurred and there were no instrumentation problems.

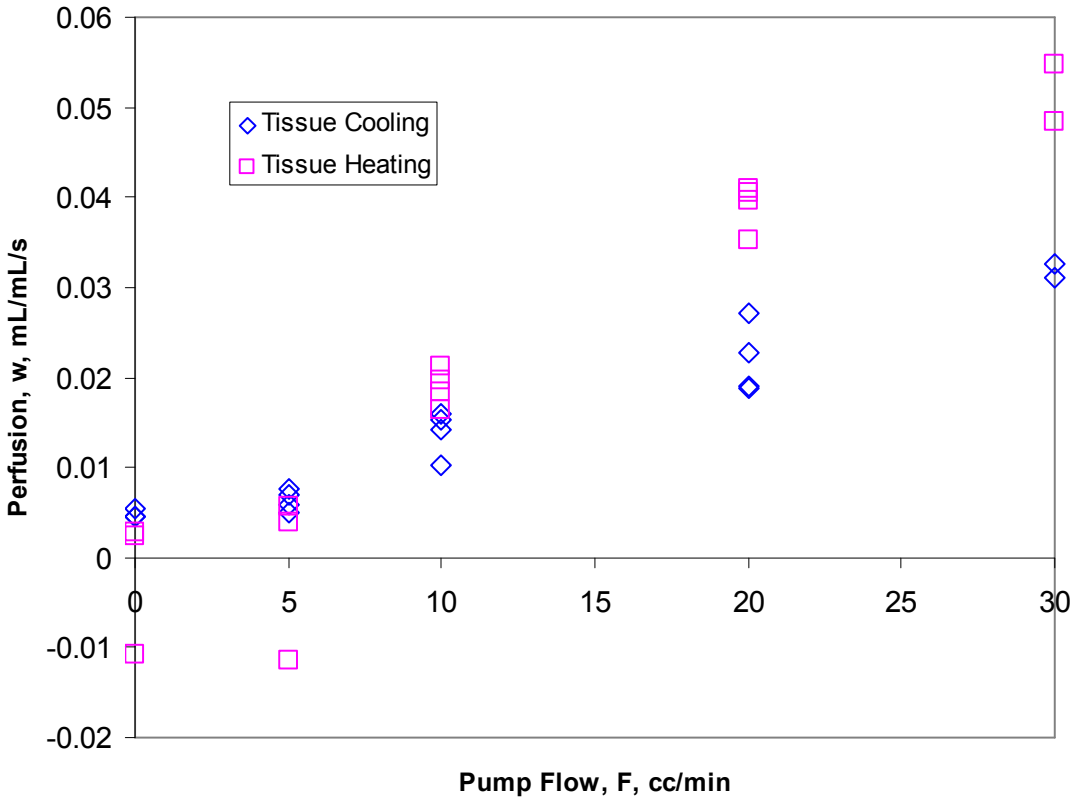

Figure 7.11. Perfusion estimates for the 69 minute test with the first version of the Blood Perfusion Probe's perfusion estimation program

The next step was to compare the average perfusion values for the tissue cooling results and the tissue heating results. Therefore, Figure 7.12 was constructed with the overall average perfusion values plotted with their 95% confidence interval. The 95% confidence interval for the 30 cc/min flow rate was not graphed because it was extensive and would not fit the scale of the graph. The heating portion of the cycle produced an upward trend with an offset of -0.00187 mL/mL/s. This offset is negligible. The heating results showed the expected upward trend. It was slightly concerning that the perfusion estimates for the 0 cc/min flow rate and the 5 cc/min flow rate were close. The cooling results also showed the expected upward trend. The cooling results had an offset of 0.0049 mL/mL/s. Again it was slightly concerning that the 0 cc/min flow rate and the 5 cc/min flow rate produced almost identical values. When the heating and cooling results were combined, an overall offset of 0.0015 mL/mL/s resulted. The reason the perfusions at a 0 cc/min flow rate and at a 5 cc/min flow rate were almost identical was because the

water doesn't reach the skin. It was shown in the computational model that at very low flow rates (5 cc/min or less), the water can't flow to the top of the sponge.

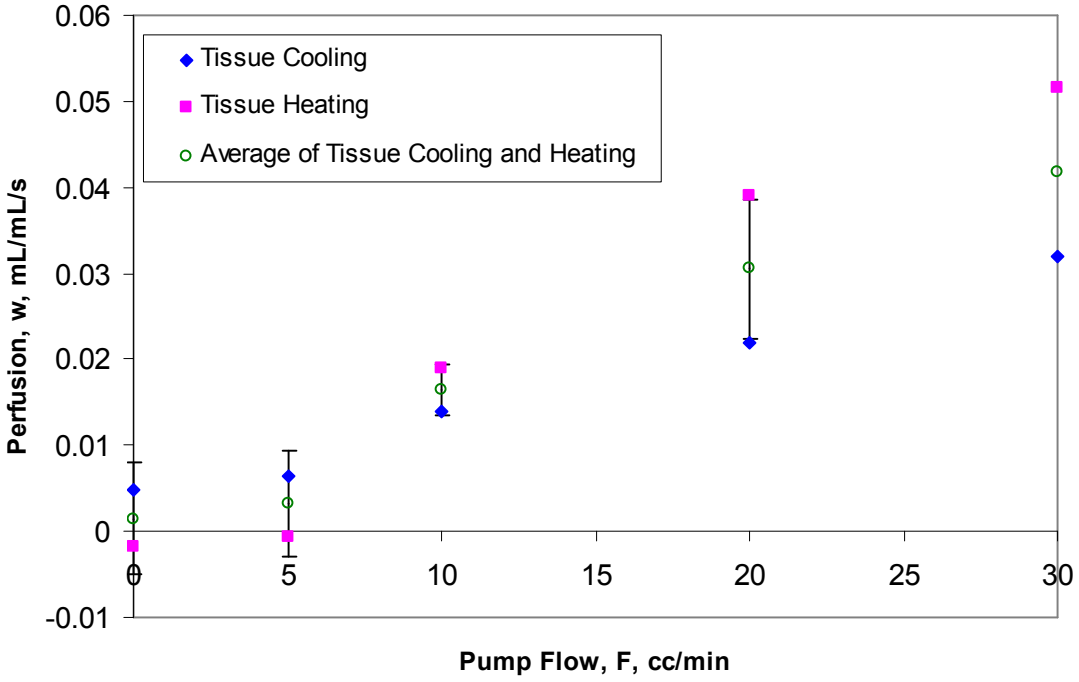

Figure 7.12. The average perfusion values for the 69 minute test using the Thermoelectric Perfusion Probe's first generation perfusion estimation program

7.4.3 Continuous Test Results with the final version of the Thermoelectric Perfusion Probe's Perfusion Estimation Program

The next step was to determine the perfusion estimates based on the extended test when temperature recycling was added to the Thermoelectric Perfusion Probe's estimation program, Figure 7.13. To make the temperature profile for the first thermal event (cooling) in the first cycle, an average arterial temperature was used. The average arterial temperature was determined based on the arterial temperatures recorded throughout the experiment. This Figure showed the expected upward trend for the tissue cooling results and the tissue heating results.

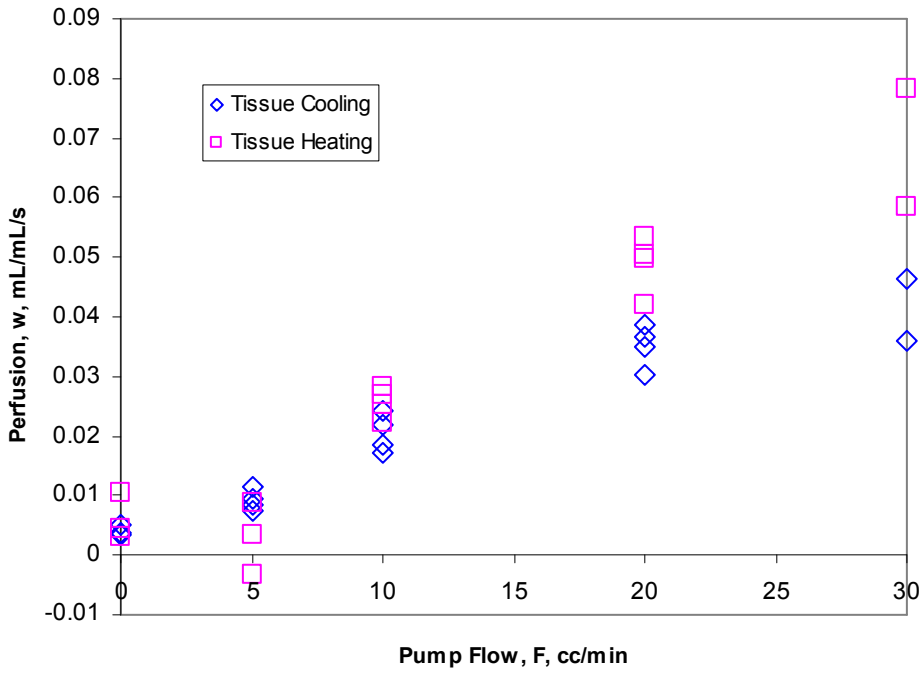

Figure 7.13. Perfusion estimates for the 69 minute test with the final version of the Blood Perfusion Probe's perfusion estimation program

Figure 7.13 does not allow for a good comparison of the difference between the tissue cooling results and the tissue heating results. Therefore, the average values for the tissue cooling and the tissue heating are presented in Figure 7.14. The average of the tissue cooling results and the tissue heating results are plotted with their 95% confidence interval. From these results both the cooing and the heating data produce the expected linear trend. The tissue cooling produced reasonable results and had an offset of 0.0041 mL/mL/s. The tissue heating resulted in a larger offset of 0.0059 mL/mL/s. When all the results were combined, the test showed an overall offset of 0.004985 mL/mL/s. It was promising that the offsets for both the cycles were close. The only concerning result was that the average tissue heating perfusion at 0 cc/min was higher than the average tissue heating perfusion at 0 cc/min.

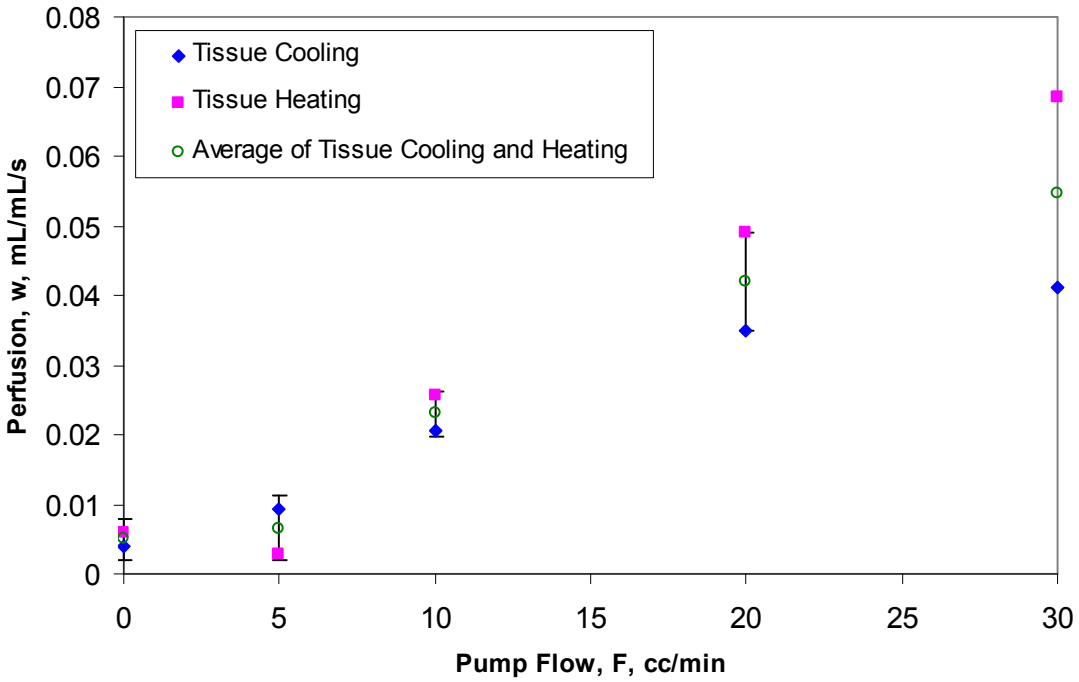

Figure 7.14. The average perfusion values for Tissue Cooling and Tissue Heating

7.4.4 A comparison the two versions of the Thermoelectric Perfusion Probe's Perfusion Estimation Program

The next step was to determine if using temperature recycling in the Thermoelectric Perfusion Probe's perfusion estimation program improved the results. Early, it was shown how much the results were improved for the curve matching. Therefore, the perfusion estimates that were obtained from the first version of the Thermoelectric Perfusion Probe's perfusion estimation program were compared to the results from the final version of the Thermoelectric Perfusion Probe's estimation program. These results were also compared to the Fluent® results (CFD Flow Model), Figure 7.15. The CFD Flow Model is the best estimate as to the actual perfusion in the phantom tissue test stand. Both versions of the Thermoelectric Perfusion Probe's perfusion estimation program produced lower results in comparison to the CFD Flow Model. It is believed this was caused by poor contact between the sensor thermocouple and the skin. However, it is very clear that the Thermoelectric Perfusion Probe has the same trend as the CFD Flow Model results. The implementation of temperature recycling into the Thermoelectric Perfusion Probe's perfusion estimation program caused

the perfusion estimates to be closer to the CFD Flow Model for high flow rates, as it appeared to move the perfusion values up.

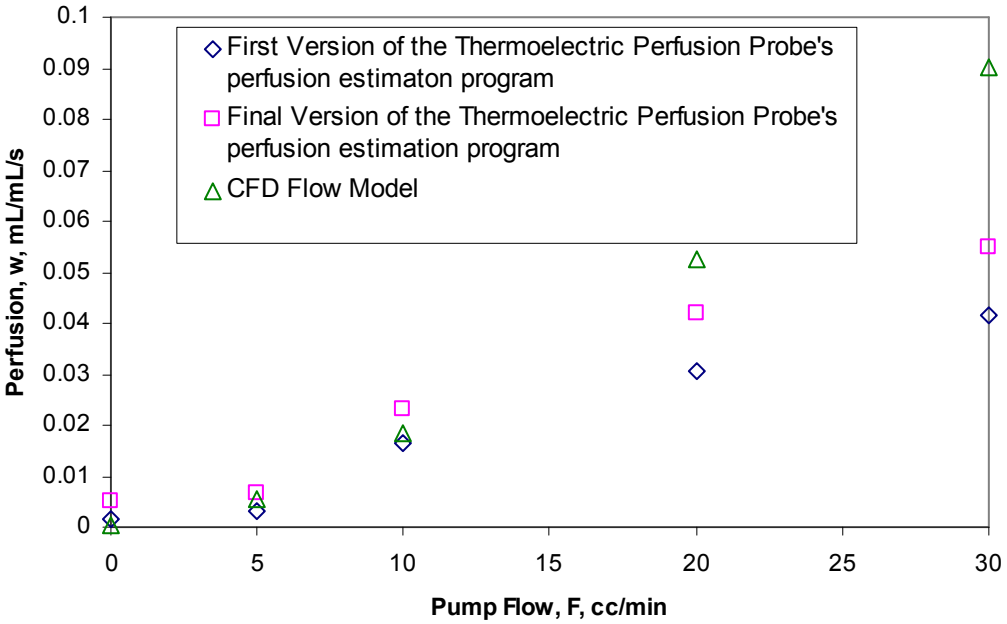

Figure 7.15. The average perfusion estimates for the 69 minute test.

It still remained difficult to draw conclusions because of the offsets associated with the perfusions based on the CFD Flow Model, the Thermoelectric Perfusion Probe's perfusion estimation with temperature recycling, and the Thermoelectric Perfusion Probe's perfusion estimation without temperature recycling. Therefore, the offsets were removed and the graph was reproduced, Figure 7.16. As can be seen from the Figure with the offset removed, the results with Temperature Recycling (the final version of the Thermoelectric Perfusion Probe's perfusion estimation program) were much better than results without temperature recycling (the first version of the Thermoelectric Perfusion Probe's perfusion estimation program). Temperature recycling caused the results at higher perfusions to increase. The results are still much lower than the CFD Flow Model; however, it is within range considering the limitations of the experimentation.

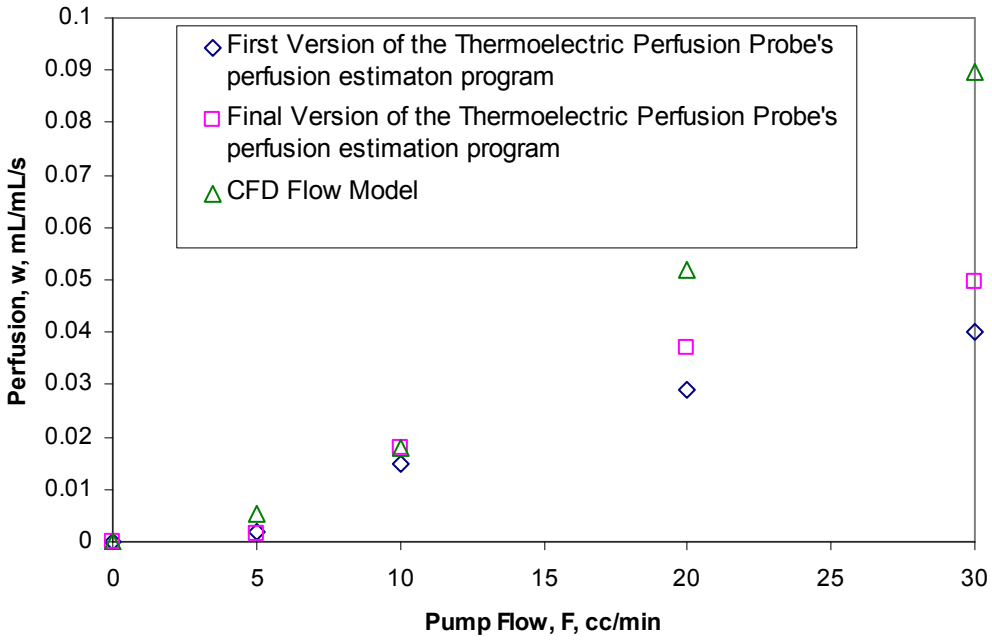

Figure 7.16. The average perfusion estimates the 69 minute test with the offset removed.

The next step was to determine if the time the experiments were taken had any effect on the perfusion estimates, Figure 7.17. Theoretically, the perfusion estimates would be independent of when they were conducted in the experiment. In Figure 7.17 a trend did not appear, the estimates were randomly distributed. This proved the perfusion estimates were independent of when they were taken in the experiment. The only area of concern was at 30 cc/min, where the decreasing flowrates produced higher perfusion estimates than increasing flowrates. This was probably due to the fact that the increasing flowrates data incorporated the cooling portion of the cycle when the flow was increased to 30 cc/min. The decreasing flowrates data incorporated the heating portion of the cycle when the flow had already been set to 30 cc/min for two minutes (during the cooling portion of the cycle).

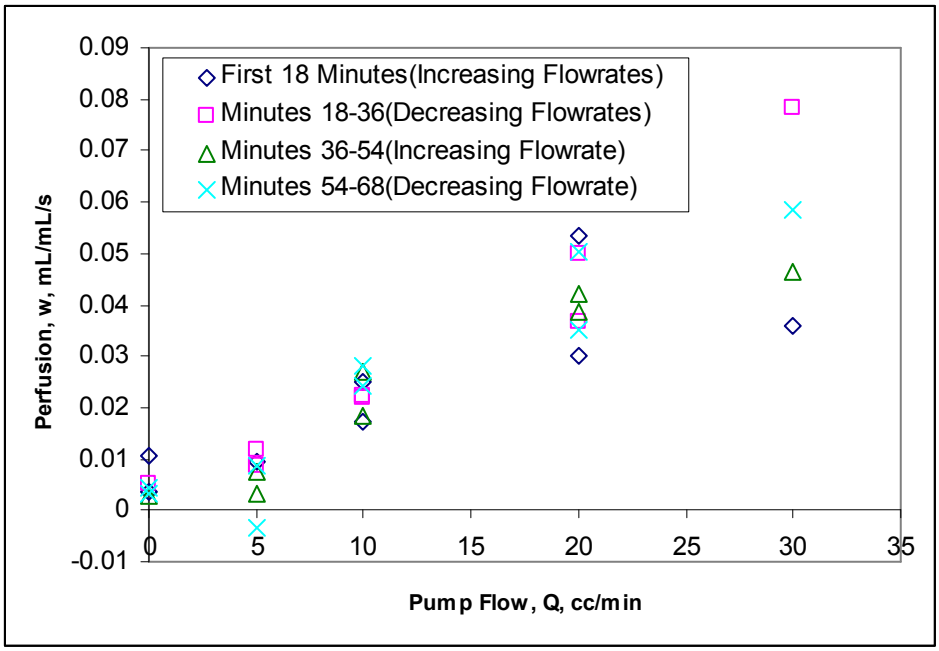

Figure 7.17. Perfusion Estimates for the 69 minute tests with the results broken up to when they were taken in the experiment.

7.5 Comparison of Thermoelectric Perfusion Probe to the Convective Perfusion Probe and the Fluent® Model

All the perfusion estimates from the experimentation with the Thermoelectric Perfusion Probe including the sensitivity tests and the continuous monitoring tests, were combined to determine how well the Thermoelectric Perfusion Probe performed compared to the CFD Flow Model and the Convective Perfusion Probe, Figure 7.18. The perfusion estimates for the all the experiments were obtained with the Thermoelectric Perfusion Probe's perfusion estimation program. The perfusion estimates for the Convective Perfusion Probe where obtained from 13 experiments at each flow rate. The average perfusion values for the Thermoelectric Perfusion Probe and their 95% confidence intervals were based on the results from all the sensitivity experiments (1 cycle) and the continuous measurement experiment (34 cycles). All three perfusion determining methods showed an upward trend with the CFD Flow Model producing the largest perfusion values, while the Convective Perfusion Probe produced slightly smaller perfusion estimates, and the Thermoelectric Perfusion Probe produced the smallest perfusion estimates. The CFD Flow Model and the Convective Perfusion Probe had a negligible offset while the Thermoelectric Perfusion Probe had an offset of 0.0027

mL/mL/s. This Figure is remade in Appendix D with the offset removed. These are very encouraging results because it shows the perfusion estimates from experimentation with the Thermoelectric Probe produced the expected trend and is also within range of both the Convective Perfusion Probe's perfusion estimates and the CFD Flow Model's perfusion estimates. All the Convective Perfusion Probe and the CFD Flow Model perfusion estimates were very close to the Thermoelectric Perfusion Probe's 95% confidence interval except at a flow rate of 30 cc/min.

Analysis of variance was then completed for all the Thermoelectric Perfusion Probe data. The data was broken up into five sections according to the flowrate it was recorded at. This statistical test calculates the probability that all five population means corresponding to the flowrates are the same. The probability that all the population means were the same was 5.5×10^{-28}. This means there is a 99.99999% chance that at least one of the population means was different. Then, a multiple comparison test was performed for both data sets, with a significance level of 0.05; an example plot can be seen in Appendix D. This test compares a pair of the flowrate data to determine if there is greater than 5% chance that the population means are the same. Then, the test compares another pair of flowrate data, until all pairs are compared. Therefore, it can be determined if all flowrates are statistically different one another. This test proved that all pairs of means were statistically different except the means at 0 cc/min and the means at 5 cc/min. Therefore, the mean perfusions corresponding to 10 cc/min 20 cc/min and 30 cc/min are statistically different then the mean perfusions corresponding to 0 cc/min and 5 cc/min. Therefore, it can be concluded that the perfusion values for the Thermoelectric Perfusion Probe has been proven to be dependent on flowrate above a 5 cc/min flowrate.

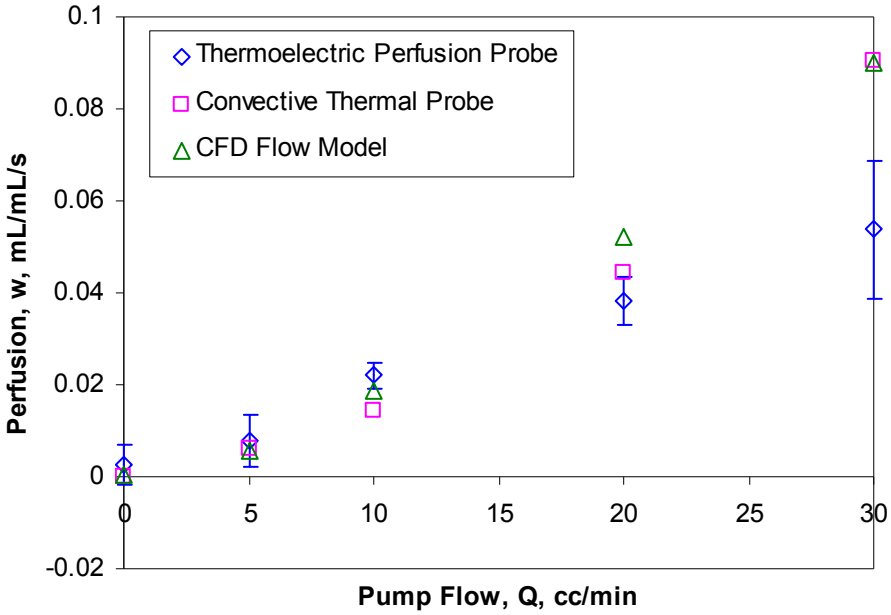

Figure 7.18 Comparison plot of the average Thermoelectric Perfusion Probe, Convective Perfusion Probe, and Fluent®

The final step was to determine if there was a significant difference between the tissue cooling portion of the cycle and the tissue heating portion of the cycle for the Thermoelectric Perfusion Probe. Therefore, the average tissue cooling and tissue heating perfusions for the Thermoelectric Perfusion Probe were plotted against the perfusion estimates produced from the CFD Flow Model and from experimentation with the Convective Perfusion Probe. The results, Figure 7.19, showed that at certain flow rates the cooling portion of the cycle produced higher perfusions, while at other flow rates the tissue heating portion of the cycle produced larger perfusion values. This Figure is remade in Appendix D with the offset removed. For all flow rates, they are both very reasonable and close to the Convective Perfusion Probe's perfusion values and the CFD Model's perfusion values. Overall, the offset for the Thermoelectric Perfusion Probe Tissue cooling was 0.0051 mL/mL/s while the offset for the Thermoelectric Perfusion Probe Tissue heating was -0.0003 mL/mL/s. These offsets are very small and are reasonable for there experiments.

Analysis of variance, previously explained, was then completed on both the cooling data and the heating data. The probability that the means were the same for the cooling data was 6.7×10^{-13}. The probability that the means were the same for the

heating data was 1.56 x 10^{-9}. Then, a multiple comparison test, previously explained, was performed for both data sets, with a significance level of 0.05. These tests proved that all pairs of means were statistically different for tissue cooling. The mean perfusion values for tissue cooling at flowrates of 0 cc/min 5 cc/min 10 cc/min 20 cc/min and 30 cc/min are statistically different; and therefore, the perfusion for tissue cooling has been proven to be dependent on flowrate. These tests proved that all pairs of means were statistically different for tissue heating except the means at 0 cc/min and the means at 5 cc/min The mean perfusion values for tissue heating at flowrates of 10 cc/min 20 cc/min and 30 cc/min are statically different than the perfusion values at 0 cc/min and 5 cc/min. Therefore, it can be concluded that the perfusion for tissue heating has been proven to be dependent on flowrate above a 5 cc/min flowrate.

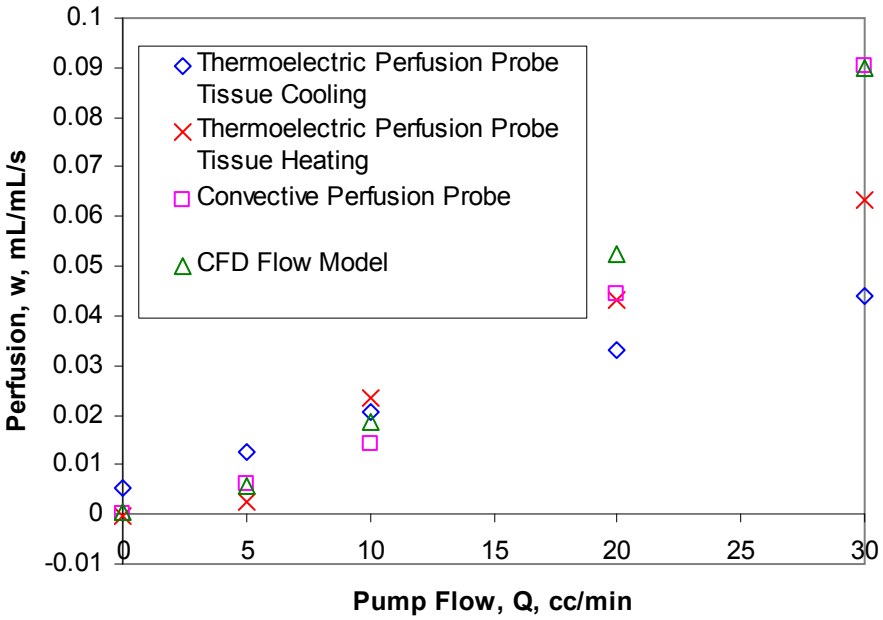

Figure 7.19. Comparison plot showing the difference between the perfusion predictions of the tissue cooling portion of the cycle and the tissue heating portion of the cycle.

7.6 Experimental Conclusions

Based on the experimentation with the Thermoelectric Perfusion Probe, the probe was proven to be repeatable and sensitive during continuous testing. Overall, it was shown that the Thermoelectric Perfusion Probe showed sensitivity and had statistically different means at all flowrates besides 0 and 5 cc/min. The Thermoelectric Perfusion

Probe displayed the same trend as both the CFD Flow Model and the Convective Perfusion Probe. The heat sink was proven to be sufficient to remove all excess heat.

Chapter 8 Conclusions

Based on the research presented in this document, it is clear that the Thermoelectric Perfusion Probe is a viable option for measuring perfusion. The current research has shown that the Thermoelectric Perfusion Probe is repeatable, sensitive, and can be used for continuous measurements. The current research has also shown that a pressed sensor in conjunction with the Thermoelectric Perfusion Probe's perfusion estimation program is a viable way to measure perfusion.

The Convective Perfusion Probe tests proved the Thermoelectric Perfusion Probe's perfusion estimation program was more repeatable then the Convective Perfusion Probe's perfusion estimation program. This is because the results produced by the Thermoelectric Perfusion Probe's perfusion estimation program had smaller confidence intervals for all flowrates than the results produced by the Convective Perfusion Probe's perfusion estimation program. The Convective Perfusion Probe experiments also proved a pressed sensor in conjunction with the Thermoelectric Perfusion Probe's perfusion can determine perfusion regardless of how the thermal event is created

The Thermoelectric Perfusion Probe's perfusion estimation program with temperature recycling had smaller sum of squares than the Thermoelectric Perfusion Probe's perfusion estimation program without temperature recycling. This means temperature recycling greatly improved curve matching. Through experimentation it was proven the Thermoelectric Perfusion Probe's heat sink could remove enough heat to keep the device at a constant temperature. The testing also showed the Thermoelectric Perfusion Probe could run for long periods of time without malfunctioning.

The Thermoelectric Perfusion Probe experiments also proved the Thermoelectric Perfusion Probe had reasonable sensitivity and repeatability for continuous monitoring. When all the experimental results were combined, the Thermoelectric Perfusion Probe results had very small confidence intervals, less than ±0.006 mL/mL/s except at a flowrate of 30 cc/min. The large confidence interval at 30 cc/min, ±0.014 mL/mL/s could be due to not having enough experiments at this flowrate, or the fact that errors get amplified at high flowrates. Also, the Thermoelectric Perfusion Probe proved to have

very good repeatability based on the testing. Slight differences still occur between perfusion estimates for the heating portion and the cooling portions of cycles, however, these differences are small. The difference between the heating portion and the cooling portions of cycles was less than 0.01 mL/mL/s except at a flowrate of 30 cc/min.

When all the experimental results were combined a multi-comparison test proved that the average perfusion values for the flowrates of 10 cc/min 20 cc/min and 30 cc/min were different than the average perfusion values for the flowrates of 0 cc/min and 5 cc/min. Therefore, the Thermoelectric Perfusion Probe's perfusion estimates were proven to be dependent on flowrate above 5cc/min of flow.

Overall the results from the Thermoelectric Perfusion Probe did not completely match the Convective Perfusion Probe' results or the computational fluid model's results. However, the Thermoelectric Perfusion Probe's results displayed the same trend as the Convective Perfusion Probe's results and the computational fluid model's results. The difference could easily be explained by experimental problems associated with the sensor temperature measurements.

Through extensive work on the perfusion estimation program and experimentation on the phantom tissue test stand, the Thermoelectric Perfusion Probe has been proven as a perfusion measuring system. The device is sensitive, repeatable, and can be used for continuous measurements. This work is proof that this concept of the Thermoelectric Perfusion Probe can be developed into a Medical Device.

Chapter 9 Recommendations

It has been shown that the Thermoelectric Perfusion Probe is a viable option to measure perfusion. However, there are a few steps that need to be completed to turn this probe from a concept into a working medical device. Also, work needs to be completed to turn the phantom tissue test stand into a calibration system for all perfusion measuring systems. There are a few alterations that need to be made to the Thermoelectric Perfusion Probe. Also, the perfusion estimation program needs to be simplified and altered to increase speed and accuracy. Finally, the phantom tissue test stand must be redesigned so it is constructed out of all plastic.

9.1 Recommendations for the Thermoelectric Perfusion Probe

One important aspect of making the Thermoelectric Perfusion Probe into a working device is to have it be a completely integrated system. Therefore, it would be preferable to have one cord coming from the probe that would act as a data collection/controller unit. Currently, this is not possible because multiple thermocouples require an extra thermocouple reader. Therefore, thermistors are currently being tested to replace thermocouples. Also, another important aspect is to make the Thermoelectric Perfusion Probe more automated. To do this, the electrical current driving the Thermoelectric Perfusion Probe needs to be computer controlled.

Thermocouples have the ability to measure voltage differences quite well. However, they can't be used to measure absolute temperatures. Also, the voltage outputs by thermocouples are very small and require an amplifier. Therefore, the goal is to begin using thermistors in place of thermocouples. A thermistor is a device that varies its resistance with temperature, Figure 9.1. As can be seen the resistance varies nonlinearly with temperature. Therefore, a fourth-order equation is used to relate the resistances with temperature. This relationship was for the GE NTC Thermistors: Type MA which has a diameter of 0.762 cm (0.3 in). These thermistors were chosen because they are designed

specifically for medical use and they were very small. Small thermistors are preferable because the goal is to have a compact perfusion measuring system.

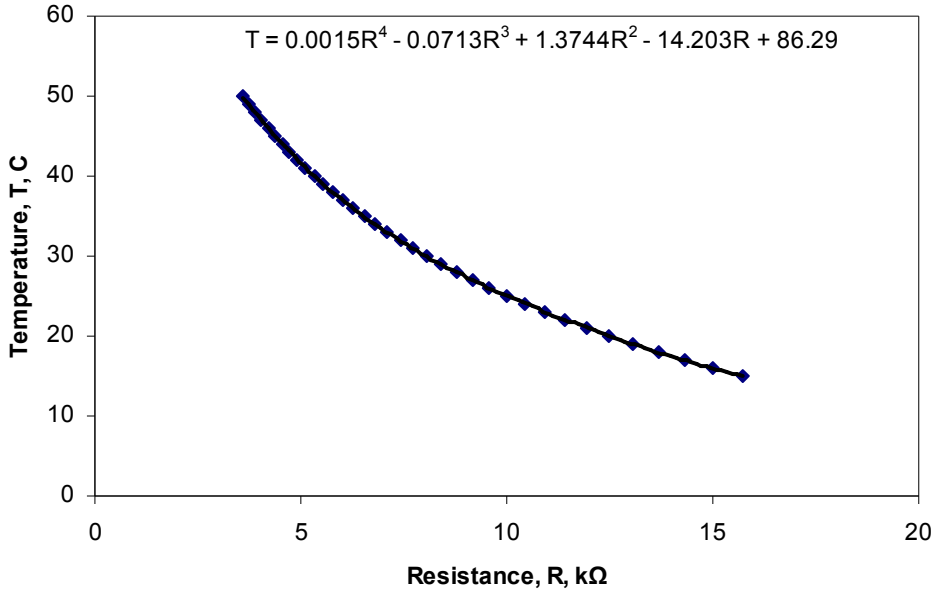

Figure 9.1. Temperature vs. Resistance plot for the GE NTC Thermistors: Type MA.

Another advantage of thermistors is they allow the user to determine the order of magnitude of the output voltage. To determine the resistance of the thermistors, a known voltage has to be placed over a voltage divider. In the voltage divider, one resistor's resistance will be known while the other resistor will be the thermistor which is unknown. Then, the voltage across the thermistor can be used to determine the resistance of the thermistor based on Equation 4,

$$R_{Thermistor} = \frac{V_{Thermistor} * R_{Known}}{V_{Input} - V_{Thermistor}} \qquad 4$$

where $V_{Thermistor}$ is the voltage measured across the thermistor, V_{Input} is the voltage input into the voltage divider, and R_{Known} is the resistance of the known resistor. Then, the temperature can be derived based on the fourth-order equation in Figure 9.1. Therefore, the order of magnitude of thermistor voltage can be set by adjusting the resistance of R_{Known}.

The next step was to determine how to incorporate this system into the current data recording system. The NI DQ PAD 6015 which we use to record the data also has the ability to output DC voltages. Therefore, a special VI was developed to output a DC voltage from the DAQ, Appendix E. The DAQ is limited to outputting small currents, therefore the R_{Known} had to be very high. Also, after experimentation it was found that there was noise while using the thermistors in conjunction with the DAQ and therefore a low pass filter was needed. The reason for the noise was due to the fact the voltage source was from the DAQ, which was deriving the voltage from an AC voltage. In total four thermistors will be needed for the measuring system.

Therefore, a circuit was created that allowed the DAQ to supply the voltage to the thermistors and then record the voltage across the thermistor, Figure 9.2. The DAQ outputs 1.25V and then the three individual thermistor circuits are placed in parallel from this output. The voltage for each thermistor goes through a 100kΩ resistor for the voltage dividing, and then through the thermistor which is connected to the ground of the DAQ. The voltage across the thermistor is split off into parallel and put through a low pass filter. The low pass filter is designed to filter all AC voltages above 6Hz. The low pass filter is made of an 8.66kΩ resistor and a $3.3\mu F$ capacitor. Then, the signal is measured by the DAQ. This system has been developed and used for preliminary testing,

results are in Appendix E. However, this system needs to be refined and validated.

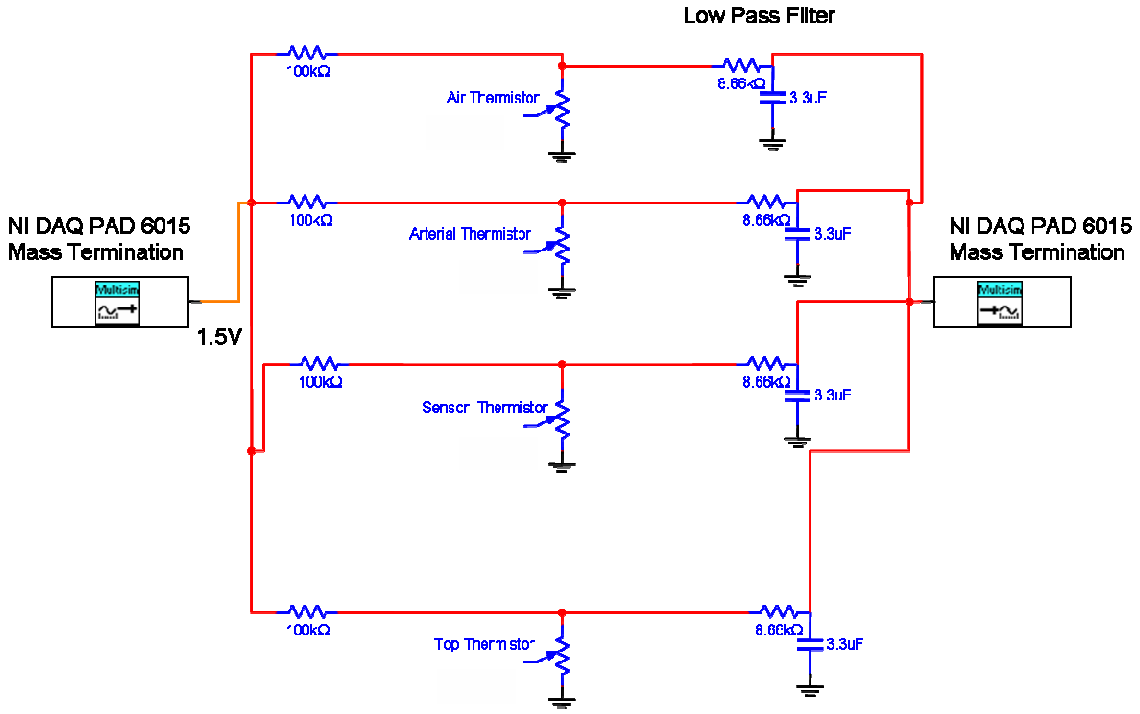

Figure 9.2. The circuit diagram for the thermistor system

Another important step will be to develop the circuitry so the DAQ can control the voltage into the TEC. A limitation of the DAQ is it can only output 50mA. The TEC requires a current of up to two amps. Therefore, a voltage to current circuit needs to be developed to allow the DAQ to output a certain voltage and then the circuit will output the required current for the TEC. This will give the system great flexibility and control as can be seen in Figure 9.3. With this new system a feedback loop can be made so the temperature along the skin can be monitored and controlled. This will allow for a more automated system and will prevent patients from burning. Also, this will allow for a finer control of the thermal event which will allow for a more precise thermal event and a better perfusion estimate. The combination of the new circuitry and the thermistors will make this a completely integrated electronic system

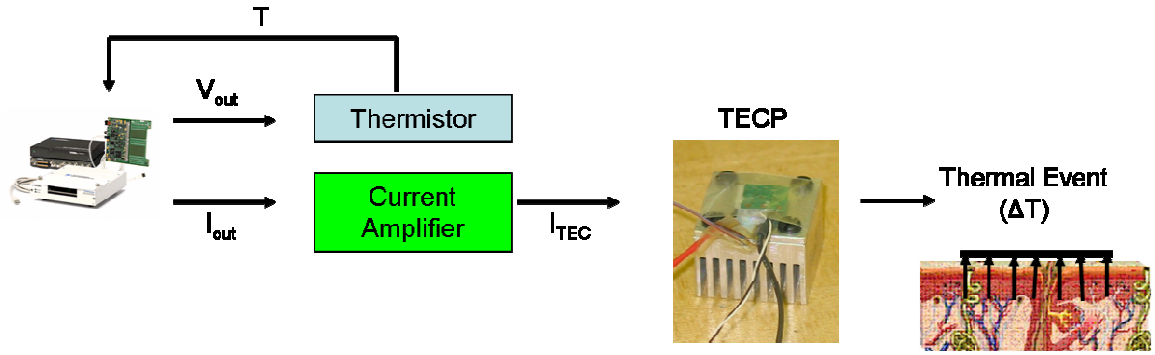

Figure 9.3. A schematic of the integrated Thermoelectric Perfusion Probe.

Another recommendation for the Thermoelectric Perfusion Probe is to redesign the heat sink and holding plate. Both of these parts are much larger than the TEC and cause the Thermoelectric Perfusion Probe to be cumbersome. The probe is heavy and hard to balance on the tissue. The probe should be redesigned so the heat sink and the holding plate have a similar length and width as the heat flux sensor.

. The TEC requires a large current, which can result in a large magnetic field. This could possibly interfere with other medical devices. Therefore, a study needs to be completed to determine the impact of this magnetic field. It is believed that by slowly ramping to the desired voltage, the current will be controlled. This will result in fewer problems. Since, the interference will mainly occur during large current switches.

9.2 Recommendations for the Perfusion Estimation Program

The current results proved that it is reasonable to use the temperature measured at the skin heat sink interface for parameter estimation. However, this code does not exactly model the current system and complicates the system. Therefore, the next step will be to develop a finite difference code that will model the exact system, Figure 9.4. As can be seen from the figure the new system greatly reduces the modeling requirements. Then based on this new system, it will not matter how the thermal event is imposed on the top side of the heat flux sensor.

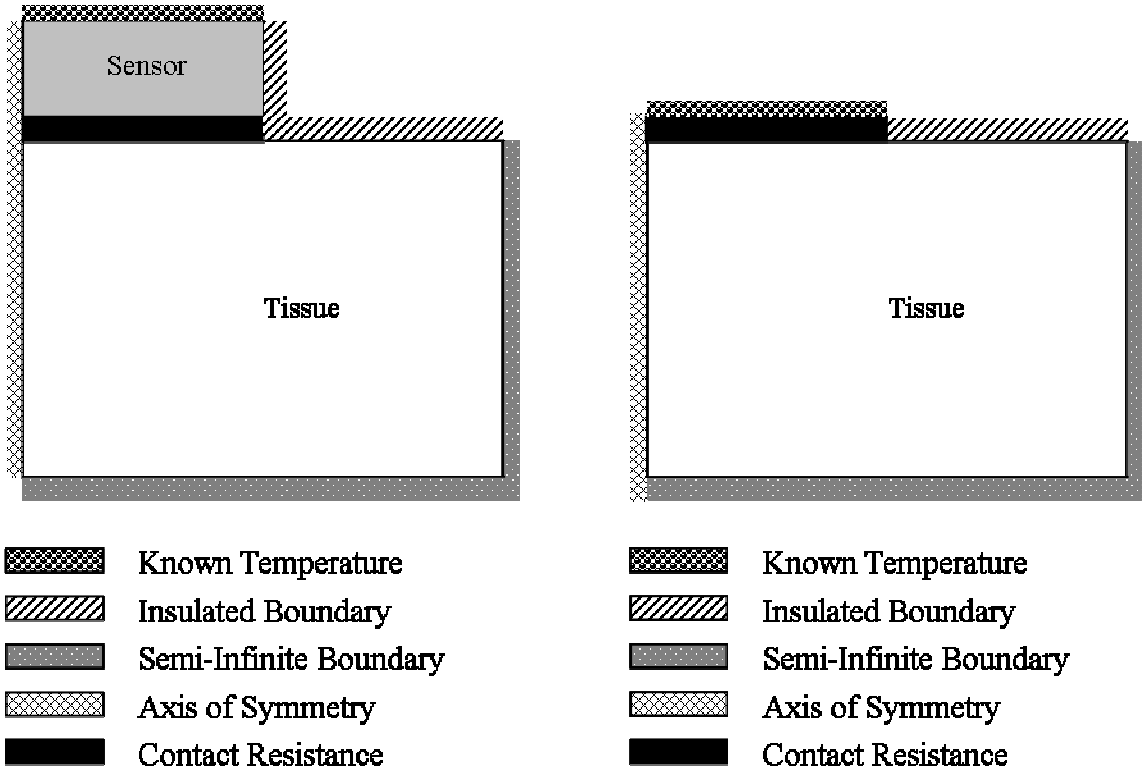

Figure 9.4. Schematic of the finite difference model for the Thermoelectric Perfusion Probe(Left) and the next generation finite difference model (Right).

These proposed changes will improve all aspects of perfusion estimation by simplifying data collection and modeling of the system. Therefore, the system will be more reliable because there will be fewer areas for failure. In earlier programs it was problematic to use the air temperature and a convective boundary condition because the exact convection coefficient is not exactly known. Furthermore, the value for the convective coefficient changes from day to day. Also, there are inaccuracies associated with the thermocouple and the amplifier system. This system will eliminate the inaccuracies caused by measuring the air temperature. This system will also decrease the inaccuracies in the finite difference program and decrease the computational time to determine perfusion values. It is very important to decrease computational time so that perfusion estimation can take place in the time it takes to complete one half of the cycle. This will allow for continuous measurements to be produced.

9.3 Recommendations for the Phantom Tissue Test Stand

The future goal of the phantom tissue test stand is to develop it so it can be used to validate, calibrate, and test other perfusion measuring systems. The current research is to develop this system so that it can be used in an MRI machine. This will be completed in two stages, first the current test stand was built with all plastic parts. The next step is for it to be tested with the Convective Perfusion Probe. Then, this system will be tested with an MRI machine. The next goal will be to develop a new test stand that will fit the requirements of an MRI machine better. It is also hoped that testing of the Thermal Diffusion Probe can be completed on the phantom tissue test stand for a comparison with the Convective Perfusion Probe.

The current phantom tissue test stand was recreated with all plastic parts. This will allow the system to be used in a situation with a magnetic field. The flow controller was placed lower on the tank so that the inlet for the MRI pump would be lower and would allow for fully mixed flow with the dye. A thicker sponge was used (greater than 1 inch) due to the scanning thickness limitations of the MRI system. The entire system was placed deeper in the tank to allow water to be placed on top of the hoop. A plastic plug was purchased to fill the top flowmeter hole. With slight modifications, it should be easy to change out the parts and hookup the current system for use with Dr. Robert Kraft's pump.

The future direction of this system is to make it more usable in an MRI machine. The limitation of the current test stand is the size and shape of this system. First, the test stand is square and doesn't properly model the size of a human body. Secondly, this test stand is not completely inclusive and water tight. This means that the test stand can't be rotated for different configurations. Dr. Kraft, for whom we are building this system, has requested the test stand be the same size and shape of a human head and the system needs to be fully enclosed to allow for different configurations. Therefore, an initial concept has been developed, Figure 9.5. This system will have an outlet from a pump that is split with a T into two tubes. Then, these tubes will enter into the hole for the inlets on either side of the sponge. The water will go through the sponge and then out two outlets. These outlet tubes will be joined by a T and then the water will flow into the pump inlet. This

entire unit will fit into a cylinder that is about the size of a human head. This tissue phantom will more accurately model perfusion because two jets of water colliding will cause substantially more convolution.

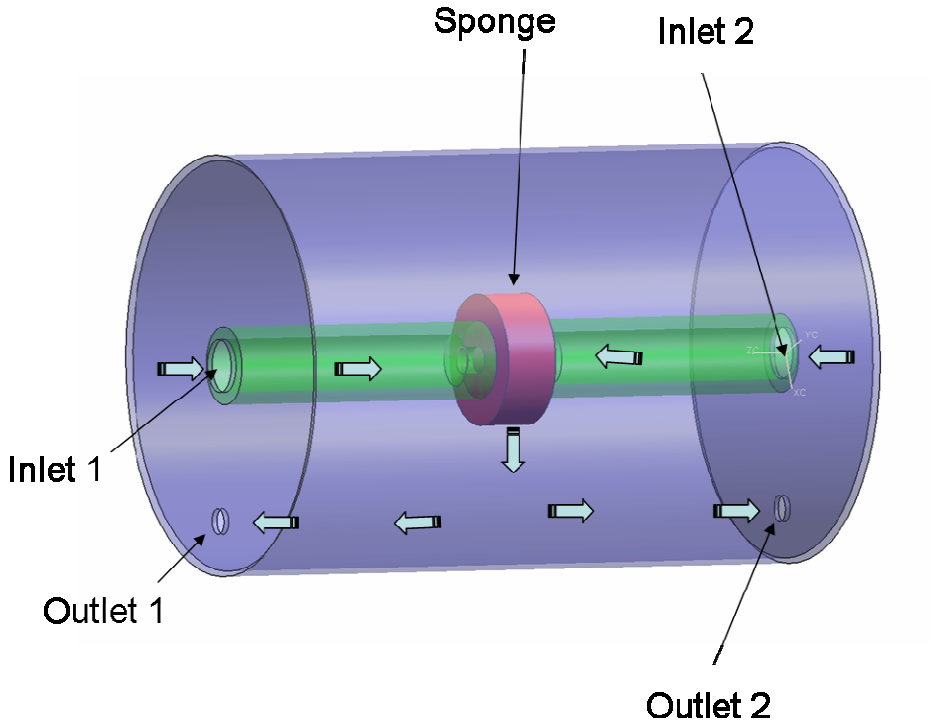

Figure 9.5. A schematic of the second generation test stand.

Bibliography

Anderson, G.T., and G. Burnside, 1990, "A Noninvasive Technique to Measure Perfusion Using a Focused Ultrasound Heating Source and a Tissue Surface Temperature Measurement," *Advances in Measuring and Computing Temperatures in Biomedicine: Thermal Tomography Techniques, Bio-Heat Transfer Models*, eds. R.G. Roemer et al., ASME, pp. 31-35.

Arnaud, F., G. Delhomme, A. Dittmar, P. Girard, L. Netchiporouk, C. Martelet, R. Cespuglio, W.H. Newman, 1994, "A Micro Thermal Diffusion Sensor for Non-Invasive Skin Characterization," *Sensors and Actuators. A, Physical*, 41-42, pp. 240-243.

Arkin, H., K.R. Holmes, M.M. Chen, W.G. Bottje, 1986a, "Thermal Pulse Decay Method for Simultaneous Measurement of Local Thermal Conductivity and Blood Perfusion: A Theoretical Analysis," *Journal of Biomechanical Engineering*, Vol. 108, No. 3, pp. 208-214.

Arkin, H., M.M. Chen, K.R. Holmes, 1986b, "Adaptive Thermal Modeling: A Concept for Measurement of Local Blood Perfusion in Heated Tissue," *Journal of Biomechanical Engineering*, Vol. 108, No. 4, pp. 306-311

Bowman, H., 1985, "Estimation of Tissue Blood Flow," in: *Heat Transfer in Medicine and Biology*, eds. A. Shitzer and R. Eberhart, Vol. 1, Chap. 9, Plenum Press, pp 193-203.

Boellaard, R., P. Knaapen, A. Rijbroek, G. J. J. Lutersema, A. A. Lammertsma, 2005, "Evaluation of Basis Function and Linear Least Squares Methods for Generating Parametric Blood Flow Images Using ^{15}O-Water and Positron Emission Tomography" *Molecular Imaging and Biology*

Brier, J. D. and Fercher A. F, 1982, "Retinal blood-flow visualization by means of laser speckle photography," *Investigative ophthalmology & visual science*. Vol 22., pp. 255-259.

Cheng, H., Q. Luo, Q. Liu, Q. Lu, H. Gong, S. Zeng., 2004, "Laser speckle imaging of blood flow in microcirculation" *Physics in Medicine and Biology*, Vol. 49., pp. 1347-1357.

Cardinali, A.V., Lanz, O.I., Diller, T.E., Scott, E.P., 2002, "Validation of a Noninvasive Blood Perfusion Measurement System using a Canine Medial Saphenous Fasciocutaneous Free Tissue Flap Model", *Proceedings of the ASME, IMECE'02, New Orleans*, Nov 17- 22, Paper No. 32354 .

Dias, M., J. Hadgraft, P. M. Glover, P. J. McDonald., 2003, "Stray field magnetic resonance imaging: a preliminary study of skin hydration" *Journal of Physics D: Applied Physics*, Vol 36., pp 364-638.

Ellis, B. E., Mudaliar, A., Ricketts, P. L, Lanz, O. I., Lee, C. Y.,Scott, E. P., and Diller, T. E., 2006, "Noninvasive Blood Perfusion Measurements of an Isolated Rat Liver and an Exposed Rat Kidney," submitted to *Journal of Biomechanical Engineering.*

Forrester, K. R., J. T. C. Leonard, C. Stewart, R. C. Bray, 2004, "A Laser Speckle Imaging Technique for Measuring Tissue Perfusion," *IEEE Transactions on Biomedical Engineering*, Vol. 51, No. 11, pp. 2074-2084.

Gregory, J. K., and J. Thirion., 2005 "Cardiovascular imaging to quantify the evolution of cardiac diseases in clinical development," Biomarkers, Vol. 10, pp. S1-S9.

Godfrey, S., 1996, "An introduction to thermoelectric coolers," *Melcor Corporation*, http://www.electronics-cooling.com/Resources/EC_Articles/SEP96/sep96_04.htm, Trenton, N.J.

Heymann, M. A., B. D. Payne, J. I. Hoffman, A. M. Rudolph, 1977, "Blood flow measurements with radionuclide-labeled particles," *Prognoses of Cardiovascular Disease,* Vol. 20, pp. 55-74.

Janssen, F.E.M, G. M. J. Van Leeuwen, A. A. Van Steenhoven, 2005, "Modelling of temperature and perfusion during scalp cooling," *Physics in Medicine and Biology*, Vol 50. pp 4065-4073.

Juillard L., M. F. Janier, D. Fouque, M. Lionnet, D. Le Bars, L. Cinotti, P. Barthez, C. Gharib, M. Laville, 2000, "Renal blood flow measurement by positron emission tomography using 15O-labeled water.," *Kidney International*, Vol. 57, pp. 2511-2518.

Khan, F., and D. J. Newton, 2003, "Laser Doppler Imaging in the Investigation of Lower Limb Wounds," *Journal of Lower Extremity Wounds,* Vol. 2, pp. 74-86.

Khot. M. B., P. K. M. Maitz, B. R. Phillips, H. F. Bowman, J. J. Pribaz, D. P. Orgill, 2005, "Thermal Diffusion Probe Analysis of Perfusion Changes in Vascular Occlusions of Rabbit Pedicle Flaps," *Plastic Reconstructive Surgery.,* Vol. 115, No. 4, pp. 1103-1109.

Kinuya, K., K. Kakuda, K. Nobata, S. Sakai, K. Yamamoto, S. Itoh, M. Ohashi, S. Kinuya, 2004, "Role of brain perfusion single-photon emission tomography in traumatic head injury," *Nuclear Medicine Communications*, Vol. 25, No 4, pp 333-337.

Kress, R., and R. Roemer, 1987, “A Comparative Analysis of Thermal Blood Perfusion Measurement Techniques,”

Leahy, M.J., de Mul, F.F.M., Nilsson, G.E., Maniewski, 1999, “ Principles and Practice of the Laser-Doppler Perfusion Technique”, *Technology and Health Care*, 7, pp. 143-162.

Li, H. J., X. X. Zhang, and Y. F. Yi, 2002, “Measurement of Blood Perfusion Using The Temperature Response to Constant Surface Heat Flux.” *International Journal of Thermophysics, Vol 2*, No. 6, pp 1631-1644.

Liebert, A., Leahy, M., Maniewski, R., 1995, “ A Calibration Standard for Laser-Doppler Perfusion Measurements”, *Rev. Sci. Instr.* 66(11), pp. 5169-5173.

Liu, J., and Xu, L.X., 1999, “Estimation of Blood Perfusion Using Phase Shift in Temperature Response to Sinusoidal Heating at the Skin Surface,” *IEEE Transactions on Biomedical Engineering*, Vol. 46, No. 9, pp. 1037-1043.

Maitz, Peter K. M, M. B. Khot, H. F. Mayer, G. T. Martin, J. J. Pribaz, H. F. Bowman, D. P. Orgill, 2005, “Continuous and Real-Time Blood Perfusion Monitoring in Prefabricated Flaps,” *Journal of Reconstructive Microsurgery.* Vol. 20, No. 1, pp. 35-41.

Martin, G. T. and Bowman, H. F., 2000, “Validation of Real-Time Continuous Perfusion Measurement,” *Med. Biol. Eng. Comput.*, Vol. 38, pp. 319-327.

Marxen, M., C. Paget, L. X. Yu, R. M. Henkelmann, 2006, “Estimating perfusion using microCT to locate microspheres,” *Physics in Medicine and Biology*, Vol. 51. pp. N9-N16.

Mileski, W. J. L. Atiles, G. Purdue, R. Kagan, J. R. Saffle, D. N. Herndon, D. Heimbach, A. Luterman, R. Yurt, C. Goodwin, J. L. Hunt, 2003, “Serial Measurements Increase the Accuracy of Laser Doppler Assessment of Burn Wounds,” *Journal of Burn Care & Rehabilitation*, Vol. 24, pp. 187-191.

Monnet, E., D. Pelsue, and C Machphail, “Evaluation of Laser Doppler Flowmetry for Measuremnts of Capillary Blood Flow in the Stomach Wall of Dogs During Gastric Dilation-Volvulus,” 2006 *Veterinary Surgery,* Vol. 35, pp. 198-205

Montet, X., M.K. Ivancevic, J. Belenger, M. Jorge-Costa, S. Pochon, A. Pechér, F. Terrier, and J. Vallé, 2003, “Noninvasive Measurement of Absolute Renal Perfusion by Contrast Medium-Enhanced Magnetic Resonance Imaging,” *Investigative Radiology*, Vol. 38, No. 9, pp. 584-592.

Mudaliar, A., 2006, Dissertation, Title Undertermined.

Mudaliar, A., Ellis, B. E., Ricketts, P. L, Lanz, O. I., Scott, E. P., and Diller, T. E., 2006, "Design of Phantom Tissue for Noninvasive Perfusion Measurements," submitted to *Journal of Biomechanical Engineering.*

Murray, A. K., A. L. Herrick, T. L. Moore, T. A. King, and C. E. M. Griffiths., 2005, "Dual wavelength (532 and 633 nm) laser Doppler imaging of plaque psoriasis." *British Journal of Dermatology*, Vol. 152, pp. 1182-1186.

Niwayama, J., and T. Sanaka, 2005, "Development of a new method for monitoring blood purification: The blood flow analysis of the head and foot by laser Doppler blood flow meter during hemodialysis," *Hemodialysis International*, Vol. 9, pp. 55-62.

Nuutilia, P. and K. Kalliokoski, 2000, "Use of positron emission tomography in the assessment of skeletal muscle and tendon metabolism and perfusion," *Scandinavian Journal of medicine & Science in Sports* Vol. 10, pp. 346-350.

Oltean, M. A. Aneman, G. Dindelegan, J. Mölne, M. Olausson, and G. Herlenius, 2005, "Monitoring of the Intestinal Mucosal Perfusion Using Laser Doppler Flowmetry After Multivisceral Transplantation," *Transplantation Proceedings*, Vol.37, pp 3323-3324.

Patel, P.A., J.W. Valvano, J.A. Pearce, S.A. Prahl, C.R. Denham, 1987, "A Self-Heated Thermistor Technique to Measure Effective Thermal Properties From the Tissue Surface," *Journal of Biomechanical Engineering*, Vol. 109, pp. 330-335.

Pennes, H. H., 1948, "Analysis of Tissue and Arterial Blood Temperatures in the Resting Human Forearm," *J. Appl. Physiol.*, Vol. 1, pp. 93-122.

Prinzen, F. W., and J. B. Bassingthwaighte, 2000, "Blood flow distributions by microsphere deposition methods," *Cardiovascular Research*, Vol. 45, pp. 13-21.

Richardson, R., L.J. Haseler, A.T. Nygren, S. Bluml, L.R. Frank, 2001, "Local Perfusion and Metabolic Demand During Exercise: A Noninvasive MRI Method of Assessment," *Journal of Applied Physiology*, Vol. 91, pp. 1845-1853.

Robinson, P. S., Scott, E. P., and Diller, T. E., 2006, "Testing of a Non-Invasive Probe for Measurement of Blood Perfusion," submitted to *Journal of Medical Devices*.

Schelbert, Heinrich R., 2000, "PET Contributions to Understanding Normal and Abnormal Cardiac Perfusion and Metabolism."*Annals of Biomedical Engineering*, Vo. 28, pp 922-929.

Slomka, P. J., H. Nishina, D. S. Berman, X. Kang, C. Akincioglu, J. D. Friedman, S. W. Hayes, U. E. Aladl, G. Germano, 2004, "Motion-Frozen: Display and

Quantification of Myocardial Perfusion," *Journal of Nuclear Medicine*, Vol. 45, pp. 1128-1134.

Stewart, C. J., R. Frank, K.R. Forrester, J. Tulip, R. Lindsay, R.C. Bray, 2005, "A comparison of two laser-based methods for determination of burn scar perfusion: Laser Doppler versus laser speckle imaging." *Journal of Burns,* Vol. 31, pp. 744-752.

Svedman, C., G.W. Cherry, E. Strigini, T.J. Ryan, 1998, "Laser Doppler Imaging of Skin Microcirculation," *Acta Dermato-Venereologica*, Vol. 78, pp. 114-118.

Vajkoczy, P., H. Roth, P. Horn, T. Lucke, C. Taumé, U. Hubner, G.T. Martin, C. Zappletal, E. Klar, L. Schilling, P. Schmiedek, 2000, "Continuous Monitoring of Regional Cerebral Blood Flow: Experimental and Clinical Validation of a Novel Thermal Diffusion Microprobe," *Journal of Neurosurgery*," Vol. 93, pp. 265-274.

Vallee, J.P., F. Lazeyras, H.G. Khan, et al., 2000 "Absolute Renal Blood Flow Quantification by Dynamic MRI and Gd-DTPA," *European Radiology*, Vol. 10, No. 8, pp. 1245-1252.

Valvano, J.W., J.T. Allen, H.F. Bowman, 1984, "The Simultaneous Measurement of Thermal Conductivity, Thermal Diffusivity, and Perfusion in Small Volumes of Tissue," *Journal of Biomechanical Engineering*, Vol. 106, pp. 192-197.

Yang, Kun and Wei Liu, 2004, "A novel model of the pulse decay method for measurement of local tissue blood perfusion," *Medical Engineering & Physics.* Vol. 26, pp. 215-223.

Appendix A: Thermoelectric Perfusion Probe Drawings

In this section the detailed drawings of the Thermoelectric Perfusion Probe are presented. All dimensions are presented in inches for both drawings, as required by the machine shop. These drawings will be presented to the machine shop if a replacement part is needed. In Figure A.1, the drawing for the holding plate, the important thing to notice is the dimensions associated with making the tiny shelf. In Figure A.2 the heat sink was presented. The heat sink has nine fins and was designed for the specific purpose of removing heat. In future designs, this heat sink should be made smaller to make the Thermoelectric Perfusion Probe less cumbersome.

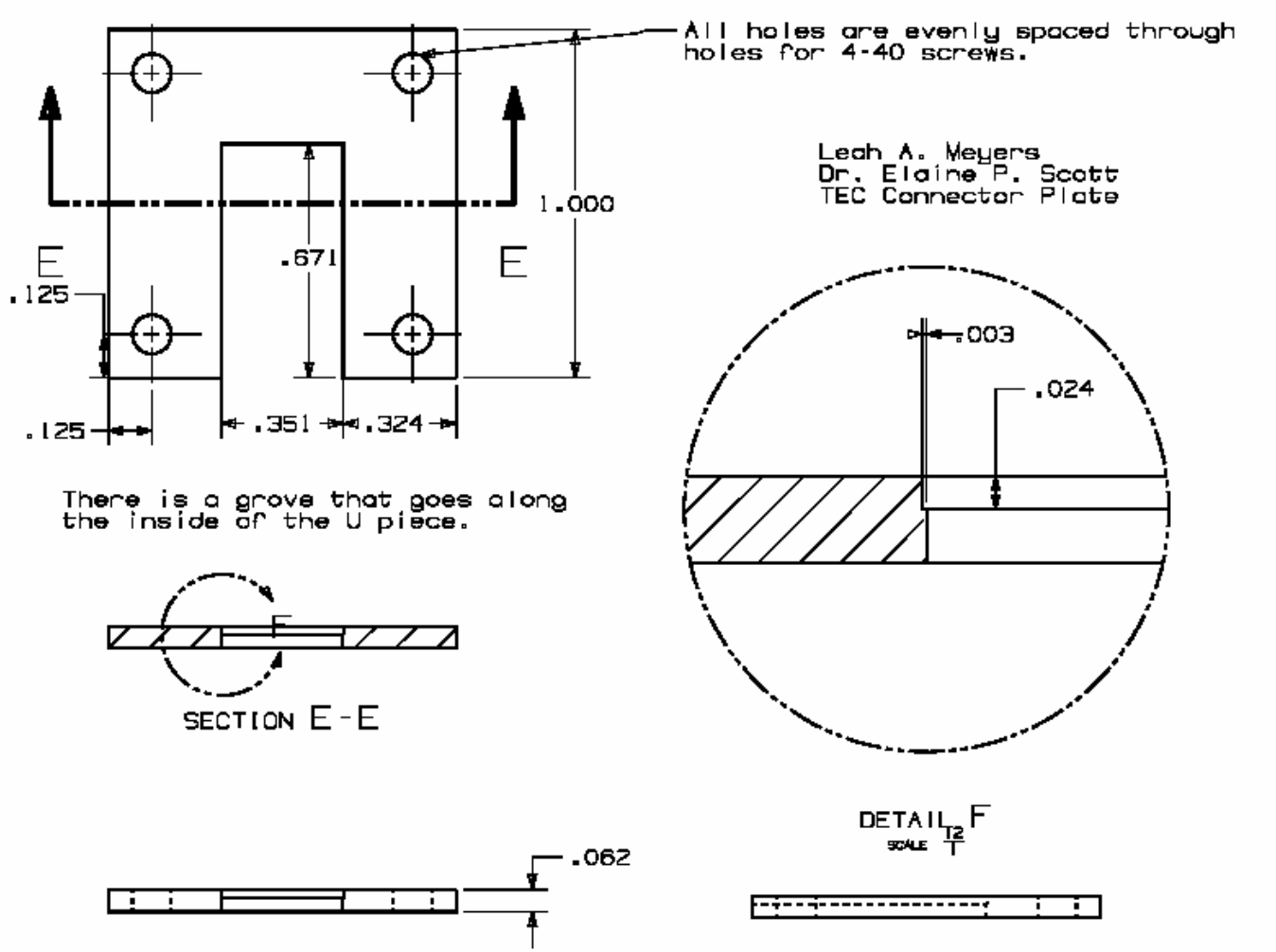

Figure A.1. The Holding Plate

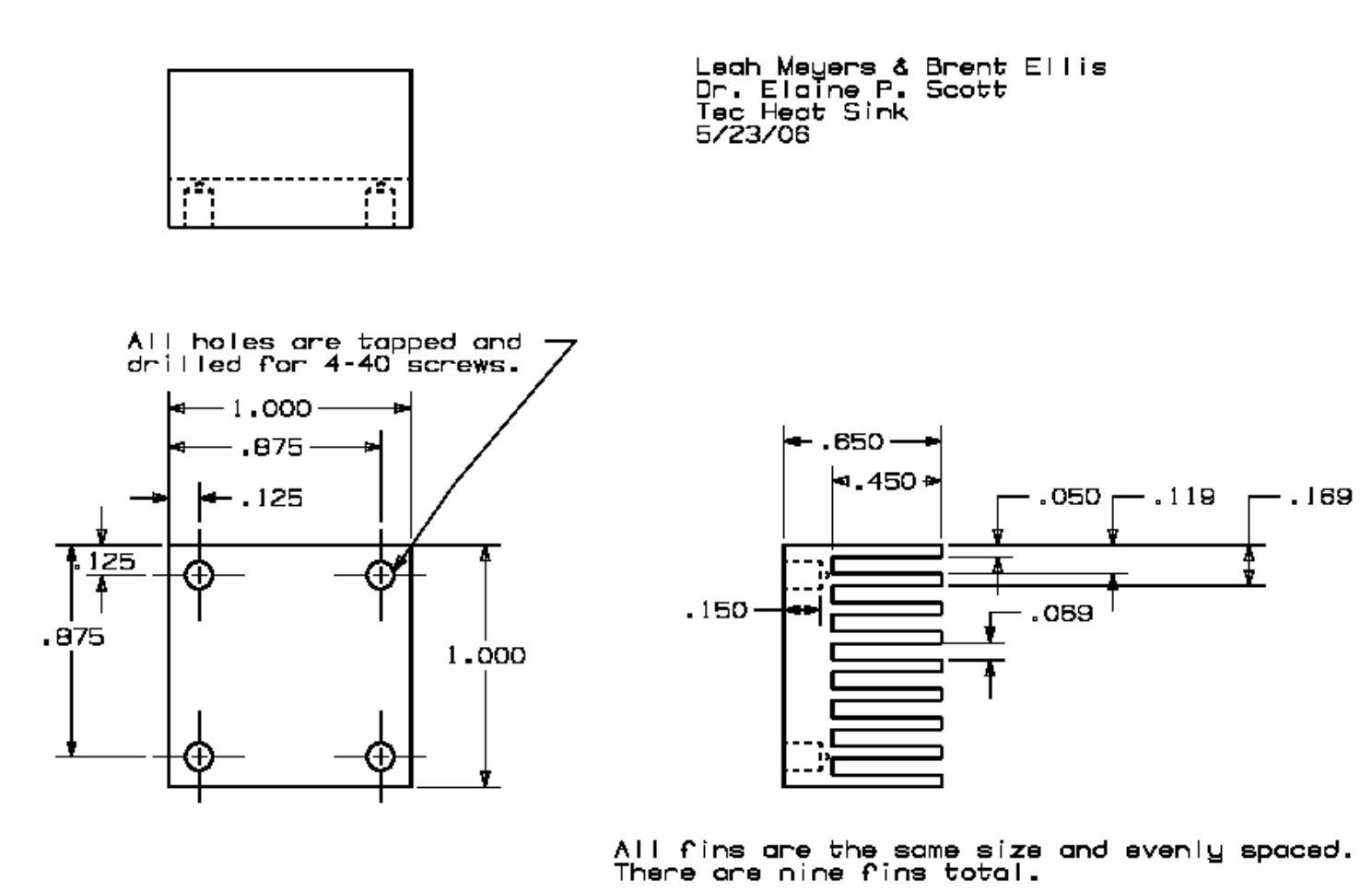

Figure A.2. The Heat Sink

Appendix B: Program Files

This appendix discusses all the programs used for the development of the Thermoelectric Perfusion Probe. This first program is a combination program that processes the files which contain one cycle. This program combines the temperature and heat flux data and breaks the data into two files: one containing the cooling portion of the cycle and the other containing the heating portion of the cycle. First, the user is prompted to input the file name containing all the data files information. Then, the user is prompted to input the number of experiments. The file containing all the data file information is then loaded and ran through a 'for loop'. In the 'for loop', the heat flux and corresponding temperature files are loaded into arrays. Then, the spline function is used to make an array, labeled z, that includes all the temperature and heat flux data with the same time step. Then, this array is splined into z2, where the time step is doubled. This larger time step helped lower run times of the program greatly. The midpoint variable finds the place according to the time of 178 seconds. Then, the portion of the array z2 corresponding to the cooling data is outputted to a new text file with the same name as the input file using a 'for loop' and the fprintf function. The cooling portion of the cycle is isolated using the limits of the 'for loop.' Then, the portion of the array z2 corresponding to the heating data is outputted to a different text file with the same name as the cooling data with a '1' on the end of it. The heating data was isolated the same way the cooling portion was isolated. The main 'for loop' is ended and the program moves to the next file.

```
fixshortfiles.m
clear all;
close all;

    filen = input('Enter the text file having heat flux and temperature info:    ');
    NumofData = input('Enter the number of Experiments:  ');
    temp = load(filen, '%f');
     char d;
    a='.txt'
    for count = 1:NumofData
        filenamenumber = temp(count,1);
        d1 = num2str(filenamenumber);
        zname = char(d1);
```

```
        q = [zname,a];
        filename =q;
        filenamenumber=temp(count,2);
        d2 = num2str(filenamenumber);
        zname = char(d2);
        q = [zname,a];
        filename2=q;
        y1 = load(filename, '%f');
        y2 = load(filename2, '%f');
        y1(:,1)=y1(:,1)*2;
        z(:,1)=y2(:,1);
        z(:,2)=y2(:,2);
        z(:,3)=spline(y1(:,1), y1(:,2), y2(:,1));
        dt=y2(2,1)-y2(1,1);
        dt2=dt*2;
        z2(:,1)=0:dt2:z(end,1);
        z2(:,2)=spline(z(:,1),z(:,2), z2(:,1));
        z2(:,3)=spline(z(:,1),z(:,3), z2(:,1));
        place=round(50/dt2);
        %offset=mean(z2(1:place,2));
        %z2(:,2)=z2(:,2)-offset;
        midpoint=round(178/dt2)
        endfirst=round(174/dt2);
        start=round(58/dt2);
        zname = 'C:\MATLAB701\work\ashvintec\spline\Results\';
        q=[zname,d1];
        filepath=q;
        suffix='.txt';
        fullout=strcat(filepath,suffix);
        q=[zname,d2]
        filepath=q
        fullout2=strcat(filepath,suffix)
        fid = fopen(fullout,'w');

        newlen=length(z2);
        figure(1);
        plot(z2(start:endfirst, 1), z2(start:endfirst, 2));
        figure(2)
        plot(z2(midpoint:newlen, 1), z2(midpoint:newlen,2));
        for count = start:endfirst
           fprintf(fid,'%10.5f \t %28.5f \t %26.5f \n', (z2(count, 1)-z2(start,1)), z2(count, 2), z2(count,3));
        end
        fclose(fid);
        fid =fopen(fullout2,'w');
        for count = midpoint:newlen
           place=count+1-midpoint;
           fprintf(fid,'%10.5f \t %28.5f \t %26.5f \n', (z2(place, 1)), z2(count, 2), z2(count,3));
        end
        fclose(fid);

    end
```

The next program that was developed was to deal with the data from the test with 17 cycles. This program was very similar to the program developed to deal with the files containing one cycle. First, the user is prompted to input the name of the file containing the experimental heat flux and temperature data and the number of cycles in the experiment. The experimental heat flux and temperature data had previously been combined into one file. Then, this file is loaded into an array. The time step and the place corresponding to the first thermal event are determined and stored in an array. Then, a 'for loop' is started that is set to run for the number of total half cycles. Variables are set to the place corresponding to the start of current half cycle and the stop of the current half cycle. Then, a 'for loop' is used to output the temperature and heat flux data for that particular half cycle. The limits of the 'for loop' are used to output just the current half cycle. The file is named for the current half cycle in the series. Finally, the 'for loop' is ended.

```
Fixlongfiles.m
clear all;
close all;

      filen = input('Enter the text file having heat flux and temperature info:    ');
      NumOfData = input('Enter the number of Cycles:  ');
      temp = load(filen, '%f');
      dt=temp(2,1)-temp(1,1);
      NumOfData=NumOfData*2;
      newdt=dt;
      %dtemp(:,1)=0:newdt:temp(1,end);
      place=round(55/newdt);
     % offset=mean(temp(1:place,2));
    %  temp(:,2)=temp(:,2)%-offset;
      for i=1:NumOfData
         d1 = num2str(i);
         zname = 'C:\MATLAB701\work\ashvintec\spline2\Results\';
         q=[zname,d1];
         filepath=q;
         suffix='.txt';

         fullout=strcat(filepath,suffix);
         fid = fopen(fullout,'w');
         start=round(((58+(i-1)*120))/newdt);
         stop=start+round(120/newdt);
         for count = start:stop
            fprintf(fid,'%10.5f \t %28.5f \t %26.5f \n', temp(count, 1), temp(count, 2), temp(count,3));
         end
         fclose(fid);
      end
```

The Thermoelectric Perfusion Probe's perfusion estimation program was developed by modifying the Blood Perfusion Probe's perfusion estimation program. As mentioned above the program was altered to match the thermal conditions in the thermoelectric perfusion probe and to allow for temperature recycling. The Thermoelectric Perfusion Probe's perfusion estimation program is made of five Matlab.m files. Throughout the five programs the difference between the Thermoelectric Perfusion Probe's perfusion estimation program and the Blood Perfusion Probe's perfusion estimation program are highlighted and explained. These are the only alterations that were made to the Blood Perfusion Probe's perfusion estimation program. Ashvin Mudaliar's dissertation (2006) will explain the other computer codes.

The first program that is being discussed is the driver program. This program controls the user interface and allows for user input. The first two changes that were made to this program were made to streamline the program. Currently, the small sensor is the only sensor being used and parameter estimation is the only portion of the code being used. Then a 2D array, TD, was initially set to zero. This array will store the first temperature profile for the current half cycle (heating or cooling). Then, in two places the function call was changed to send the file name and this temperature array to the Phantom_ParameterEstimation program. The Phantom_ParameterEstimation program returns the temperature profile at the end of that heating/cooling portion of the cycle, TSTART. Finally, TD is set to TSTART which will set the initial temperature profile for the next cycle.

```
TPP_DriverProgram.m
global R_Temp Art_Temp Top_Temp Skin_Temp Rs MFP MFS
clear all;
close all;
clc;
% This driver program written by Ashvin Mudaliar on 27th of May 2006. This
% code is used to run one or multiple set of experimental data at one shot.

Run_Choice = 1%input('Enter 1 to run Parameter Estiamtion and 2 Finite Difference Model:  ');

if Run_Choice == 2
   Phantom_BloodPerfusion;
else

   Probe_Choice =2% input('Enter 1 for big probe and 2 for small probe:  ');

   if Probe_Choice == 1
      Rs = 0.00953; % Radius of the cut out section in the probe housing
```

```
    MFP = 1.2; % Since the sensing are of the sensor is bigger than the
          % area exposed to air jets, so the heat flux measured will
          % be higher than the measured
  elseif Probe_Choice == 2
    Rs = 0.004275; % Equivalent radius based on sensing area of 57.4 mm^2
    MFP = 1; %Whole of the senor is exposed to the air jets
  end

  MFS = input('Enter the multipication factor of the sensor:  ');

  Input_Choice = input('Enter 1 for one set of data and 2 for multiple set of data:   ');

  a = '.txt';
  TD=zeros(260,32);
  if Input_Choice == 1
    R_Temp = input('Enter the Reference Temperature in deg C:   ');
    Art_Temp = input('Enter the Arterial Temperature in deg C:   ');
    Skin_Temp = input('Enter the Skin Temperature in deg C:   ');
    Test_type = input('Enter 1 for phantom test and 2 for animal test:  ');
    if Test_type == 1
     Top_Temp = input('Enter the Top Thermocouple Temperature in deg C:   ');
    elseif Test_type == 2
      Top_Temp = Skin_Temp;
    end

    filenamenumber = input('Enter the filename: ');
    d = num2str(filenamenumber);
    z = char(d);
    q = [z,a];

    [FinalP2, FinalCR2, FinalSS2,TSTART] = Phantom_ParameterEstimation(q,R_Temp,Art_Temp,Top_Temp,Skin_Temp,Rs,MFP,MFS,d,TD, 1);

  else

    filename = input('Enter the text file having heat flux and temperature info:    ');
    NumofData = input('Enter the number of Experiments:  ');
    char d;
    y1 = load(filename, '%f');

    for count = 1:NumofData
      filenamenumber = y1(count,1);
      d = num2str(filenamenumber);
      z = char(d);
      q = [z,a];
      R_Temp = y1(count,2);
      Art_Temp = y1(count,3);
      Top_Temp = y1(count,4);
      Skin_Temp = y1(count,5);

      [FinalP2, FinalCR2, FinalSS2,TSTART] = Phantom_ParameterEstimation(q,R_Temp,Art_Temp,Top_Temp,Skin_Temp,Rs,MFP,MFS,d,TD, count);

      Perfusion(count) = FinalP2;
      CR(count) = FinalCR2;
      SS(count) = FinalSS2;
```

```
        TD=TSTART;
    end

    filepath = 'C:\MATLAB701\work\tec code to use for continuous-9-29-06\FinalResults\FinalEstimates';
    suffix = '.txt'
    fulloutputname = strcat(filepath,suffix);
    fid = fopen(fulloutputname,'w');
    fprintf(fid,'***Parameter Estimation for All Runs***\n\n');
    fprintf(fid,'Perfusion (ml/ml/s) \t Contact Resistance (m^2-K/W) \t Sum of the Squares \n');
    fprintf(fid,'--------------------\t ---------------------------- \t --------------------\n');

    for count = 1:NumofData
        fprintf(fid,'%10.5f \t %28.5f \t %26.5f \n', Perfusion(count), CR(count), SS(count));
    end
    fclose(fid);
  end
end
```

The Phantom_ParameterEstimation program is the brains of the perfusion estimation program. This program sends the information out to the other programs and determines if the predicted heat flux is close enough to the experimental heat flux. The initial function call had to be altered to accept the number corresponding to the filename, and the temperature array containing the initial temperature profile. Then, an 'if else' is used to set the initial temperature profile to send to the finite difference program. The blue text shows the 'if' statement that was used if the program is working for one experiment with many cycles. The current 'if' statement was for processing the one cycle files in order. This 'mod' function was used to find the odd file numbers, signifying the cooling portion of the cycle.

Then, if the filename is odd that indicates that this is the very first cooling part of a cycle and therefore, a temperature profile has to be made. This temperature profile is a linear gradient based on the initial temperatures measured from the Doric thermocouple reader. If the filename is even, the temperature profile is set to the temperature profile sent from the driver program. Next the Phantom_Model function call and the PhantomSensitivityCoefficient call where changed to send the initial temperature gradient. These functions also return the temperature profile from the final finite difference time step. This temperature profile is eventually returned to the driver program for the next cycle.

```
function[FinalP, FinalCr, FinalSS,TSTART] = Phantom_ParameterEstimation(filename1,R_Temp,Art_Temp,Top_Temp,Skin_Temp,Rs,MFP,MFS,d, TD, place)

% ************************************************************************* %
%% PARAMETER ESTIMATION ROUTINE
%%          by Ashvinikumar Mudaliar
%% This program is modified from Caroline program to take the air
%% temperature variation and inital temperature for sensor and tissue

%% This is the program that executes the paramter estimation routine if
%% decision = 2 in BloodPerfusion.m.  It takes in the experimental heat
%% flux data and compares it to the data from the model.  The unknown parameter
%% values, perfusion and contact resistance are adjusted accordingly after each
%% iteration in order to achieve convergence between the experimental and
%% calculated heat flux data.
%%
%%
%%     Inputs: filename1: filename of the file containing the experimental
%%                 heatflux data (written as a string i.e.
%%                 filename1.txt')
```

```
%%            filename2: filename of the file containing the experimental
%%                temperature data (written as a string i.e.
%%                'filename1.txt')\
%%
%%     Outputs: opens Estimates.txt in a new m-file window.  This file contains
%%        the parameter estimates and sum of squares for each iteration and
%%        the final perfusion and contact resistance estimates.  It also
%%        contains the heat flux convergence plot data (time, experimental q"
%%        and calculated q").  The convergence plot is also opened when
%%        the program is done running.\
% ************************************************************************** %

global N NP temperatures
global start stop

    % starts clock for program run-time

% ********************** Call ExpDataFormatting m-file ********************** %
%[variables,initial_guesses,temperatures,dataout] = ExpDataFormatting_SP(filename1,filename2);
[time,FD_tstp,initial_guesses,temperatures,variance,SmoothAirTemp,heat_flux,const5]                    =
Phantom_ExpDataFormatting(filename1,R_Temp,Art_Temp,Top_Temp,Skin_Temp,Rs,MFP,MFS,d);

Y = heat_flux';
NTSTP = const5;
%Var = dataout(3,:)';
Var = variance';
MaxIt = 30;
BS = initial_guesses;
NP = 2;
```

```
Tair = temperatures(1); Tart = temperatures(2); Tinit1 = temperatures(3); Tinit2 = temperatures(4);Tsensor
= temperatures(5);
Tair_smooth = SmoothAirTemp;

z='C:\MATLAB701\work\tec code to use for continuous-9-29-06\FinalResults\Estimates';
q=[z,d];
filepath=q;   % ---> Make sure you have the correct
suffix='.txt';                          % directory name for MatLab on
fulloutputname=strcat(filepath,suffix);       % the computer you are using.

fid=fopen(fulloutputname,'w');
fprintf(fid,'***PARAMETER ESTIMATION ROUTINE*** \n\n');
fprintf(fid,'Input Files: %s, ', filename1); %fprintf(fid,'%s \n', filename2);
fprintf(fid,'Date & Time: %4.0f/%02.0f/%02.0f, %02.0f:%02.0f:%02.0f\n\n', clock);
fprintf(fid,'T_arterial = %4.2f \n',Tart);
fprintf(fid,'T_air = %4.2f \n',Tair);
fprintf(fid,'T_TopThermocouple = %4.2f \n',Tinit2);
fprintf(fid,'T_BottomThermocouple = %4.2f \n',Tinit1);
fprintf(fid,'T_Sensor = %4.2f \n\n',Tsensor);
fprintf(fid,'Starting Line #: %5.0f \n', start);
fprintf(fid,'Ending Line #: %5.0f \n\n', stop);
fprintf(fid,' Perfusion (mL/mL/s) \t Contact Resistance (m^2-K/W) \t Sum of Squares\n');
fprintf(fid,'-------------------- \t ---------------------------- \t ---------------- \n');


% ************************************************************************** %
```

```
% ************** Start of Sequential Gauss Estimation Scheme *************** %

ConvTest = 0;
control =1;
% % ************************** Call MODEL m-file ***************************** %
%       [TIME, SMOOTHPQ] = Phantom_MODEL(BS, temperatures, NTSTP,Tair_smooth, FD_tstp, Rs);
% % ************************************************************************** %
%       Qpredicted = SMOOTHPQ;         % save for plotting on final iteration
%
% % ***************** Call SENSITIVITY COEFFICIENTS m-file ******************* %
%             SC = Phantom_SensitivityCoefficients(BS,temperatures, SMOOTHPQ, NTSTP,Tair_smooth,
FD_tstp, Rs);
%
%if place==1
if mod(place,2)~=0
   place
   Nodes_Radial = 15;
   Nodes_Rs = Nodes_Radial+2; % number of nodes in radial direction on the Sensor
   Nodes_Rt = 2*Nodes_Rs-2;%2*Nodes_Rs; % number of nodes in radial direction on Tissue
   Nodes_Zs = 5; % number of nodes along the sensor thickness
   Nodes_Zt = 51*Nodes_Zs; % number of nodes along thickness of the tissue

   Tair = temperatures(1);
   Tart = temperatures(2); %Arterial Temperature
   TopT = temperatures(4);
   Tinit_sen = temperatures(5); %Initial Temperature of sensor deg C
   Tinf = Tair_smooth;
   TempGrad = (TopT - Tart)/(Nodes_Zt-1);

   Ta = Tart; % Just alloting Ta as Arterial Temperature
%Initial Condition for the Sensor and Tissue
   for i = 1:Nodes_Zs
      for j = 1:Nodes_Rs
         TS(i,j) = Tinit_sen; % Initial Temp condition for the sensor
      end
   end

   for i = Nodes_Zs+2:(Nodes_Zs+Nodes_Zt)
      for j = 1: Nodes_Rt
         TS(Nodes_Zs,Nodes_Rs:Nodes_Rt) = TopT; %Initial Temp for ghost cells for open tissue portion
         TS(Nodes_Zs+1,j) = TopT; % Initial Temp condition as Temp gradient
         TS(i,j) = TS(i-1,j)+ TempGrad;
      end
   end
else
   TS=TD
end

while control < MaxIt

   if ConvTest == 0


% ************************** Call MODEL m-file ***************************** %
```

```
    [TIME, SMOOTHPQ, TSTART] = Phantom_MODEL(BS, temperatures, NTSTP,Tair_smooth,
FD_tstp, Rs, TS);
% ************************************************************************** %
    Qpredicted = SMOOTHPQ;        % save for plotting on final iteration

% ***************** Call SENSITIVITY COEFFICIENTS m-file ******************** %
    [SC, TSTART] = Phantom_SensitivityCoefficients(BS,temperatures, SMOOTHPQ,
NTSTP,Tair_smooth, FD_tstp, Rs, TS);
% ************************************************************************** %

%% ----- Calculate the sum of squares (SSy)
    Resid = Y - SMOOTHPQ;
    SSy = sum(Resid.^2./Var);
%       RSSy = sum(RS.^2);
%
%% ----- Calculate the "C" matrix
    for k = 1:NP
       for k1 = 1: NP
          C(k1,k) = sum(SC(:,k).*SC(:,k1)./Var);
       end
    end

%% ----- Calculate "D"
    for k = 1:NP
       D(k) = sum(SC(:,k).*Resid./Var);
    end

%% ----- Calculate the "P" matrix from the "C" matrix coefficients
    PINV = C;

    if NP == 1
       P(1,1) = 1./PINV;
    else
       P = inv(PINV);        % invert C matrix
    end

    DeltaB = [0 0];
    for k = 1:NP
       for j = 1:NP
          DeltaB(k) = DeltaB(k) + (P(j,k)*D(j));
       end
    end

    for k = 1:NP
       B(k) = BS(k) + DeltaB(k)/2;
    end

%       if B(1) <= 0
%          B(1) = 0.000001;
%       end
    if B(2)<=0
       B(2) = 0.000001;
    end

    for k = 1:NP
       CI(k) = sqrt(abs(P(k,k)))*1.96;     % 95% confidence interval
```

```
      end

% ********** End of Sequential Gauss Estimation Scheme ********** %
% ************************************************************************ %

%%% Check the parameter estimates for w and Rc against the criteria for a
%%% converged solution (ratio <= 0.0001).  Update "change" accordingly.

      change = 0;

      for j = 1:NP
         Ratio = abs((B(j) - BS(j))./BS(j));
         if Ratio <= 0.0001
            change = change +1;
         end
      end

%%% Check to see that both paramters have converged.  If not, check to see if
%%% the maximum number of iterations have been used.  If not, then program
%%% runs through Gaussian estimation loop again using the updated
%%% parameter estimates as the initial guesses.

      outputs(1,control) = B(1);
      outputs(2,control) = B(2);
      outputs(3,control) = SSy;
      outputs';

      if change == NP
         control = MaxIt + 1;
         fprintf(fid,'%10.5f %28.5f %26.5f \n\n',outputs);
         fprintf(fid,'Final Perfusion Estimate (mL/mL/s) = %6.5f \n', B(1));
         fprintf(fid,'Final Contact Resistance Estimate (m^2-K/W) = %6.5f \n', B(2));
         fprintf(fid,'Sum of Squares for Final Estimates = %6.5f \n', SSy);
%           fprintf(fid,'Sum of Residual Squares for Final Estimates = %6.5f \n', RSSy);
         fclose(fid);
         figure(1)
         plot(time,Y, time,Qpredicted,'--r');
         xlabel('Time (sec)');  ylabel('Heat Flux (W/m^2)')
         legend('Experimental','Predicted')
         title('Heat flux data for the Flow =     cc/min');
         grid on;
      else
         BS = B;
         control = control+1;
      end

      if control == MaxIt
         fprintf(fid,'%13.5f %28.5f %26.5f \n\n',outputs);
         fprintf('Maximum number of iterations reached.');
         fclose(fid);
      end

   end    % end "if" statement
end    % end "while" statement
plot(time,Y, time,Qpredicted,'--r');
B(1)=BS(1);
```

```
B(2)=BS(2);
FinalP=B(1)
FinalCr=B(2)
FinalSS=SSy
%open Estimates.txt
h=figure(1);
z='C:\MATLAB701\work\tec code to use for continuous-9-29-06\FinalResults\Fig';
q=[z,d];
filepath=q;
suffix='.fig';
fullout=strcat(filepath,suffix);
saveas(h,fullout);


close all;


  % t - total run time for program
```

The Phantom ExpDataFormatting program is used to process the data to get everything ready for the finite difference program. Only two minor changes had to be made to this program. First, the thermal event starting time was set as the first experimental data point. This was because during the file processing the initial minute for determining the heat flux offset was removed. The second change that was made was related to the input air temperature. The exact temperature was recorded by the DAQ and therefore, a conversion was not needed to convert a voltage into the temperature.

```
function [time,FD_tstp,initial_guesses,temperatures,variance,SmoothAirTemp,...
  heat_flux,const5]                                                                    =
Phantom_ExpDataFormatting(filename1,R_Temp,Art_Temp,Top_Temp,Skin_Temp,Rs,MFP,MFS,d)

format short e;

global N NP
global start stop
% My Modification dated 16th Sept 2005
 y=load(filename1, '%f');
 [maxv ind1] = max(y(1:end,2));
 start=1;% ind1;%input('Enter starting point of thermal event: ');
 stop= length(y(1:end,2));
 % initial guesses for perfusion (1) and contact resistance (2)
 initial_guesses(1)=0.0001;
 initial_guesses(2)=0.0001;
   RefT = R_Temp; %input('Enter the Reference Temperature:  ');            %Required to convert the voltage
into Temp CJC
   InletTemp= Art_Temp; %input('Enter the Arterial Temperature:    ');         %z(:,4); % Channel 4 reading
from DAQ
   TissueTemp= Skin_Temp; %input('Enter the Skin Temperature:    ');         %z(:,3); % Channel 3 reading
from the DAQ
   TopTemp = Top_Temp; %input('Enter the Top Thermocouple Temperature:       '); %Temperature
measured from Doric

   TempTime = y(:,1);          % With Old DAQ %Actual time is used with new DAQ
   dt = TempTime(2)- TempTime(1);             % time step for temperature measurement
   Tstart = (TempTime(start)); % Rounding off the starting point
   Tend = (TempTime(stop)); % Rounding off the ending point
   % Temperatures from the DAQ
   AirTemp= y(:,3);%y(:,3)./(40.6e-04) + RefT; % Experimental Air Temp. , Channel 3 reading from Old
DAQ

   % Protocol Established by Ashvin, Caroline and Dr. Diller for Initial
   % Condition
   InitialTemp1 = InletTemp;     %mean(InletTemp(1:Tstart-1)) with new DAQ;
   InitialTemp2 = TopTemp;       %mean(TopTemp(1:Tstart-1)); with new DAQ
   AirT=AirTemp(start:stop-1);   % Truncated Air temperature during the thermal event

   temperatures(1) = mean(AirTemp(start:stop));       % air temp.
   temperatures(2) = InletTemp;                    % arterial temp.
   temperatures(3) = InitialTemp1;                  % Initial Temperatures for tissue and sensor are different
```

```
   temperatures(4) = InitialTemp2;                  % Finalized by Ashvin, Dr. Scott and Dr. Diller Dated 23rd
Sept 2005
   temperatures(5) = TissueTemp;%mean(SensorTemp(1:Tstart-1));        % Sensor Initial Condition

% Removing the zero offset in heat flux measurement from the Amplifier
   q = y(:,2).*MFS;       %Voltage converted into Heat flux;
   offset = 0%mean(q(1:start-1)); %calculating the offset heat flux
   const3 = length(q);          %length of the Experimental heat flux

for i=1:const3
   Actual_heat_flux(i) = q(i)- offset; %Removing the offset in the measurement
end

  heat_flux = Actual_heat_flux(start:stop-1)*MFP; % Scaling factor taken in consideration because of the
change in sensing area
  consthf = length(heat_flux);
  time = 0:(Tend-Tstart)/(consthf-1):(Tend-Tstart);

   FD_Time = 0:time(2)/2:time(end);% Finite Difference time
   FD_tstp = FD_Time(2)-FD_Time(1);
   SmoothAirTemp = spline(time,AirT,FD_Time);
   const5 = length(FD_Time);


% Variance for the heat flux data
   Var1 = var(heat_flux);

   % Weighing the residual by factor of 100000. The first 15 seconds of data
   % is dominated contact resistance. The region of interest is after 15
   % seconds where perfusion is dominant
   for i = 1:consthf
      if i <= round(7/FD_tstp);
         variance(i) = Var1*100000;
      else
         variance(i) = Var1;
      end
   end

%************End of Formatting Experimental Data**************************
```

The PhantomSensitivityCoefficients program had to have three alterations to be made to allow for temperature recycling. First, the initial function call had to be altered to input the initial temperature profile, TS, and to output the final temperature profile, TNEW. Also, the Phantom_MODEL function call had to be adjusted to send out the initial temperature profile, TS, and accept the final temperature profile, TNEW. This function call was altered in two places.

```
function [SC, TNEW] = Phantom_SensitivityCoefficients(BS, temperatures, SMOOTHPQ,NTSTP,Tair_smooth, FD_tstp, Rs, TS)

% ********************************************************************** %
%% SENSITIVITY COEFFICIENTS
%%       by Caroline Comas
%%
%% This program calculates the sensitivity coefficients for heat flux
%% sensitivity to perfusion and contact resistance, which are used in the
%% parameter estimation routine.
%%
%%     Inputs: BS:  [perfusion, contact reistance]
%%             temperatures:  passes air, arterial and initial
%%                temperatures, which are used in MODEL.m
%%             SMOOTHPQ:  passes the calculated heat flux for the
%%                parameters, BS
%%
%%     Outputs:  SC:  Sensitivity coefficients
% ********************************************************************** %

global N

Beta1 = BS(1);
Beta2 = BS(2);

Factor = 1.001;
Beta1P = Beta1*Factor;
Beta2P = Beta2*Factor;

[TIME, SMOOTHPQ1, TNEW] = Phantom_MODEL([Beta1P,Beta2], temperatures, NTSTP,Tair_smooth, FD_tstp, Rs, TS);
[TIME, SMOOTHPQ2, TNEW] = Phantom_MODEL([Beta1,Beta2P], temperatures, NTSTP,Tair_smooth, FD_tstp, Rs,TS);


SC(:,1) = (SMOOTHPQ1 - SMOOTHPQ)./(Beta1P - Beta1);
SC(:,2) = (SMOOTHPQ2 - SMOOTHPQ)./(Beta2P - Beta2);
```

The final program that had to be changed was the Phantom_MODEL program. This program is where the finite difference procedure is completed and the result is a time based heat flux. Alterations had to be made to this program to allow for temperature recycling and to adjust the finite difference model to fit the thermal diffusion probe. The first change that had to be made was to the function call. This had to be altered to accept the initial temperature profile, TS, and to return the final temperature profile, TSTART. The second change that was made was to increase the convective coefficient to $1{,}000{,}000\frac{W}{^{\circ}C\,m^2}$. The convective coefficient was taken out of all equations; however, this change was made just as a precautionary measure. The next change was to comment out the temperature profile maker, shown in green. Then, the initial temperature profile T, was set to the temperature profile sent to the program. The next change that was made was to change equation C2, the inverse of the convective coefficient was taken out of this equation. The final change that was made was to return the temperature profile from the final time step.

```
function [TIME, SMOOTHQ, TSTART] = Phantom_MODEL(BS, temperatures,NTSTP,Tair_smooth,FD_tstp, Rs,TS)
% This code is being developed to replace the code written by Mitchener,
% Robinson, Cardinali and Comas. The code written by them was in
% non-dimensional form and the current code is in dimensional form. This
% code is written by Ashvinikumar Mudaliar on 17th of April 2006
format long e;
Rt = Rs*2; %Tissue Radius
Tiss_t = 0.0127; %input(' Thickness of the Tissue'); % Sponge thickness
Sens_t = 0.00025; % input(' Thickness of the Sensor'); % Sensor thickness


Nodes_Radial = 15;
Nodes_Rs = Nodes_Radial+2; % number of nodes in radial direction on the Sensor
Nodes_Rt = 2*Nodes_Rs-2;%2*Nodes_Rs; % number of nodes in radial direction on Tissue
Nodes_Zs = 5; % number of nodes along the sensor thickness
Nodes_Zt = 51*Nodes_Zs; % number of nodes along thickness of the tissue

dr = Rs/(Nodes_Rs-2); %spacing between the nodes in radial direction
r = dr/2:dr:Rt; % Radius discretized
dz = (Sens_t)/(Nodes_Zs); % Node spacing in axial direction
z = dz/2:dz:(Sens_t+Tiss_t)-dz/2; % Thickness discretized


% Properties of the sensor
rho_s = 1250; % Density of sensor kg/m^3
sp_heat_s = 1340; % Specific heat of the sensor J/kg-K
k_s = 0.25;% Thermal condcutivity of the sensor W/m-K
alpha_s = k_s/(rho_s*sp_heat_s); % Thermal diffusivity of the sensor m^2/s
```

```
% Properties of the Tissue
rho_t = 998.2; %density of tissue in kg/m^3
sp_heat_t = 4182; %Specific heat of tissue J-kg/K
k_t = 0.5723;% Thermal conductivity of tissue W/m-K
alpha_t = k_t/(rho_t*sp_heat_t); %Thermal diffusivity of the tissue

%Fluent® Time Step
dt1 = FD_tstp; %time step sec

%Initial Temperature and other required data
Tair = temperatures(1);
Tart = temperatures(2); %Arterial Temperature
TopT = temperatures(4);
Tinit_sen = temperatures(5); %Initial Temperature of sensor deg C
Tinf = Tair_smooth;
% TempGrad = (TopT - Tart)/(Nodes_Zt-1);

Ta = Tart; % Just alloting Ta as Arterial Temperature
h = 1000000; %Convective heat transfer coefficient W/m^2-K
Rc = BS(2); %Contact resistance m^2-K
w =  BS(1); %blood perfusion in ml/ml/s

%Initial Condition for the Sensor and Tissue
% for i = 1:Nodes_Zs
%     for j = 1:Nodes_Rs
%         T(i,j) = Tinit_sen; % Initial Temp condition for the sensor
%     end
% end
%
% for i = Nodes_Zs+2:(Nodes_Zs+Nodes_Zt)
%     for j = 1: Nodes_Rt
%         T(Nodes_Zs,Nodes_Rs:Nodes_Rt) = TopT; %Initial Temp for ghost cells for open tissue portion
%         T(Nodes_Zs+1,j) = TopT; % Initial Temp condition as Temp gradient
%         T(i,j) = T(i-1,j)+ TempGrad;
%      end
% % end
%
%  ytemps = load('1temps.txt', '%f');
%  T=ytemps;
   T=TS;
%_____________________________________________________________________________
%Defining constants for Sensor
 As = -alpha_s*dt1/(2*dz^2);
 Bs = 1 + (alpha_s*dt1/(dz^2));
 Ds = 1 - (alpha_s*dt1/(dr^2));
 for j = 2: Nodes_Rs-1
    Cs(j-1) = (alpha_s*dt1/(2*dr))*(1/dr-1/(2*r(j-1)));
    Es(j-1) = (alpha_s*dt1/(2*dr))*(1/dr+1/(2*r(j-1)));
 end
%_____________________________________________________________________________
 %Defining constants for Tissue
  A1t = -alpha_t*dt1/(2*dz^2);
  B1t = 1 + (alpha_t*dt1/dz^2)+ w*dt1/2;
  B2t = 1 + (alpha_t*dt1/dr^2)+ w*dt1/2;
  D1t = 1 - (alpha_t*dt1/dr^2) ;
```

```
  D2t = 1 - (alpha_t*dt1/dz^2) ;
  for j = 2:Nodes_Rt-1
     C1t(j-1) = (alpha_t*dt1/(2*dr))*(1/dr-1/(2*r(j-1)));
     E1t(j-1) = (alpha_t*dt1/(2*dr))*(1/dr+1/(2*r(j-1)));
  end

%_____________________________________________________________________________

 %_____________________________________________________________________________
%Tridiagonal Matrix elements for axial sweep in sensor

 C1 = k_s/dz;
 C2 = ( dz/(2*k_s));
 C3 = (dz/(2*k_s) + Rc + dz/(2*k_t));

 for j = 2:Nodes_Rs-1
    A(1,j) = 0;
    B(1,j) = 1+ C1*C2;
    C(1,j) = -C1*C2;

    A(Nodes_Zs,j)= -C1*C3;
    B(Nodes_Zs,j) = 1 + C1*C3;
    C(Nodes_Zs,j) = 0;
 end

 for i = 2:Nodes_Zs-1
    for j = 2:Nodes_Rs-1
       A(i,j) = As;
       B(i,j) = Bs;
       C(i,j) = As;
    end
 end
 %_____________________________________________________________________________

 % Trididgonal Matrix elements for Radial sweep in Sensor

 for i = 1:Nodes_Zs
    D(i,1) = 0;
    E(i,1) = 1;
    F(i,1) = -1;

    D(i,Nodes_Rs) = -1;
    E(i,Nodes_Rs) = 1;
    F(i,Nodes_Rs) = 0;
 end

 for i = 1:Nodes_Zs
    for j = 2:Nodes_Rs-1
       D(i,j) = -Cs(j-1);
       E(i,j) = 2-Ds;
       F(i,j) = -Es(j-1);
    end
 end
 %_____________________________________________________________________________
  % Matrix elements for Axial sweep in Tissue
```

```
    C4 = k_t/dz;
    C5 = rho_t*sp_heat_t*w*dz;
    C6 = rho_t*sp_heat_t*w*dr;

    for j = 2:Nodes_Rs-1
      A(Nodes_Zs+1,j) = 0;
      B(Nodes_Zs+1,j) = 1 + C4*C3+ C3*C5;
      C(Nodes_Zs+1,j) = -C4*C3;

      A(Nodes_Zs+Nodes_Zt,j) = -1;
      B(Nodes_Zs+Nodes_Zt,j) = 1;
      C(Nodes_Zs+Nodes_Zt,j) = 0;
    end

    for j = Nodes_Rs:Nodes_Rt-1
      A(Nodes_Zs+1,j) = 0;
      B(Nodes_Zs+1,j) =  C4 + C5;
      C(Nodes_Zs+1,j) = -C4;

      A(Nodes_Zs+Nodes_Zt,j) = -1;
      B(Nodes_Zs+Nodes_Zt,j) = 1;
      C(Nodes_Zs+Nodes_Zt,j) = 0;
    end

    for i = Nodes_Zs+2:Nodes_Zs+Nodes_Zt-1
      for j = 2:Nodes_Rt-1
         A(i,j) = A1t;
         B(i,j) = B1t;
         C(i,j) = A1t;
      end
    end
%_____________________________________________________________________
 % Matrix elements for Radial sweep in Tissue
   for i = Nodes_Zs+1: Nodes_Zs+Nodes_Zt
      D(i,1) = 0;
      E(i,1) = 1;
      F(i,1) = -1;

      D(i,Nodes_Rt) = -1;
      E(i,Nodes_Rt) = 1;
      F(i,Nodes_Rt) = 0;
   end

   for i = Nodes_Zs+1: Nodes_Zs+Nodes_Zt
      for j = 2:Nodes_Rt-1
         D(i,j) = -C1t(j-1);
         E(i,j) =  B2t;
         F(i,j) = -E1t(j-1);
      end
   end
%_____________________________________________________________________
  %*********************************************************************



for t = 1:NTSTP %time counter
```

```
%_____________________Axial Sweep_____________________________________
    %Top and Bottom boundary condition RHS for Sensor
    for j = 2:Nodes_Rs-1
        RHS1(1,j) = Tinf(t);
        RHS1(Nodes_Zs,j)= T(Nodes_Zs+1,j); %T(Nodes_Zs+1,j);
    end
   %Top and Bottom boundary condition RHS for Sensor

    %Middle Columns of the Sensor
       for i = 2:Nodes_Zs-1
          for j = 2:Nodes_Rs-1
             RHS1(i,j)=  Cs(j-1)*T(i,j-1)+Ds*T(i,j)+Es(j-1)*T(i,j+1);
          end
       end
     %Middle Columns of the Sensor

     %Thomas Algorithm starts
       for j = 2:Nodes_Rs-1
          PS1(1,j) = B(1,j);
          QS1(1,j) = RHS1(1,j)/PS1(1,j);

          for i = 2:Nodes_Zs
             PS1(i,j) = B(i,j)-A(i,j)*C(i-1,j)/PS1(i-1,j);
             QS1(i,j) = (RHS1(i,j)-A(i,j)*QS1(i-1,j))/PS1(i,j);
          end

             T(Nodes_Zs,j) = QS1(Nodes_Zs,j);

       %Backward substitution

          for k = Nodes_Zs-1:-1:1
             T(k,j) = QS1(k,j) - C(k,j)*T(k+1,j)/PS1(k,j);
          end
       end
        %Thomas Algorithm ends

          T(1:Nodes_Zs,1) = T(1:Nodes_Zs,2);
          T(1:Nodes_Zs,Nodes_Rs) = T(1:Nodes_Zs,Nodes_Rs-1);

 %_____________________________Axial Sweep_____________________________

 %_____________________________Axial Sweep for Tissue__________________
%Top & Bottom boundary condition
    for j = 2:Nodes_Rs-1
          RHT1(Nodes_Zs+1,j) = T(Nodes_Zs,j)+ C3*C5*Ta;
          RHT1(Nodes_Zs+Nodes_Zt,j) = 0;
    end

    for j = Nodes_Rs:Nodes_Rt-1
          RHT1(Nodes_Zs+1,j) = C5*Ta;
          RHT1(Nodes_Zs+Nodes_Zt,j) = 0;
    end
%Top & Bottom boundary condition

%Middle Columns of the Tissue
```

```
      for  i = Nodes_Zs+2:Nodes_Zs+Nodes_Zt-1
         for j = 2:Nodes_Rt-1
           RHT1(i,j) = C1t(j-1)*T(i,j-1) + D1t*T(i,j) + E1t(j-1)*T(i,j+1)+ Ta*w*dt1/2;
         end
      end

%Middle Columns of the Tissue


  %Thomas Algorithm starts
   for j = 2:Nodes_Rt-1
      PT1(Nodes_Zs+1,j) = B(Nodes_Zs+1,j);
      QT1(Nodes_Zs+1,j) = RHT1(Nodes_Zs+1,j)/PT1(Nodes_Zs+1,j);

      for i = Nodes_Zs+2:Nodes_Zs+Nodes_Zt
         PT1(i,j) = B(i,j)-A(i,j)*C(i-1,j)/PT1(i-1,j);
         QT1(i,j) = (RHT1(i,j)-A(i,j)*QT1(i-1,j))/PT1(i,j);
      end
         T(Nodes_Zs+Nodes_Zt,j) = QT1(Nodes_Zs+Nodes_Zt,j);

         %Backward substitution

         for k =Nodes_Zs+Nodes_Zt-1:-1:Nodes_Zs+1
            T(k,j) = QT1(k,j) - C(k,j)*T(k+1,j)/PT1(k,j);
         end
   end
%     Thomas Algorithm ends


   %Temperature updated to satisfy boundary condition
   T(Nodes_Zs+1:Nodes_Zs+Nodes_Zt,1) = T(Nodes_Zs+1:Nodes_Zs+Nodes_Zt,2);
   T(Nodes_Zs+1:Nodes_Zs+Nodes_Zt,Nodes_Rt) = T(Nodes_Zs+1:Nodes_Zs+Nodes_Zt,Nodes_Rt-1);
  %*****************************Axial Sweep for Tissue ends************
  %_____________________________Radial Sweep_____________________________

%        LHS and RHS boundary condition
       for i = 1:Nodes_Zs
          RHS2(i,1) = 0;
          RHS2(i,Nodes_Rs)= 0;
       end
      %LHS and RHS boundary condition

      %Middle Columns of the Sensor
       for  j = 2:Nodes_Rs-1
          for i = 2:Nodes_Zs-1
            RHS2(i,j) = -As*T(i-1,j) + (2-Bs)*T(i,j) -As*T(i+1,j);
          end
       end
      %Middle Columns of the Sensor

      %Thomas Algorithm starts
        for i = 2:Nodes_Zs-1
          PS2(i,1) = E(i,1);
          QS2(i,1) = RHS2(i,1)/PS2(i,1);

          for j = 2:Nodes_Rs
```

```
            PS2(i,j) = E(i,j)-D(i,j)*F(i,j-1)/PS2(i,j-1);
            QS2(i,j) = (RHS2(i,j)-D(i,j)*QS2(i,j-1))/PS2(i,j);
          end

            T(i,Nodes_Rs) = QS2(i,Nodes_Rs);

         %Backward substitution
          for k = Nodes_Rs-1:-1:1
            T(i,k) = QS2(i,k) - F(i,k)*T(i,k+1)/PS2(i,k);
          end
       end
       %Thomas Algorithm ends
%           T(1,2:Nodes_Rs-1) = (T(2,2:Nodes_Rs-1)*C1*C2 + Tinf(t))/(1+C1*C2);
%                                   T(Nodes_Zs,1:Nodes_Rs-1)   =   (T(Nodes_Zs-1,1:Nodes_Rs-1)*C1*C3   +
T(Nodes_Zs+1,1:Nodes_Rs-1))/(1+C1*C3);

 %_____________________________Radial Sweep_____________________________
 %_____________________________Radial Sweep of Tissue begins_____________________

 %LHS & RHS boundary condition

 for i = Nodes_Zs+1:Nodes_Zs+Nodes_Zt
    RHT2(i,1) = 0;
    RHT2(i,Nodes_Rt) = 0;
 end

%LHS & RHS boundary condition

%Middle Columns of the Tissue
       for  j = 2:Nodes_Rt-1
          for i = Nodes_Zs+2:Nodes_Zs+Nodes_Zt-1
            RHT2(i,j) = -A1t*T(i-1,j) + D2t*T(i,j) -A1t*T(i+1,j)+ Ta*w*dt1/2;
          end
       end

 %Middle Columns of the Tissue

 %Thomas Algorithm starts for the region below the sensor
  for i = Nodes_Zs+2:Nodes_Zs+Nodes_Zt-1
      PT2(i,1) = E(i,1);
      QT2(i,1) = RHT2(i,1)/PT2(i,1);

      for j = 2:Nodes_Rt
         PT2(i,j) = E(i,j)-D(i,j)*F(i,j-1)/PT2(i,j-1);
         QT2(i,j) = (RHT2(i,j)-D(i,j)*QT2(i,j-1))/PT2(i,j);
      end
         T(i,Nodes_Rt) = QT2(i,Nodes_Rt);

         %Backward substitution

         for k = Nodes_Rt-1:-1:1
            T(i,k) = QT2(i,k) - F(i,k)*T(i,k+1)/PT2(i,k);
         end
  end
  %Thomas Algorithm ends for the region below the sensor
```

```
%_____________________________________________________________________
        r1 = r(1:Nodes_Rs-2);
        C7 = 2*k_s/dz;
    for i = 2:Nodes_Rs-1
        q(i-1)= k_s/(z(Nodes_Zs)-z(1))*(T(Nodes_Zs,i)- T(1,i));
        TopT(i-1) = T(1,i-1);
        BotT(i-1) = T(Nodes_Zs,i-1);
        Tw(i-1) = (T(1,i)*(C2*C7-1)+Tinf(t))/(C2*C7);
        Tr1(i-1) = T(Nodes_Zs+1,i);
        Tr2(i-1) = T(Nodes_Zs,i);
    end
        qcond(t) = sum(q*r1')/sum(r1);
        Twall(t) = sum(Tw*r1')/sum(r1);
        Top(t) = sum(TopT*r1')/sum(r1);
        Bot(t) = sum(BotT*r1')/sum(r1);
        qres(t) = ((sum(Tr1*r1')/sum(r1))-(sum(Tr2*r1')/sum(r1)))/C3;
        qconv(t) = h*(Twall(t)-Tinf(t));
        MP = qcond';
        length(MP);
        SMOOTHQ = MP(1:2:end);
        length(SMOOTHQ);
        TIME(t) = t*dt1;

end
 TSTART=T;
```

Appendix C: Phantom Tissue Test Stand Drawings

In this section, the drawings related to the phantom tissue test stand are presented. First, the drawing for the newest inlet plate is presented, Figure C.1. This inlet plate was designed originally for Dr. Kraft's phantom tissue test stand with a 2.54 cm (1 inch) sponge. This piece is 1.27 cm (0.5 in.) wide to account for the large sponge. The original inlet plate is shown in Figure C.2. It is very important that the tapping be completed from the bottom side, or the pipe will not fit properly and leaking will occur. Also, the inlet for the pipe is 0.635 cm (0.25 in). For Dr. Kraft's model the plastic inlet pipe had to be drilled out to this diameter. The diameter size is very important for the computational flow model and therefore must be kept constant. The tank for the phantom tissue test stand had to be altered so that the tissue system, the heater, and the flow meter could be mounted to the tank, Figure C.3. A slot was added for an easy exit for the pump cord. The important thing to note was the direction where the pipe threads are tapped from. The flowmeter tappings must be started from the inside and moved to the outside. The heater tapping has to be started on the outside of the tank. Figure C.4 displays the three-way valve holder's dimensioned drawings. The three-way valve is ziptied to the holding plate which is bolted to the tissue system. Figure C.5 and Figure C. 6 show the two components that compose the bracket. Figure C.5 shows the side of the bracket which the inlet plate will sit on. Figure C. 6 shows the back of the bracket which will be attached to the tank through the slots. It is important to note that these dimensioned drawings show all the screw holes as being 10-32 holes. The old version of the phantom tissue test stand was made with 10-32 screws while the newer version was made with 10-24 screws. Therefore, the screw size will need to be adjusted depending on which size is required.

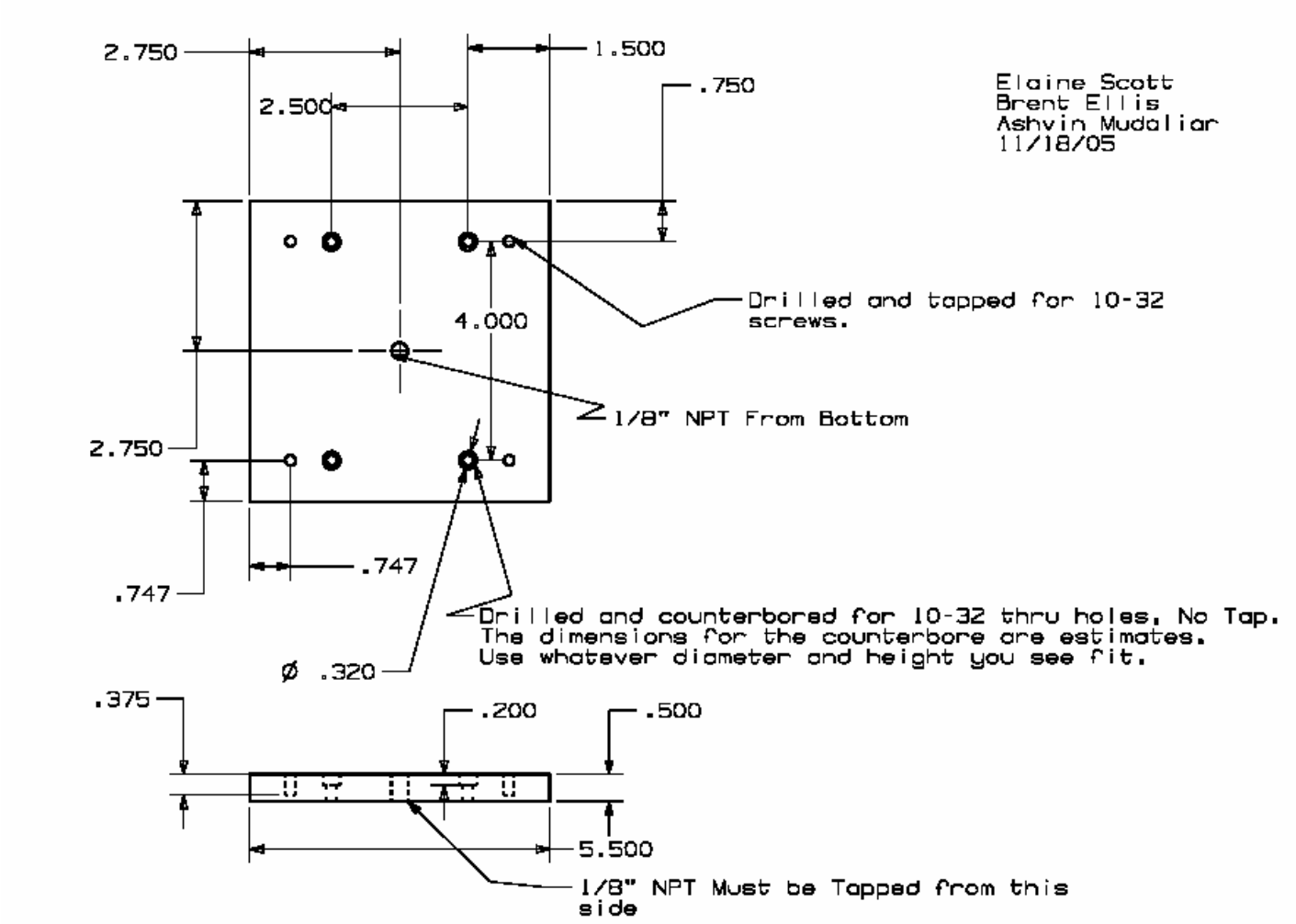

Figure C.1. The Inlet Plate for a thicker sponge

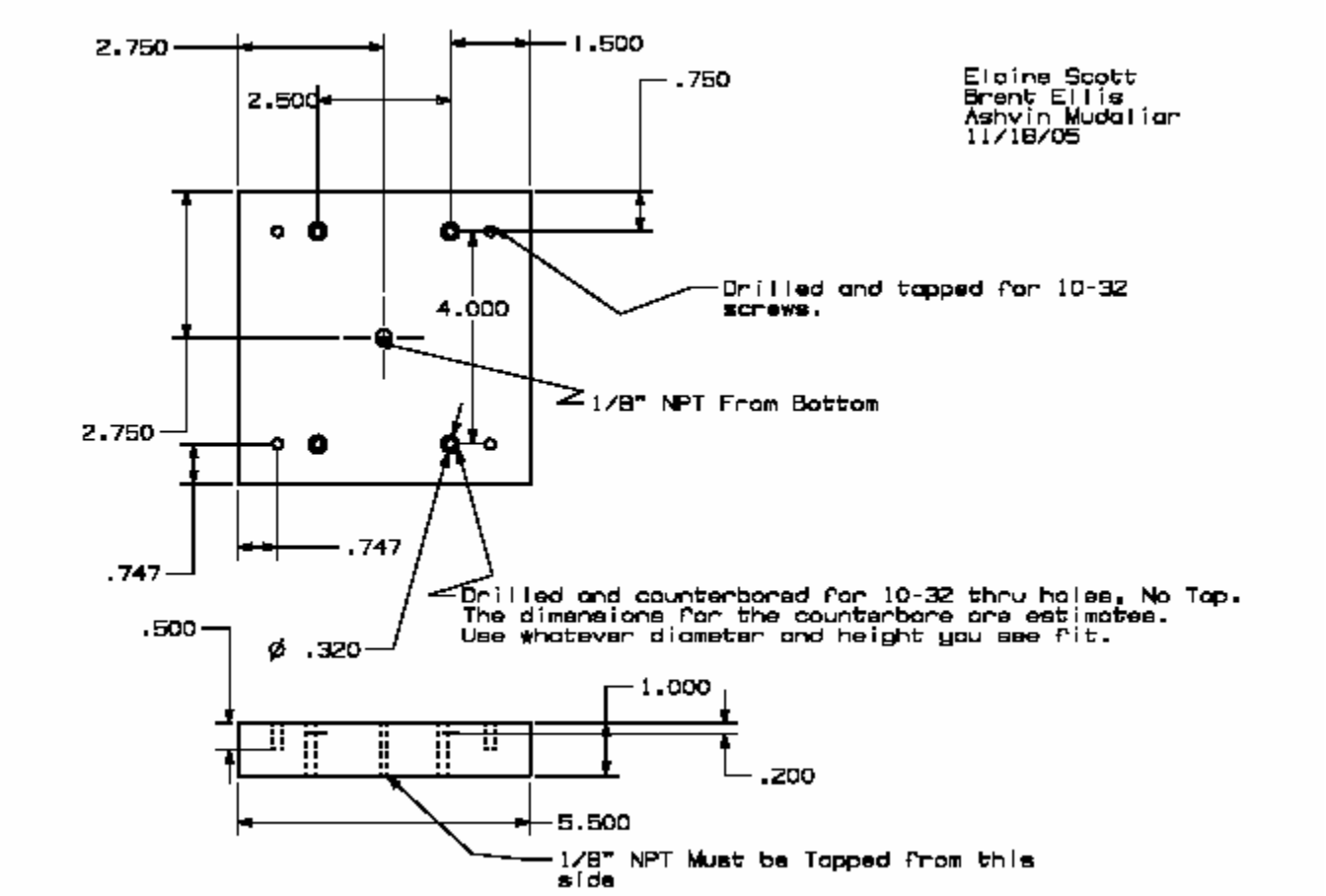

Figure C.2. The Inlet Plate for a thin sponge

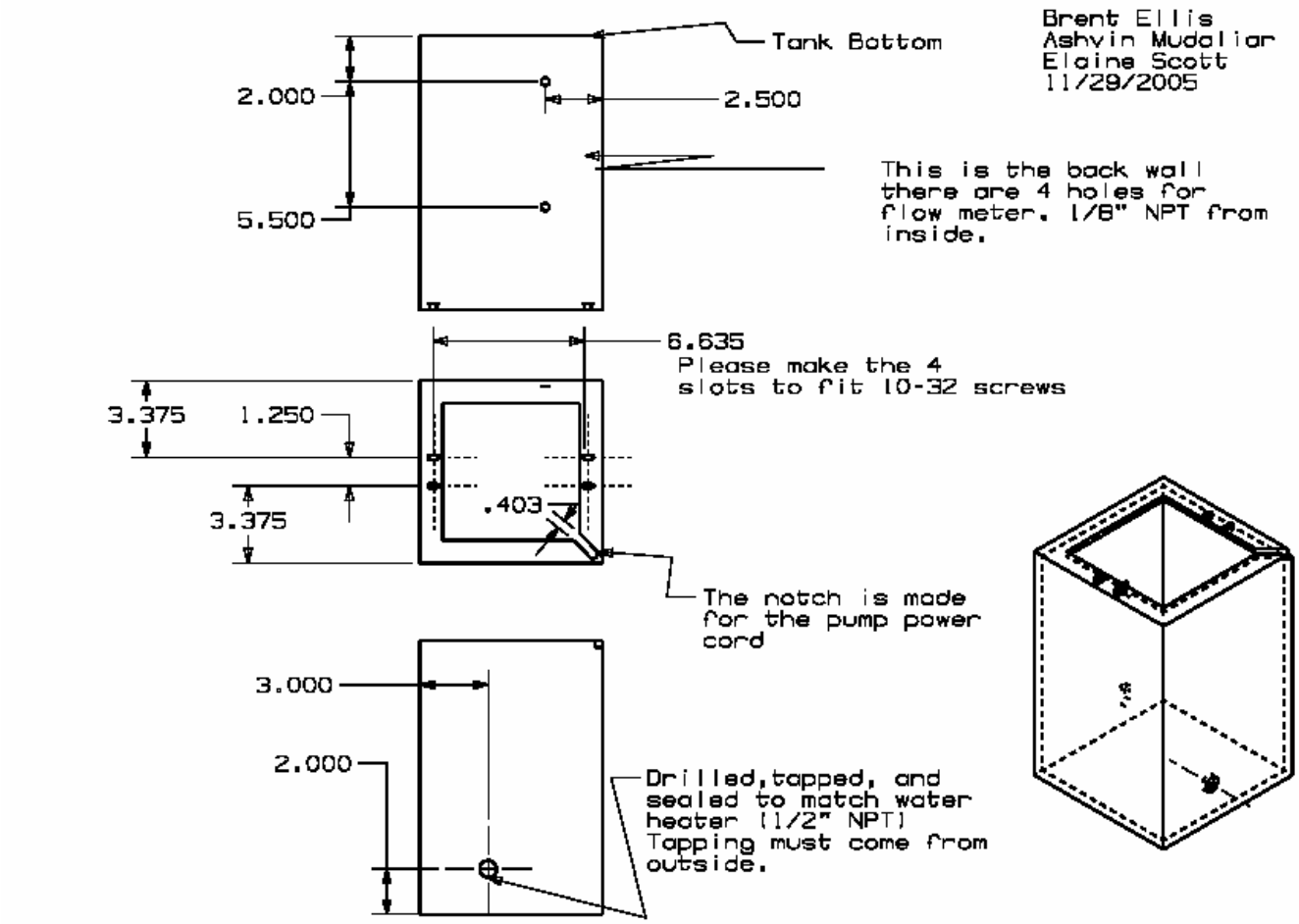

Figure C.3. The Fish Tank

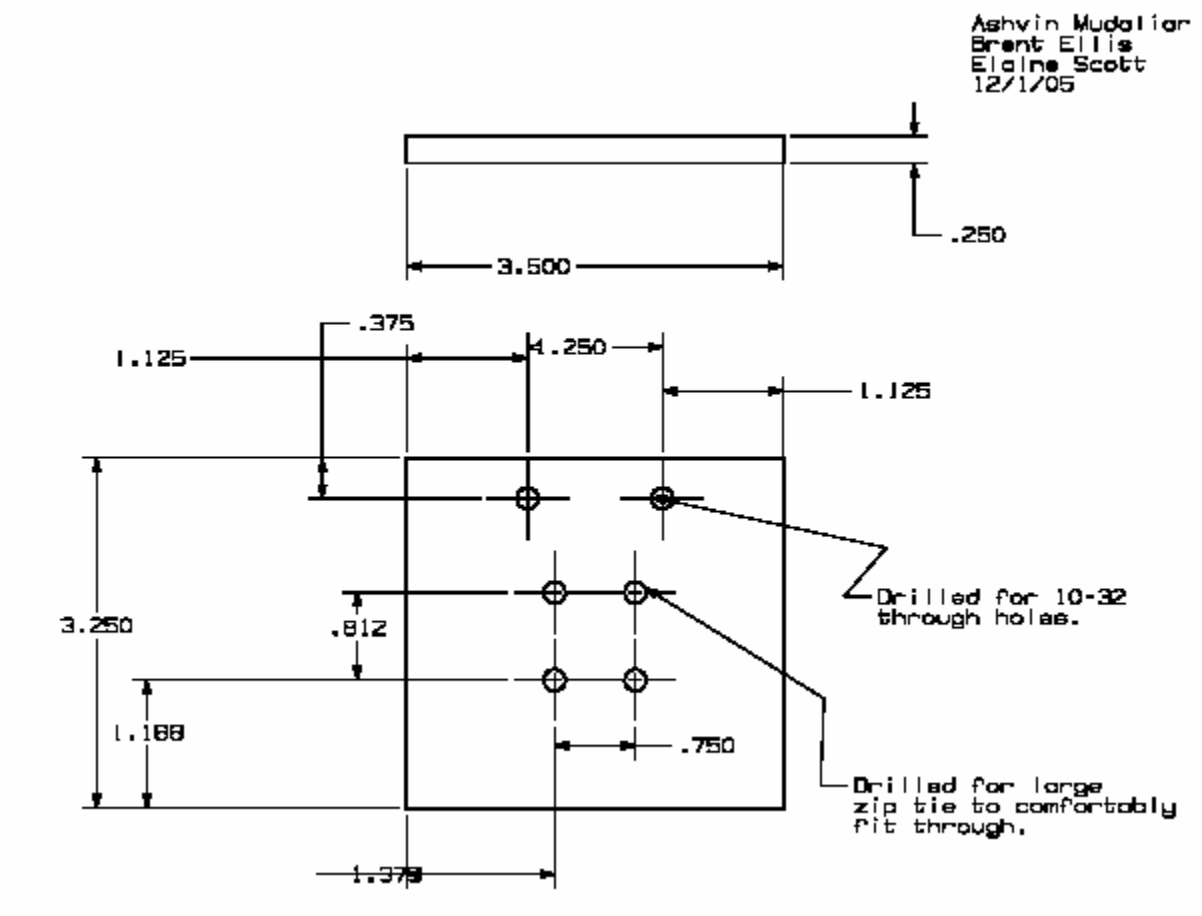

Figure C.4. The Convective Perfusion Probe's Holding Plate

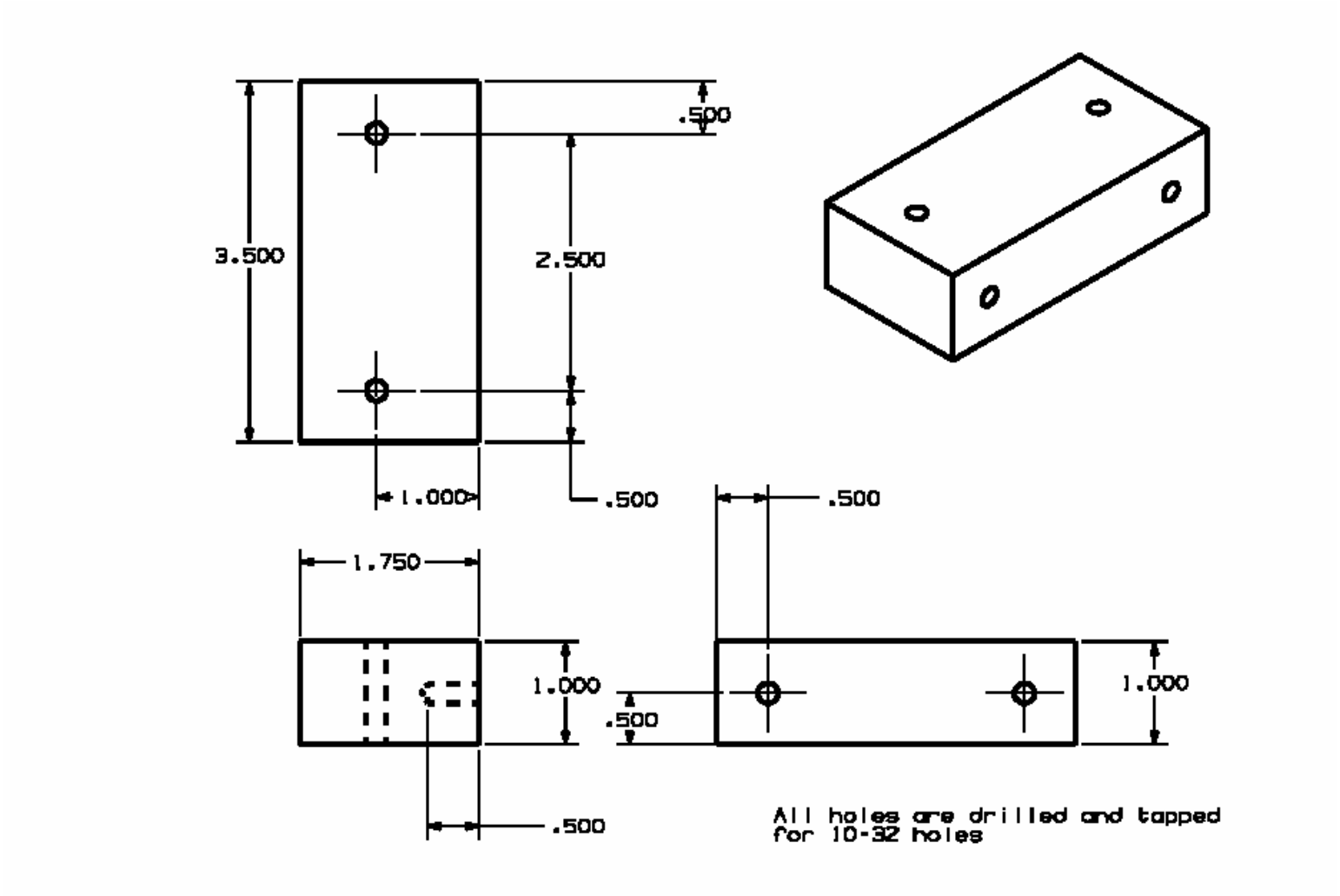

Figure C.5. The side of the bracket

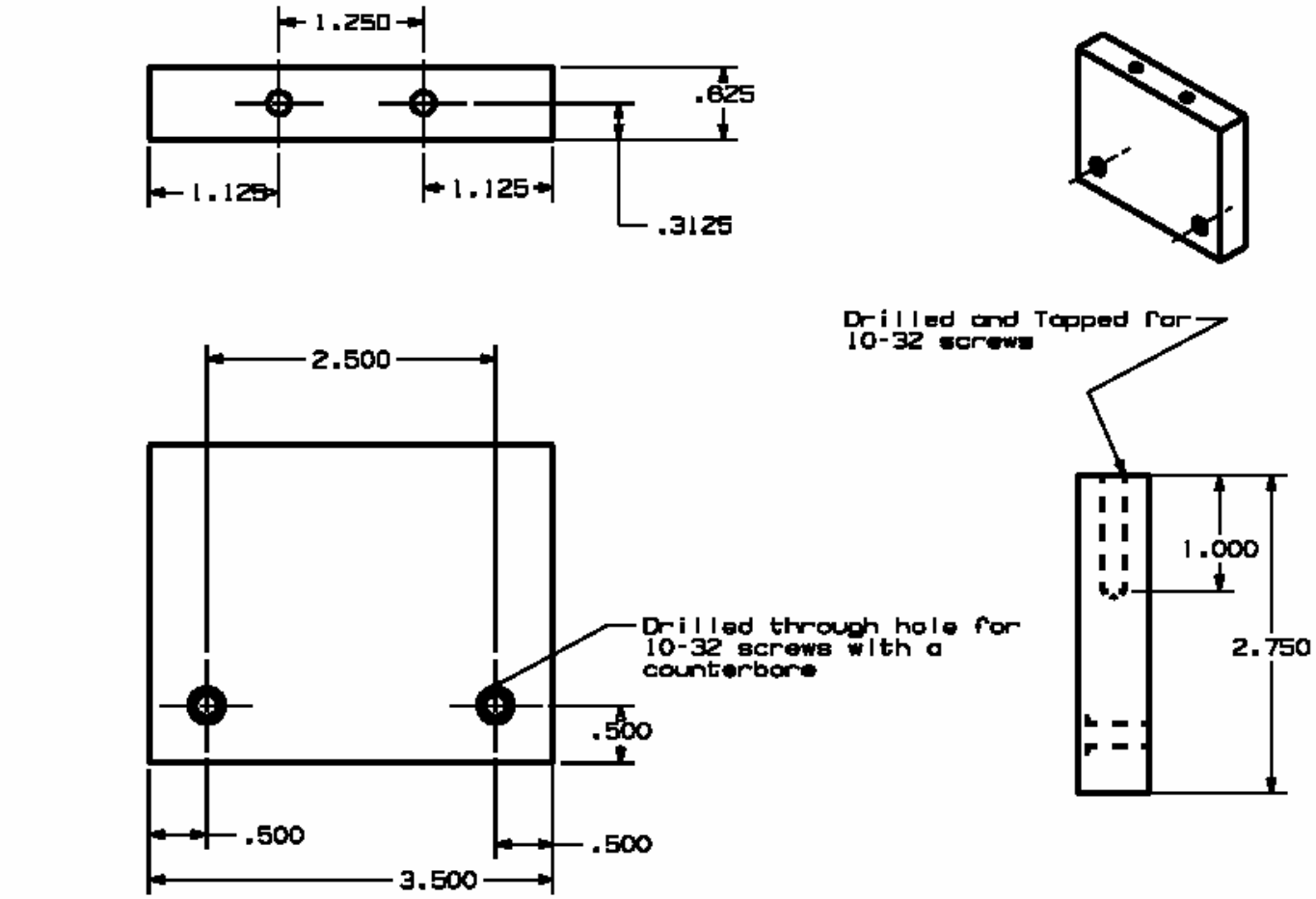

Figure C. 6. The back of the bracket

Appendix D: Experimental Results

In this section the extra graphs described in Chapter 7 are presented. Figure D.1 shows a comparison of the heat flux curves produced by cooling with the convective perfusion probe and the thermoelectric perfusion probe. These heat flux curves correspond to a flow rate of 30 cc/min. It is very important to notice how the shape of the curve is different for the two different probes. The shape of the curve is important for determining perfusion. This is because the thermoelectric cooler takes time to get the desired amount of cooling, while the cooling caused by the convective perfusion probe is instantaneous.

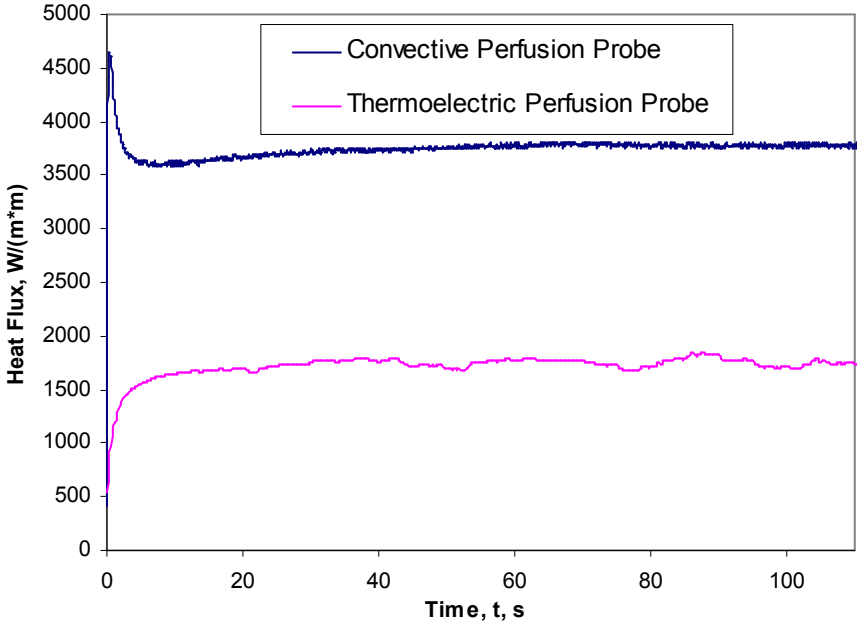

Figure D.1. Comparison the of the Thermal Event for the Convective Perfusion Probe and the Thermoelectric Perfusion Probe

Figure D.2 shows the repeatability graphs for the heating portion of the cycle. This graph was the results of experimentation at 0 cc/min flow rate. The repeatability of the heat flux during Thermoelectric Perfusion Probe is not as good as the Convective

Perfusion Probe because the voltage into the TEC isn't exactly controlled. Finally, Figure D.3 displays the sensitivity of the heat flux.

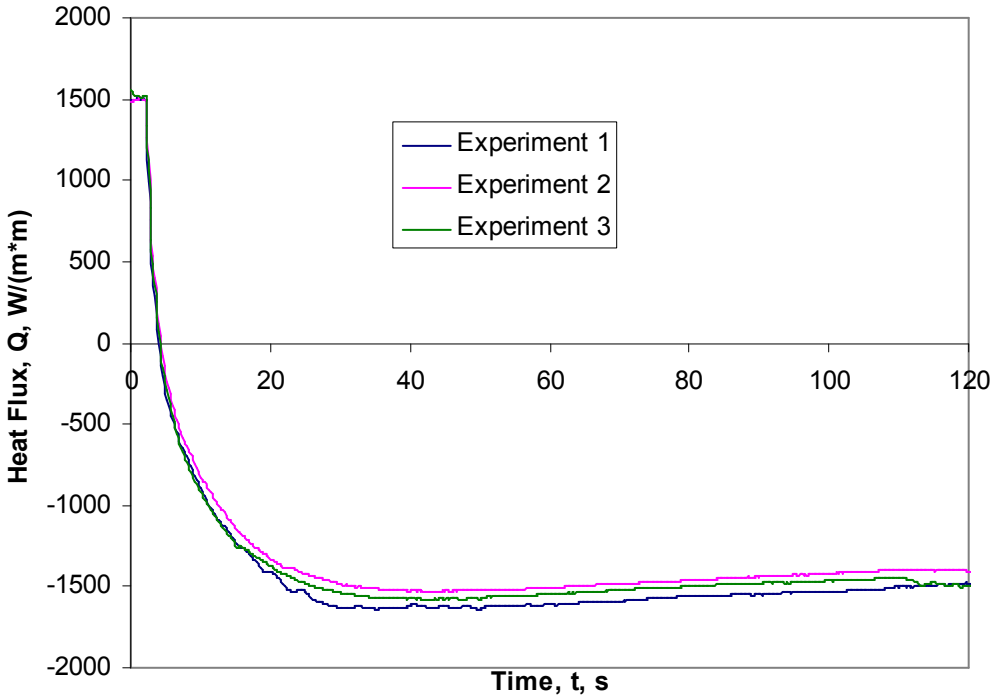

Figure D.2. The repeatability graph for the heating cycle

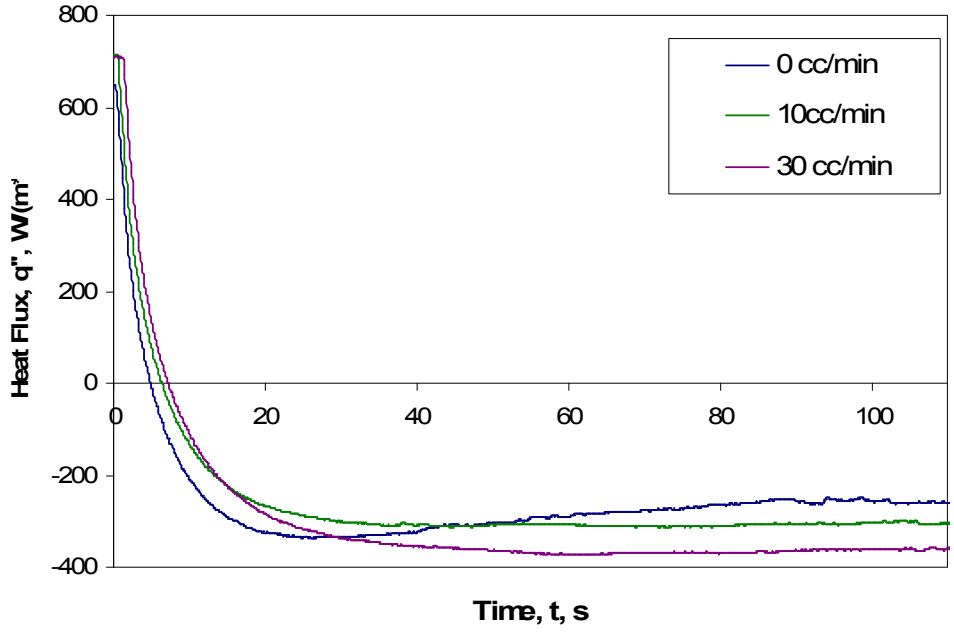

Figure D.3. The sensitivity results for the heating portion of the cycle

The perfusion results with the offsets removed are presented in Figure D.4, Figure D.5, and Figure D.6. Figure D.4 shows the perfusion estimation results when the single cycle data is processed. Figure D.5 displays the average perfusion estimates for the Thermoelectric Perfusion Probe compared to the Convective Perfusion Probe and the CFD Flow model. Figure D.6 displays the Thermoelectric Perfusion Probe's cooling and heating results. Figure D.7 displays an example of a multi-comparison statistical test.

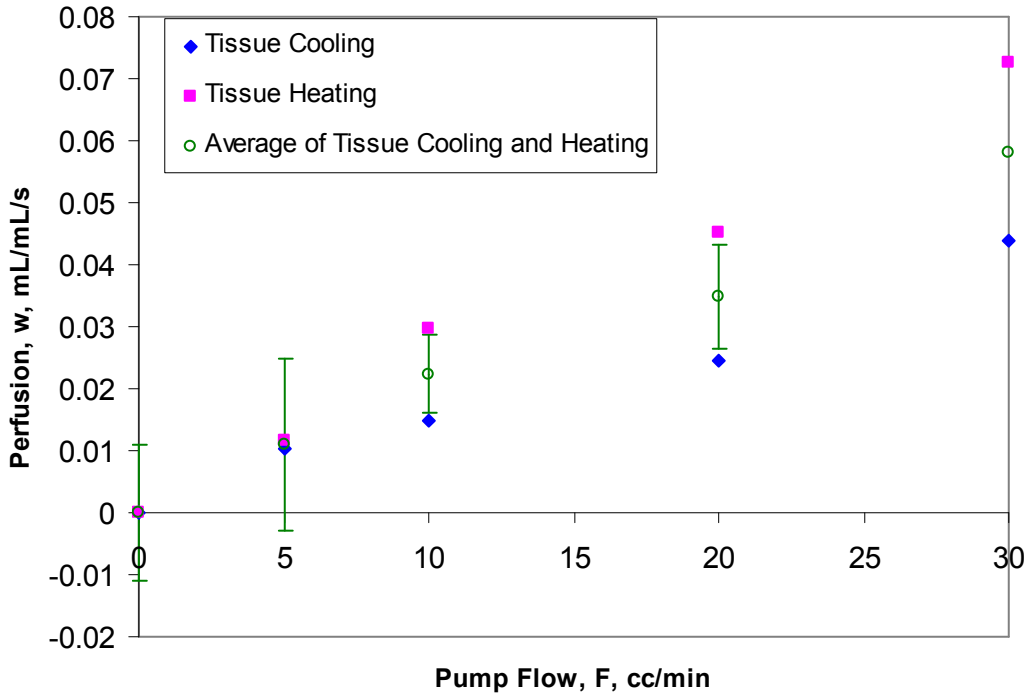

Figure D.4. Perfusion values for Tissue cooling and Tissue heating for a single cycle with the offsets removed.

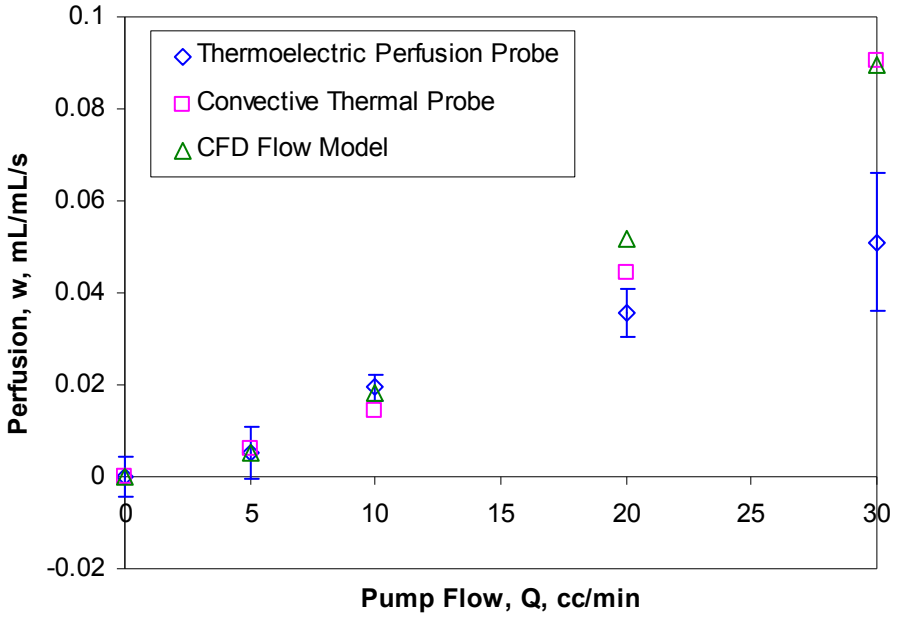

Figure D.5. Comparison plot of the average Thermoelectric Perfusion Probe, Convective Perfusion Probe, and the CFD Flow Model with all the offsets removed.

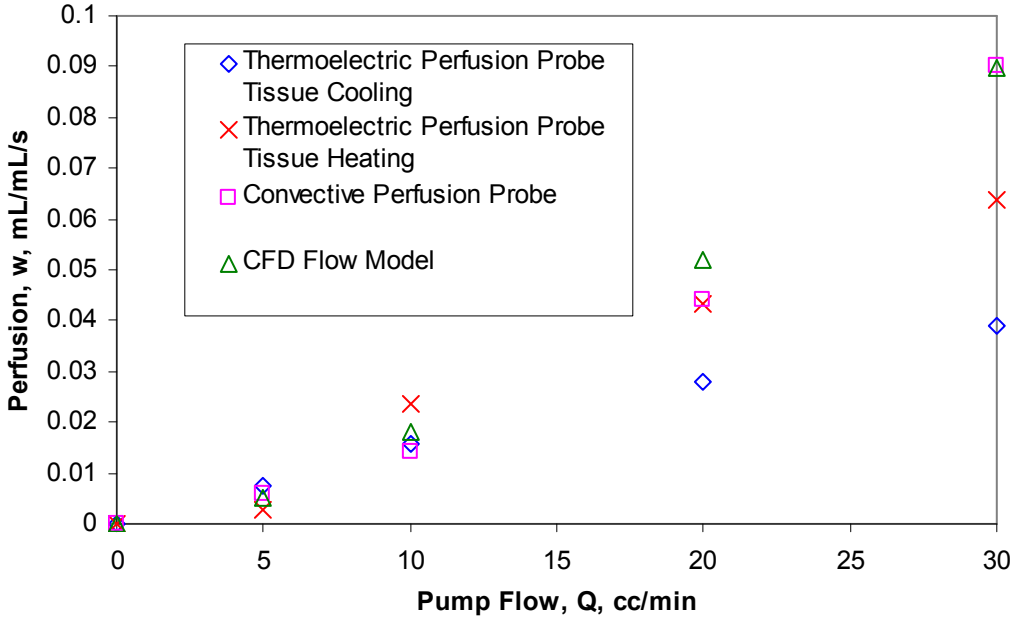

Figure D.6. Comparison plot showing the difference between the perfusion predictions of the tissue cooling portion of the cycle and the tissue heating portion of the cycle with the offsets removed.

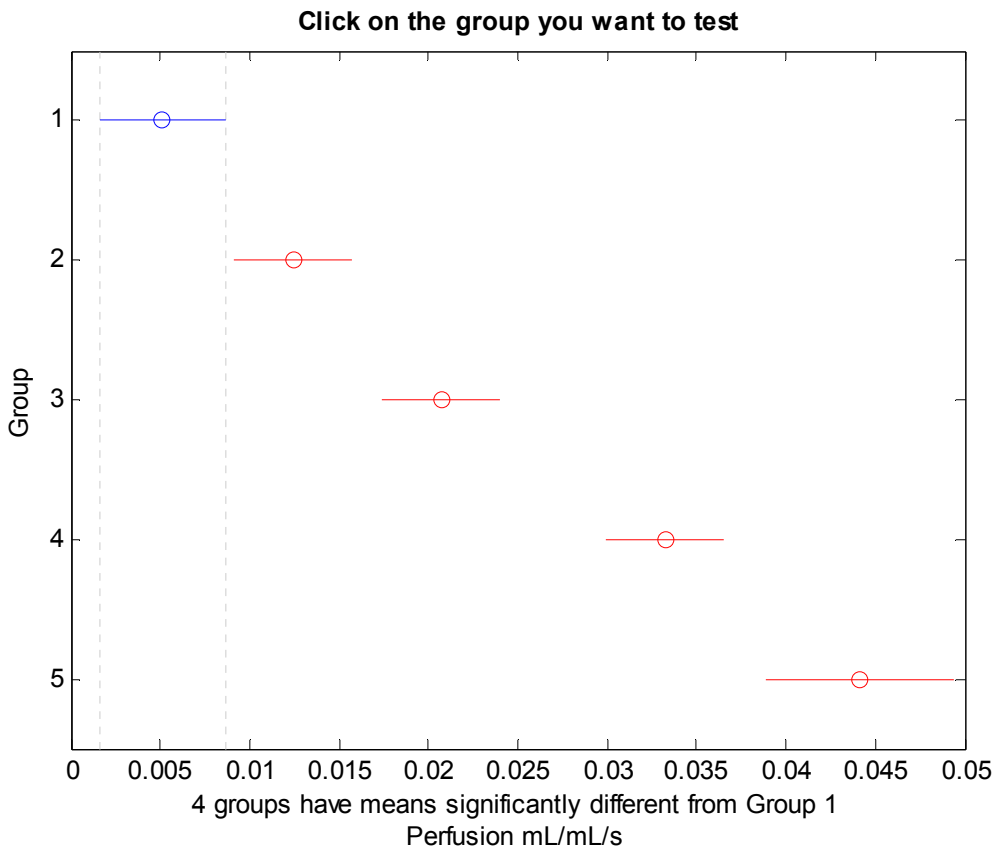

Figure D.7. Comparison of Means Results for Tissue Cooling

Appendix E: Thermistors' Labview Program and Results

As discussed above this section discusses the Labview 7.0 program developed to drive and record the information from the thermistors. Also, in this section are some results using thermistors as the temperature recording device. Figure E.1 shows the front panel, the data collection interface, associated with the Labview Thermistor program. This particular Labview program was developed specifically for animal testing and allows for the heat flux to be recorded, all the voltages produced by thermocouples corresponding to temperatures, and all the voltages based on thermistors corresponding to temperatures. As can be seen in Figure, the recorded voltages for the temperature and heat flux measurements are continuously updated on all the graphs. This front panel allows the user to see if the experimental data recording is successful. This program allowed for two temperature measurement systems to be used at once. As can be seen in the Figure, the continuously recorded voltages are displayed on the graphs.

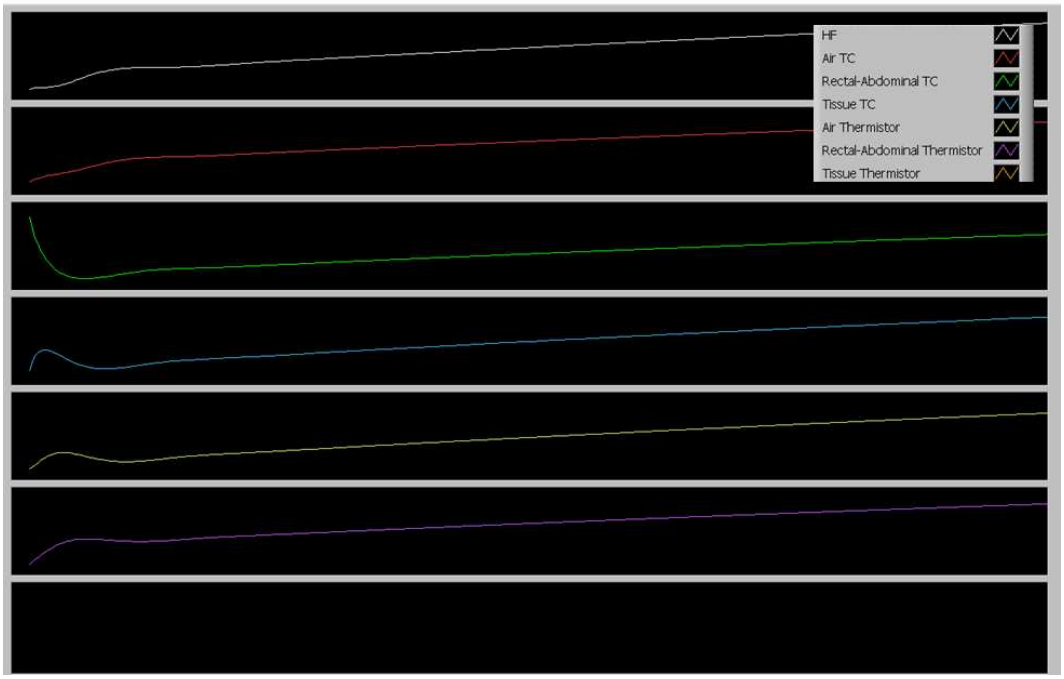

Figure E.1. Front Panel of the Labview Thermistor Program

Figure E.2 shows the back panel, the pictoral programming part of the Labview program. The red block highlights the **DAQ Assistance2** which has to be adjusted to include all input channels. The black block highlights the main addition to the Labview program. The **Simulated Signal** combined with the **DAQ Assistant** is used to output a desired DC voltage, 1.25V, to a particular channel. The connector block has a diagram that shows the location of the different output channels. This program uses output channel a0.

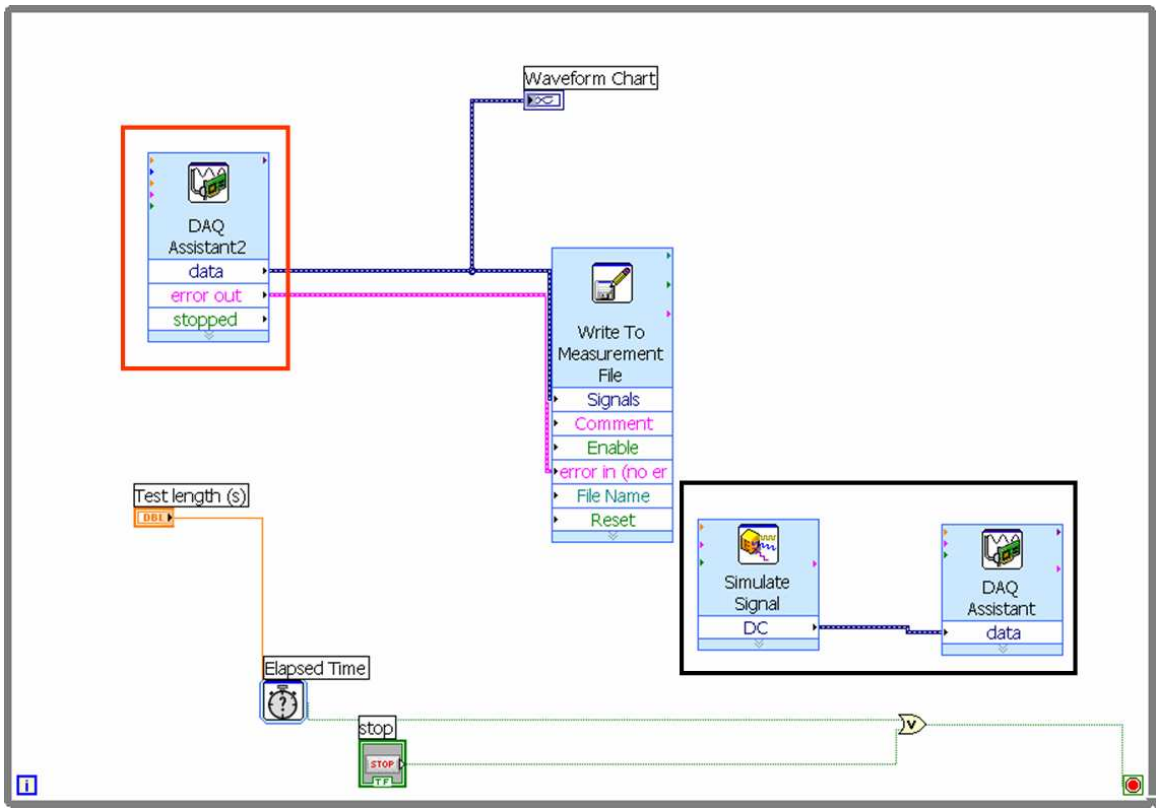

Figure E.2. The Labview Program

Tests were performed on the experimental test stand with the Convective Perfusion Probe where the temperature data was recorded by both the thermocouples and the thermistors. Nine total experiments were completed, three experiments at flow rates of 0, 15, and 30 cc/min. Figure E.3 shows an example graph of the temperatures recorded with the both the thermocouples and the thermistors. Overall, the biggest difference occurred between the air temperature measured by thermistors and by thermocouples. Perfusion estimates were found using the two different temperature measurement systems in conjunction with the heat flux data, Figure E.4. As can be seen from the Figure, the perfusion estimates based on thermistors proved to be larger than the perfusion estimates based on the thermocouples. Also, the difference between the estimates for the two different measuring systems grows with an increase in flowrate. To this point neither measuring system has been proven more accurate.

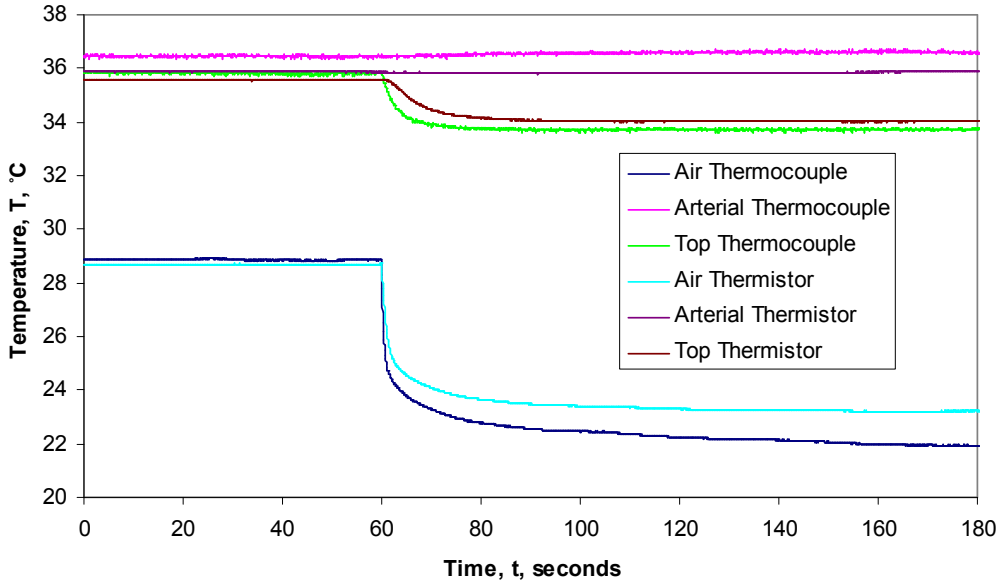

Figure E.3. The Recorded Temperatures from an Experimental Test

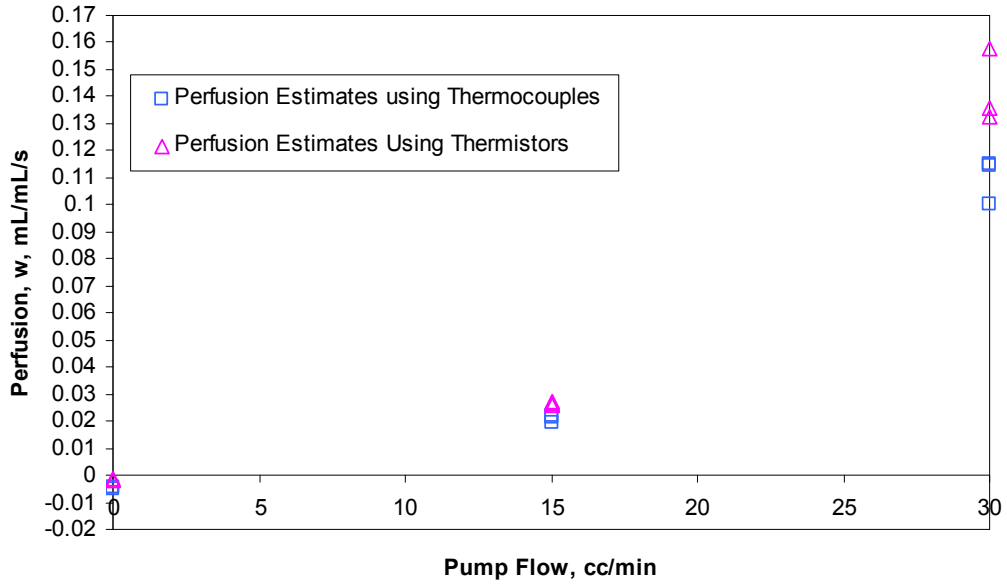

Figure E.4. Perfusion Estimates using Thermistors and Thermocouples